QUALITATIVE AND SEMI-QUANTITATIVE PHYSICO-CHEMICAL CHARACTERIZATION OF SOME CALCIUM PHOSPHATE IMPLANT AND BONE SAMPLES

By

GUSTAV JOSEPH SCHINDLER

Dissertation presented to the
University of Cape Town
in fulfilment of the requirements
for the degree of

MASTER OF SCIENCE

Department of Chemistry

September 1991

ACKNOWLEDGEMENTS

I would like to express my gratitude to:

Professor Allen L. Rodgers for his invaluable guidance throughout the duration of this study.

Professor M. Spector of the Department of Orthopedic Research, Brigham and Women's Hospital, Harvard Medical School, Boston, Massachussetts, for his expert advice and provision of the implant materials studied.

Professor A. Morris of the Department of Anatomy and Cell Biology, Medical School, University of Cape Town, for the provision of the human bones studied.

Dr.C.J. Lombard of the Institute for Biostatistics of the Medical Research Council, Tygerberg for his evaluation of part of the data obtained during this study.

Bruno Pougnet for his valuable assistance and guidance on the ICP-AES and AAS techniques.

The Council for Scientific and Industrial Research (CSIR) for financial assistance.

CONTENTS

ABSTRACT

Ten calcium phosphate implant substances (six of natural origin, four of synthetic orign) and several bone samples from a single human skeleton have been qualitatively and semi-quantitatively characterized with respect to several physico-chemical properties. Analysis involved the techniques of X-ray powder diffraction, infra-red spectroscopy, inductively-coupled plasma atomic emission spectroscopy, atomic absorbtion spectroscopy, and thermal decomposition. In addition, a series of adsorption/exchange experiments were conducted in which implant and bone samples were exposed to progressively increasing concentrations of aqueous Ca^{2+} and Na^{+} ions.

X-ray powder diffraction showed that the implants consist of only hydroxyapatite while bones contain small amounts of CaO as well. a-Cell parameters of the implants of natural origin were larger than those of both synthetic implants and bones. The a-cell sizes of the latter two types of samples resembled each other. The c-cell sizes were similar for all samples. The degrees of crystallinity of all implants were higher than those of bone, possibly indicating lower CO_3 contents in the former.

%Mass contents of various elements were determined by ICP for implants and bones. Statistical analysis on the bone values showed that variation of elemental concentrations not attributable to experimental error occurred in bone from different regions of the body, but not across the surface of any particular bone. Ratios of Ca/P and Mg/Ca were calculated for all samples, and showed differences between implants and bone due to higher calcium levels in the former.

Infrared spectroscopy was used in order to determine $\%CO_3$ values in all the samples. It is suggested that bone contains higher levels of CO_3 than the implants. This was confirmed by analysis of the shapes of certain bands in the spectra of all samples and correlated with XRD results.

All samples were subjected to heat up to a maximum of 900°C. XRD scans were recorded after heating to 650°C and 900°C. Percentage mass losses were also recorded at various stages throughout the heating process. Some of the implants revealed traces of tricalcium phosphate (β-TCP) and CaO after heating to 900°C. All bones revealed traces of CaO after heating to 900°C. a-Cell parameters were calculated for all samples and revealed very slight changes in size. Implants exhibited most of these changes after heating to 650°C, while bones did so only after heating to 900°C.

Surface chemistry studies further confirmed chemical differences between implants and bone by virtue of the fact that neither exogenous Ca^{2+} nor Na^{+} adsorbed/exchanged with ions in the implants, while bone exhibited a clear saturation curve for each exogenous ion.

It is suggested that the techniques and experiments described in this thesis might be utilized by other investigators in the hope of establishing guidelines for the selection of appropriate implant substances.

1. INTRODUCTION

1.1 THE NEED FOR IMPLANT MATERIALS

It has always been an appealing possibility for mankind to be able to replace damaged body tissue with foreign materials. As a consequence, materials science has progressed in recent years to include the development of new porous solids for prosthetic applications, especially for synthetic teeth and bone replacement.

Unlike lower life forms, the human body is substantially limited in its capacity to regenerate components that are lost, damaged or diseased. Furthermore, there are great problems associated with implanting foreign substances within the human body and these tend to persist even though much work has been done in this field. Ironically, the remarkable improvement in medical techniques during the past decade has only further aggravated the situation, as many severely injured patients now have higher survival rates, and this results in a growing population with serious disabilities (Cur62). Autogenous transplants (Cur62), a method whereby living tissue of one part of the body is used to repair tissue of another part of the same body, are usually successful, but there is an obvious restriction on the quantity of material available. This type of bone tissue graft is therefore only feasible for rather minor repairs. In the case of homologous transplants, bone tissues are taken from another animal of the same species and inserted. However, only in unusual instances are these tissues accepted by the recipient's body (Cur62). The dilemma persists even for transplants involving bone tissues from a donor of a different species. It seems that the root of the problem lies with the organic matter present in the foreign bone tissue: it cannot be removed completely, or even in minor amounts, and hence causes rejection when implanted in the human body (Wic66).

For a long time prosthetics technology was more advanced than prosthetics science. In other words, practitioners knew how to make an implant but had no understanding as to why it functioned. The situation has now been reversed by the advent of engineering studies. Scientists can determine what materials are needed for successful implant prostheses. Fundamental aspects such as tissue reaction, whether favourable or adverse, stress distribution as a function of geometry, and factors promoting tissue attachment have gained greater clarity. Today, calcium phosphate (hydroxyapatite i.e.HA) implants are being widely used (Ell69,Web93,Sar86,LeGe88a). There are different forms of these available, each incorporating varying ratios of different crystal phases.

The application of calcium phosphate materials as bone substitutes can be traced as far back as 1920, when Albee reported that a triple calcium phosphate compound used in a bony defect promoted osteogenesis or new bone formation. In 1969, Levitt et al (Lev69) and in 1971,Monroe et al (Mon71),reported a method for the preparation of a calcium phosphate ceramic, mainly calcium-fluor-apatite, and suggested it for the use of dental and medical implantation. Much progress has been made since those pioneering days, and it is largely through the simultaneous but independent efforts of various researchers in the USA and in Europe (LeGe88a), that the potential of these ceramics as bone grafts or substitutes in dentistry has been furthered to the extent that they could become commercially available. At present there are several commercial outlets in the United States as well as in Europe that are marketing these materials under various names depending upon their composition and function (See "TYPES OF CERAMIC IMPLANTS AVAILABLE" p.8)

Before studying the function of these materials within the human body, the structure, formation and function of bone tissue must be considered.

1.2 BONE AND ITS STRUCTURE:

The composition of bone is mainly a tough organic matrix that is greatly strengthened by deposits of calcium salts (Mor66). The matrix content in average bone is 70% while that of salt is 30% (Mor66). It is only newly-formed bone that differs appreciably from this ratio in that it contains a considerably higher percentage of matrix in relation to salts.

A closer investigation of the matrix reveals that it consists of about 90 to 95% of collagen fibres. The remainder is a homogenous medium called "ground substance" (For87,Sel88). The collagen fibres extend primarily along the lines of tensional force, that is, the lines of greatest stress in the bone. These fibres lend the bone its great tensile strength (Cur62).

On the other hand, the bone salts within the organic matrix of bone are composed principally of calcium phosphate, otherwise known as hydroxyapatite:

$$Ca_{10}(PO_4)_6(OH)_2$$

Each bone crystal is about 400 Å long, 10-30 Å thick and 100 Å wide and is shaped like a long, flat plate (Mor66). The relative ratio of Ca to P can vary markedly under different substitutional conditions; on a mass basis it ranges from 1.3 to 2.0. (For87, Gan89).

Mg^{2+}, Na^{+}, K^{+} and CO_3^{2-} ions are also present among the bone salts (Mor66). These ions are believed to be conjugated to the hydroxyapatite crystals rather than to be organized into distinct crystals of their own. Many different types of

ions can conjugate to bone; these include ions normally foreign to bone, such as Sr^{2+}, Pb^{2+}, Au^{+}, as well as many major radioactive ions.

1.3 TENSILE AND COMPRESSIONAL STRENGTH OF BONE

In order to understand how the mechanical properties of bone are produced, attention has to be focussed on the way in which collagen and apatite combine. Every 640Å along the length of a collagen fibre there is a repeating periodic segment, adjacent to each of which lie hydroxyapatite crystals, bound tightly to it (Sel88). It is this strong bonding that prevents "shear" of the bone and lends the bone its inherent strength. In addition to this, the segments of adjacent collagen fibres overlap each other, thereby creating an overlap between the hydroxyapatite crystals. Like the collagen fibres of tendons, those of bone have great tensile strength but low elasticity, while the calcium salts, which are similar in physical properties to marble, have great compressional strength (Cur62). Hence it is more likely that the calcium salts (apatites) - effectively the ceramic component of bone - would have low tensile strength in bulk, since ceramic materials are characteristically stronger in compression than in tension (Cur62). Collagen and apatite, however, when combined, produce a third material, called bone. Bone has a high tensile strength (about 15000 $lb./in^2$) and even higher compressive strength (about 25000 $lb./in^2$) (Cur62). Any cracks that develop in the structure will spread only under the influence of very high stresses. Once they do spread, they will immediately leave the apatite crystals and enter the collagen, which will deform under their influence but not rupture. Thus, it can be appreciated that it is the combination of collagen with apatite that makes the structure of bone so tolerant to stresses.

Bone has a high tensile strength (about $1.03*10^5$ kPa) and even higher compressive strength (about $1.72*10^5$ kPa) (Cur62).

1.4 BONE AND BIOMATERIAL

When hard tissue is replaced, or limb prostheses permanently attached, or even teeth implanted, the critical requirement is that the biomaterial must interface with bone. The natural response of healing tissue to an implanted foreign body is to encapsulate it in scar. Thus, contrary to natural healing, continuity of tissue is never fully restored as long as the implant remains to occupy space which would otherwise be filled by scar. The root of the problem thus lies in the fact that all man-made substances differ from bone in some or other respect.

1.5 BODY RESPONSE

The greatest obstacle for the successful implant of prosthetic devices in the body stems from the body's elaborate immune system. It is extremely efficient in identifying foreign objects, either seeking to destroy the intruder, or if unable to do so, then at least to neutralize it in some way. Phagocytic cells are available to digest the smaller particles of foreign matter such as bacteria and viruses (Sch68). These phagocytic cells can also be prompted into response by chemical stimuli. Three grades of response can follow in such a case:

Grade 1: If there is an absence of corrosion, a very thin membrane separates the implant from surrounding healthy tissue;

Grade 2: If small areas of corrosion are detectable, discoloration of the surrounding tissue occurs. The surrounding membrane is then thicker;

Grade 3: If there is severe corrosion, extensive discoloration of the surrounding tissue occurs. Thick scar tissue surrounds the bone and numerous inflammatory

cells are present. Many cells die, and pus is created. If this is not treated in due course, the patient may die.

Healing around an implant as outlined above, involves its total encapsulation. When the implant is partially exposed, healing may cause its rejection because the surface tissue (i.e. epithilium) will grow into the capsule-implant interface (Dav68). Granulation tissue is far more susceptible to destruction by sepsis and irritation than is cutaneous epithilium. It is surmised (Dav68), that a partially exposed prosthesis will be unstable as long as there is no secure, real bond between the surface of the implant and the connective tissue capsule.

It is apparent from the above discussion that the problem of biocompatibility imposes a severe restriction upon the choice of materials to be used in prosthetic applications.

1.6 PREREQUISITE PROPERTIES OF IMPLANT MATERIALS:

As we have seen from the previous discussion, the most important property of an implant material is its compatibility with body tissues and fluids. In order to blend with its surroundings in the human body, the implant must be non-toxic and non-irritating to the adjacent cells (Gro66).

Biodegradation of implant materials is characterized by alterations in the physicochemical properties of the material after implantation (LeGe88b). Factors that tend to increase the rate of biodegradation include ionic substitutions in the apatite lattice, like CO_3^{2-}, Mg^{2+}, and Sr^{2+} (LeGe88b). In the case of calcium phosphate ceramic implants, physical changes may include disintegration, loss of mechanical strength and changes in porosity; chemical changes that may occur

include dissolution, formation of other CaP phases, and also possible transformation of these phases on the ceramic surfaces.

1.7 SURGICAL USES

Implant materials can be used in two different applications: (Gro66)

1) fixation devices, and
2) prostheses.

The former have the primary role of serving as "splints" during healing and regrowth of damaged bone tissue, whereas the latter have generally stronger mechanical requirements, for the following reasons:

i) the prosthesis must retain adequate strength for a long time, and

ii) the strength that it retains must be sufficient so as not to impose any restrictions upon the activities of the recipient (Gro66).

In the case of a fixation implant the surgeon may order a restriction on activities such as walking, but only for enough time to allow reasonable healing. A hip prosthesis, for example, which is used to replace the head of the femur, has to be capable of tolerating loads of up to six times the body weight, depending upon the individual's activities (Wei68). Fixation devices, such as plates, nails, pins and staples are not designed for weight-bearing use, but rather to hold bones in proper alignment until healing occurs. They should be sufficiently strong to serve for their intended purpose as well as withstand occasional overloading.

The unique feature that commends calcium phosphates as implants is their ability to become directly bonded to bone (Cal84). This means that the bone forms or grows directly on the implant surface, producing a continuum of calcium substance from itself, through the interface and into the implant. The strong bond associated with these implants has been attributed to a "bonding zone" described as dense "amorphous" material (LeGe88a,Dac90). Thus, stimulation of bone growth by the implant occurs.

Another benefit of the calcium phosphate implants is that they can be made resorbable so that they can eventually be entirely replaced by host bone.

Many investigators (Heu88,LeGe88a,LeGe88b,Dac90) have studied the changes that occur with time after the implantation has been completed. The exact mechanism for the formation of the "bonding zone" is not known (LeGe88a). The ultrastructural characterization of the interface is yet to be completed.

1.8 TYPES OF CERAMIC IMPLANTS AVAILABLE

There are several types of calcium phosphate ceramic implants (Table 1.1) available commercially today, each differing from the next with respect to preparation and composition (LeGe88a).

TABLE 1.1 : Calcium Phosphate Materials currently used (LeGe88a)

TYPE	CRYSTALLOGRAPHIC SOURCE
Calcium phosphate ceramics	1. Calcium Hydroxyapatite. Commercial names: Calcitite,

	Periograf, Durapatite etc.
	2. β-Tricalcium Phosphate.
	Commercial names: Synthograf, Augmen.
	3. Biphasic Calcium Phosphates
	(mixture of HA and β-TCP).
	Commercial name: Triosit.
Calcium Phosphate Materials from Natural Products	1. Coralline HA: coral (Porites) hydrothermally converted to HA. Commercial name: Interpore 200
	2. Sintered bovine bone.
	Commercial name: Bio-oss.
Glass Ceramics	1. Prepared by melting together SiO_2,Na_2O/K_2O + CaO, and P_2O_5.
	Commercial names: Bioglass,
	Ceravital.

1.9 DIFFERENCES OF CERAMICS TO OTHER IMPLANTS

The fundamental difference in the choice of ceramic implant materials as opposed to other materials (such as metals, alumina, carbons,etc.) is that its selection is not based on inertness criteria to prevent a response from the body, but rather on its ability to provoke a reaction to their presence. Thus there are terms classifying the metal implants (and others mentioned above) as "bioinert" and the ceramic materials as "bioactive" (LeGe90). A ceramic must therefore have

a chemical composition and a microcrystalline structure almost identical to bone to make such a bioactive nature possible (Web73).

A variety of bioinert materials is available commercially, but recently, a method of application has been suggested for possible future use: a metal implant is coated with a layer of HA or Bioglass, thus combining the strength of the metal with the flexible adaptivity imposed by the HA or Bioglass coating (LeGe88a). These coating processes may have a great influence upon the properties of the newly-formed metal implant when compared to the presently-available forms, especially with respect to their biodegradability.

1.10 DENSE vs POROUS CALCIUM PHOSPHATE MATERIALS

To differentiate between the two terms, it is necessary to consider the materials on the basis of gross physical properties. Materials which are called "dense" are actually micro-porous as a consequence of the sintering conditions (i.e temperature and duration of sintering) under which they were prepared. On the other hand, porous materials are those that are macro-porous in nature, and this is due to deliberate chemical processing (e.g addition of an organic component, such as naphthalene or H_2O_2, followed by volatilization of this component before finally sintering) (LeGe88a). Materials derived from corals i.e. coralline hydroxyapatite, are macro-porous as a result of deliberate retention of the properties of the coral's $CaCO_3$ skeletal structure during the hydrothermal conversion to hydroxyapatite (Don69,Web71,Roy74,Int85,Sar86). The mechanism of bone attachment occurring with the macro-porous structure is that it allows penetration of body tissue through it and as a result, becomes an integral part of it (Web71). Macro-porosity with pores of 150μm in diameter is considered ideal for tissue ingrowth (LeGe88a), since this matches the macro-porosities in human spongy bone.

Both porous and dense materials show strong attachment to bone. The dense material has been reported to have a greater rate of healing compared to standards, while the porous materials have exhibited slower rates of healing within bony pocket confines (LeGe88a). Studies of their biodegradability have revealed that the dense variety biodegrades at a slower rate than the porous type, and mechanical strength investigations have revealed that, the dense material is stronger than the porous type (LeGe88b).

1.11 AIM OF PRESENT STUDY

From the aforegoing it is apparent that the biocompatibility of implant materials is of fundamental importance in determining whether such materials will serve usefully and function correctly. Biocompatibility, in turn, is probably dependent on numerous factors, among which the physicochemical nature of the implant materials must play a key role. It seems reasonable to suggest that of even greater importance is how these physicochemical properties compare with those of the bone in which they are to be implanted. Herein lies the aim and objective of the present study: to characterize, on a qualitative basis, the physicochemical nature of some calcium phosphate implant materials as well as some human bone tissue.

In defining these objectives it is recognized that the physicochemical properties of bone may vary from site to site within the same bone sample as well as within bones from different locations in the human body. Moreover, variation within bones from different individuals as well as male-female differences may also be expected. It is intended that the site-to-site variation and different location-type variation be addressed in the present study. However, inter-human variation of bone properties is beyond the scope of this study.

1.12 MATERIALS

1.12.1 Implant materials

Ten ceramic implant materials were supplied by the Department of Orthopaedic Research, Brigham and Womens' Hospital, Harvard Medical School, Boston, USA. Of these, six were of natural origin, while the remainder were of synthetic origin. Details are given in Table 1.2 below.

TABLE 1.2 : List of ceramic implant materials used

Implant number	Commercial brand	Description
1	S 26/T 900	Preparation: calcination at 900F
2	OsteoGen	Resorbable*; particle size: 300-400 microns
3	Porex Pha	Resorbable* particle size: 300-400 microns
4	C 0/T900	Preparation: calcination at 900F Origin: anorganic bovine bone
5	Bio-Oss	Particle size: 1-2mm Origin: anorganic bovine bone
6	Bio-Oss	Particle size: 1-2mm Origin: anorganic bovine bone
7	Calcitite	Type: calcium phosphate ceramic Mesh size: 40-60 microns Non-resorbable*
8	Calcitite	Type: calcium phosphate ceramic Mesh size: 20-40 microns Non-resorbable*
9	Interpore 500	Type: coralline HA Preparation: hydrothermal conversion of "Porites"** Pore size: 500 microns
10	Interpore 200	Type: coralline HA Preparation: hydrothermal conversion of "Porites"** Pore size: 200 microns

* "Resorbable" specifies that the material implanted becomes absorbed by the bone, thereby adopting a bone-like nature.

** "Porites" are a type of sea-coral.

1.12.2 Bone specimens

The bone specimens were provided by the Department of Anatomy, UCT Medical School and were obtained from one human cadaver. The subject was a male, aged 64. The date of death was 12th of January 1985 (at Groote Schuur Hospital), and the cause was cancer of the bronchus.

The sites sampled are listed in Table 1.3.

TABLE 1.3 : List of bone samples used

Specimen number	Location origin
1	Distal-medial segment of left humeral head - cancellous bone
2	Medial portion of distal diaphysis of left humerus - compact bone
3	Antero-lateral segment of left patella - sessamoid bone
4	Transverse process of 9th thoracic vertebra
5	Anterior (sternal) half of left 10th rib
6	Cranial vault pieces from antero-inferior aspect of right parietal bone

2. TECHNIQUE - INSTRUMENTATION AND METHODOLOGY

2.1 X-RAY POWDER DIFFRACTION

The basic principle of this method is that a powdered specimen of crystalline material is bathed in a beam of monochromatic X-rays which are diffracted by the various planes of atoms and which are then recorded as a spectrum on a strip recorder or photographic film. The diffraction pattern so obtained is a one-dimensional record of peak intensities as a function of diffraction angle (2θ). It is a unique characteristic of the crystal and is similar to a human fingerprint in that it is very useful for identification purposes.

The success of a diffraction experiment depends on the proper preparation of the sample under study. Many different methods of sample preparation have been devised for many different purposes. Ideally, samples for quantitative X-ray diffraction analysis should be prepared in such a way that particle/crystallite size distributions within the sample are uniform and matched in size (Jen81). The terms "crystallite" and "particle" size may not always be synonymous. Crystallite size refers to the size of the individual domains which diffract the X-rays in a certain coherence. Particle size refers to the grain size in a powdered specimen. Thus, particle size can be many time the crystallite size for a sample since individual grains may be made up of many crystallites (Jen81,Rah84). In general it is the crystallite size which is important when considering the orientation effects in the sample, the peak shapes and the noise levels in the background.

Preferred orientation has long been considered to be the primary source of systematic error in quantitative X-ray diffraction analysis (Rah84, Jen81). For truly quantitative X-ray diffraction analysis, it is necessary to use randomly

orientated specimens because of the dependence of the peak intensities on particle/crystallite orientation. Preferred orientation effects can be reduced by employing the side-drifting or end-loading technique (Rah84,Geh83). Gehringer et al. (Geh83) have reported reproducibility figures of 1 to 3% for this technique, which is very acceptable. Consequently, it is this technique which was used in the present study.

A common shortcoming of X-ray diffractometry is the failure to reveal the presence of constituents in mixtures when these occur in minor concentrations. This is attributable to four factors (Geh83): the first is that a constituent whose concentration is less than about 10% will give only a weak diffraction pattern which may be (partly) obscured by the major component. The second arises in those cases where several constituents have common reflections in the diffraction pattern which may make it very difficult, if not impossible, to distinguish one constituent from another. A third source of error may originate from incorrect sampling of the specimen to be tested in that certain specific deposits may be physically missed. The final source of error lies with the instrument itself, which may impose certain limitations upon the resolution of reflections. For example, use of photographic film (as opposed to strip chart recorder) may preclude the detection of low 2θ reflections.

X-ray powder diffraction was selected for use in the present study to achieve the following objectives:

(i) to identify which crystal phase of calcium phosphate is present;

(ii) to determine unit-cell parameters (which may aid in the detection of crystal lattice substitutions);

(iii) to measure the degree of crystallinity.

(iv) to monitor changes in crystal parameters and crystallinity after thermal treatment (see Thermal Decomposition, p.40).

2.1.2 Equipment and operating conditions

Portions of ~0.05g of each of the ten implant materials were roughly ground with a mortar and pestle. These were then progressively passed through a series of stainless steel sieves of size 53,45,and 38μm respectively. Thereafter, samples were packed into aluminium trays using the end-loading technique. After recording a diffraction spectrum, each sample was re-loaded and a duplicate spectrum recorded. A diffraction pattern for an empty aluminium plate was also recorded to determine its characteristic peaks. The bone samples were treated in the same way.

Diffraction patterns were recorded using a Philips PW 1050/70 automatic X-ray powder diffractometer fitted with monochromator and scintillation counter with pulse height selection. A PW2233/20 Cu normal focus tube was run at 40kV and 40mA and was used with 1° divergence and scatter slits. Peak positions and intensities were recorded on a strip chart while scanning the sample through a 2θ range of 20-54°.

Chart settings were:
Scan rate: 2 °/min
Chartdrive: 2cm/min
Range: 4000 cm/sec

2.1.3 Spectra analyses

a] Crystal Phase

The spectra obtained for the samples were examined for the presence of hydroxyapatite and β-tricalcium phosphate (Whitlockite).

b] Unit cell parameters

In order to study substitution effects in the apatite structure, unit-cell parameters have to be calculated. These have been reported to alter significantly as a result of various substitutions (LeGe65,LeGe67,LeGe69,Mco65). Unit cell measurements of apatite crystals (HasX) were obtained from the 002 and 300 X-ray diffraction lines. Since the structure is reported to be hexagonal, only the sizes of a- and c-axes needed to be measured (since b=2a) (You75,Mco65,Mac72,Ell73).

The expressions used to calculate the lattice parameters are:

$$c(\text{Å}) = 2(d_{002})$$

$$a(\text{Å}) = 3(d_{300})/\sin 60 \qquad \text{(HasX)}$$

A list of the cell-measurements for the samples tested is provided under the RESULTS section (p.52).

No internal standard was used.

c] Crystallinity

When substitution of certain ions occurs in the crystal, the degree of crystallinity may alter, depending upon the amount and type of substituent present (Sob49, Mco65, LeGe73 ,Blu81,LeGe83,LeGe84). For example, the presence of carbonate in the apatite crystal can decrease the crystallinity, whereas the presence of Fluoride can increase it (Pos63, LeGe65,LeGe67,You75,LeGe80,LeGe87). The crystallinities of the various samples were calculated from the half-height width of the peak due to the 002 reflection (HasX, Mco60, Sil86). The values obtained in this manner are not absolute values, but are rather used as relative comparison parameters and provide an *INDICATION* of the degree of crystallinity prevalent in each of the samples. Further effects of substitutions on crystallinity will be covered under the DISCUSSION section of this study (p.84).

2.2 ICP-AES TECHNIQUE INTRODUCTION

Inductively coupled plasma atomic emission spectrometry (ICP-AES), was conceived in the early 1960's and is now being used in a wide variety of applications (Pin78,Tho83,Mon87). The ICP is an effective source of atomic emission which can be used for the determination of a wide variety of elements; hence its current popularity among scientists. The major constituent parts of an ICP system are identified as (Bar81,Tho83):

(i) the sample introduction system (nebulizer);
(ii) the ICP torch;
(iii) the radio frequency generator;
(iv) the transfer optics and spectrometer; and
(v) the interface and computer.

In the simplest form of the equipment, a solution of an element whose concentration is to be determined, is introduced into the ICP torch as aqueous aerosol. The light emitted by the atoms or ions in the ICP is converted to an electrical signal by a photomultiplier in the spectrometer. The intensity of this electrical signal is compared to a previous measured intensity of a known concentration of the element, and a final concentration is computed. A schematic representation of a typical ICP system is given in Fig.2.1 (Tho83).

Fig.2.1 : Schematic diagram of a simultaneous ICP system

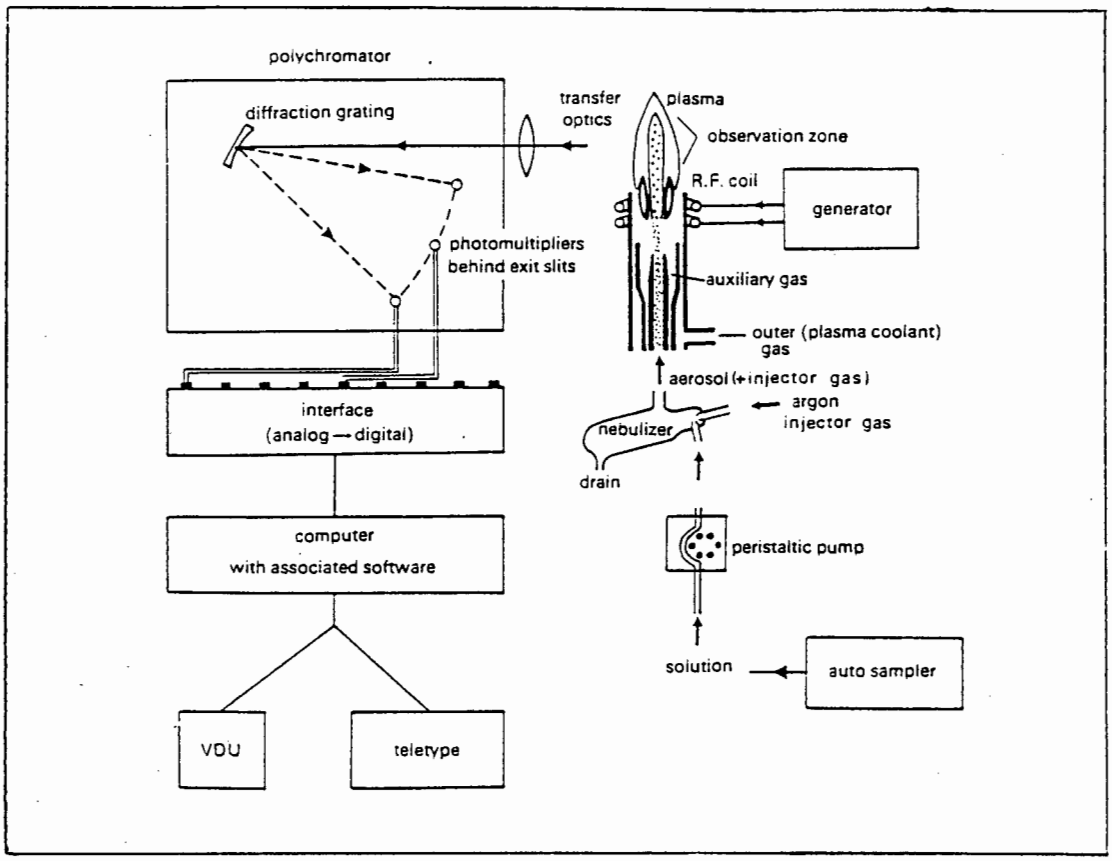

2.2.1 Instrumentation

All experimental work was performed with a Plasma-200 spectrometer fitted with two monochromators of which one operates in vacuum: monochromator B in Table 2.2, page 31 (Allied Analytical Systems). This instrument is an updated version of the IL PLasma-100 previously described in detail by Smith et al. (Smi83,Wan86).

2.2.2 Overall Description

The Plasma-200 is a self-contained ICP spectrometer system that consists of a power regulator, radio frequency power amplifier, sample pump, nebulizer and

spray chamber, torch, two monochromators - the standard air path and a vacuum monochromator which allows the observation of emission lines in a vacuum below 300nm (Wan86, AllM). The computer monitors, interrupts, controls switches and levels, and performs other input/output functions such as signal measurement, processing and the presentation of analytical results. A schematic representation of an inductively-coupled plasma source is given in Fig 2.2 (Bar81).

Fig.2.2 : Diagram of an ICP source

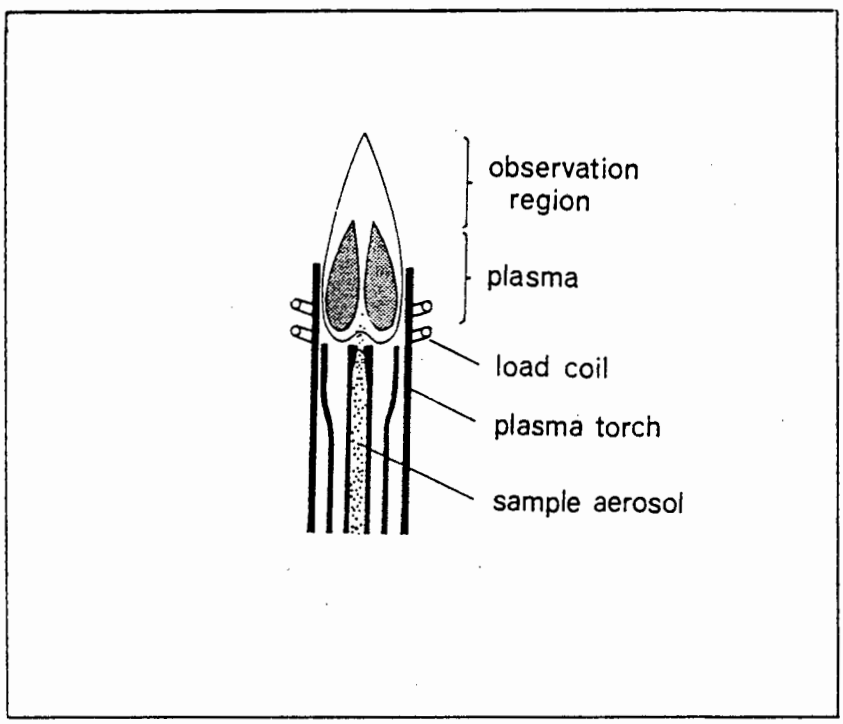

By definition, a plasma is a gaseous mixture in which a significant fraction of the atomic or molecular species originally present is in the ionic form (Lee83,Smi83,Tho83). The plasma employed for emission analyses generally consists of a mixture of argon ions and atoms. When a test sample is injected into this medium, atomization occurs as a consequence of the high temperature, which

may be as great as $1x10^4$K (Bar81,Smi83). Argon ions are formed in a plasma and are capable of absorbing sufficient power from an external source to maintain a sufficiently high temperature to continue the ionization process.

The argon stream flows through three concentric quartz tubes at a rate of between 15 and 20 litres/min. The diameter of the largest tube is 2.0cm. At the top of this tube and surrounding it is a water-cooled induction coil that is powered by a two-kilowatt radio frequency generator (AllM). A spark from a Tesla coil causes ionization of the flowing argon. The resulting ions and their associated electrons then interact with the fluctuating magnetic field produced by the induction coil. This interaction causes the ions and electrons within the coils to flow in the closed annular paths. Their resistance to this movement causes ohmic heating. Because the temperature of the plasma created in this way is very high, thermal isolation from the outer quartz cylinder is needed. This isolation is achieved by allowing argon to flow tangentially around the walls of the tube. The flow of this stream is 14 to 20 liters/min and cools the inside walls of the center tube.

2.2.3 Sample injection

The peristaltic pump is computer-controlled and varies the sample input flow rate from 0.1 ml/min to the maximum allowable value (approx. 2.2ml/min) (Smi83). When the sample is introduced, the computer automatically increases the pump rate to reduce the time required to introduce the sample into the plasma.The nebulizer is of cross-flow design with sapphire gas and sample orifices to reduce nebulizer clogging and to provide a surface that is resistant to all common solvents (Bar81,Tho83,Mon87). The sample may be an aerosol, a thermally generated vapour, or a fine powder.

The most widely used apparatus for sample injection is similar in construction to the nebulizer employed for flame methods. Here the sample is nebulized by the flow of argon, and the resulting finely divided droplets are carried into the plasma.

2.2.4 Plasma Appearance and Spectra

The typical plasma has a very intense, brilliant white, nontransparent core topped by a flame-like tail (Mah83,2I,AllX). The core, which extends a few mm above the tube, consists of a continuum upon which is superimposed the atomic spectrum for argon. The source of the continuum arises from recombination of argon and other ions with electrons. In the region above the core, the continuum fades, and the plasma is optically transparent. Spectral observations are generally made at a height of 15 to 20mm above the induction coil (Lee83b,Bra83,Wan86). Here, the background radiation is remarkably free of argon lines and is well suited for analysis. Many of the most sensitive analyte lines in this region of the plasma are from ions such as Ca(I), Ca(II), Cd(I), Cr(II), and Mn(II).

2.2.5 Analyte Atomization and Ionization

There is not a great temperature variation along a typical plasma source. For example, at a height close to the r.f.coil, the temperature is as high as $1x10^4K$, whereas at a height of 25mm, the temperature is $6x10^3K$ (Tho83,Mon87,2I). Because of these high temperatures, atomization is more complete and there are fewer interference problems due to dissociation reactions.

2.2.6 Quantitative Applications of ICP-AES

When preparing for quantitative analysis, extreme care must be taken to control the many variables involved in sample preparation. In addition, a set of carefully prepared standards for calibration purposes is required (Pin78,Bra83). These standards should closely resemble the composition and physical properties of the samples to be analysed.

2.2.7 Standard samples

In some instances, standards can be synthesised from pure chemicals. On the other hand, a large number of carefully analyzed metals, alloys, and mineral materials have been analyzed by the NBS (National Bureau of Standards), and these are available as standards. Finally, standards are also available from a number of commercial companies.

2.2.8 Operation

a] Optimisation

Once suitable standards have been chosen and prepared and the samples are ready for analysis, optimisation of the instrument is of critical importance. Usually five parameters enable the analyst to set the machine for optimal analysis (Pin78,Bra81,Smi83).These are:

(i) torch power;
(ii) plasma gas flow;
(iii) torch observation height;

(iv) carrier gas flow rate;

(v) nebulizer driving pressure.

After setting the above conditions, only the selection of the spectral line for each of the relevant elements remains. This is usually based on information from the literature and by using line coincidence tables (Mah83), in which possible interferences by other elements present in the samples are considered.

b] Detection Limits

The detection limit is usually defined as "the analyte concentration which will produce a net line intensity that is twice or three times (IUPAC recommendation) greater than the standard deviation of the background signal for a blank solution not containing the analyte, with a minimum of ten successive measurements" (Dea75,Fuw82). Three-fold differences in analyte figures are not significant, as day to day variations in the instrument as well as in operator skills can easily alter values (Mah83,Lee83b). Often however, unrealistically low detection limits are reported. These invariably are obtained by using an excessively large number of readings and long integration times (Wan86). Thus, proper lower limits of detection have to be established for each study. The upper concentration limit is the maximum concentration that can be aspirated without the signal intensity saturating the photomultiplier tube of the detection system (Mah83). Choice of a less sensitive line or use of a less efficient observation height, as well as sample dilution can help to alleviate this problem.

c] Interferences

In most analyses, there are generally two types of interferences - additive and multiplicative (Bar81,Bra83). The first type causes a change in the intercept of the

calibration curve. This occurs when the sample constituent gives rise to a signal that adds to the analyte intensity. The second type causes a change in the slope of the calibration curve and occurs when a sample constituent enhances or suppresses the analyte signal without creating a signal of its own (Mah83). Spectral interferences are generally additive and can occur as a result of emission from OH bands, for example, or even stray light. These interferences can often be eliminated by correct wavelength selection. If, however, spectral interferences cannot be avoided, correction schemes based on the measurement of the concentration of interfering elements must be used. True background shifts can be allowed for with background correction facilities such as those available on the Plasma-200 instrument used in this study: after measurement of the background intensity on one or both sides of the analyte peak, this "base line" is automatically subtracted from the emission line. As a result of this facility, it is apparent that spectral interference plays only a minor role in ICP-AES.

Chemical interferences are comprised of the "classical stable compound-formation" and ionization interferences (Tho83,Mon87). These are caused by chemical interaction of the sample constituents and are multiplicative.

Finally, physical interferences may arise from direct environmental effects(e.g temperature and pressure variations) on instrument performance, and become apparent as drift and increased noise levels during analysis (Bar81). These can be minimized by avoiding large variations in dissolved solid levels and solvent type.

d] Wavelengths

The wavelength chosen for the analytical procedure is critical to the success of the investigation. It must display minimal spectral interferences as well as sufficient sensitivity to ensure detection (Bar81,Tho83).

e] Advantages of ICP

There are several advantages of using ICP relative to other spectro- metric techniques. These include:

(i) its applicability to the analysis of most elements;

(ii) simultaneous or rapid sequential multi-element determinations are possible;

(iii) atomization occurs in a chemically inert environment, which should enhance the lifetime of the analyte;

(iv) effects such as self-absorbtion and self-reversal are not encountered as a result of the uniform cross-section temperature of the plasma;

(v) detection limits are comparable to other spectrometric techniques and are of acceptable precision and accuracy.

f] Objectives of using ICP-AES in the present study. There are several objectives associated with this part of the study:

(i) to determine concentrations of the major (Ca and P) and some of the minor (Na, Mg, Sr, K, Fe, and Zn) elements in all samples;

(ii) to calculate useful parameters from these, such as Ca/P and Mg/Ca ratios so that these may be compared with values published for similar materials;

(iii) to determine whether elemental concentrations vary laterally across a bone surface;

(iv) to determine whether elemental concentrations vary in different bones; and

(v) to compare ICP data with results obtained from the XRD and IR studies.

2.2.9 Sample preparation

Portions (1.0-1.5g) of powdered bone and implant sample were separately weighed into (100ml) Erlenmeyer flasks and 3-4ml of concentrated nitric acid was added (Bar81,Mah83,Wan86). The mixture was heated slowly on a hot plate. Hydrogen peroxide (30%) was added (dropwise to prevent foaming and loss of sample) until all organic material was destroyed (Mah83). Approximately 15-30 mins. was required for complete dissolution.

After cooling, the solution was transferred to a 50ml volumetric flask and diluted to volume with 18mohm (high-purity) water. A 1ml aliquot of this solution was placed into a 100ml volumetric flask and again diluted to volume with 18mohm water. These final dilute solutions were prepared in order to analyse for elements such as Ca, Mg, and P which are expected to be present in much higher concentrations than other elements.

Care was taken throughout the preparation to limit contamination from dirty glassware by soaking the latter overnight in a soap solution, followed by rinsing for 3-4hrs in a dilute nitric acid bath. All solutions used during the preparation were of analytical reagent grade.

The sampling technique for bone was, however, somewhat more intricate than that for the implant materials in order to meet the objectives of this study. To acquire representative samples of each bone from several regions of the body, two sites of that bone were sampled. These were analysed in duplicate using the ICP. Three readings were taken for each determination. Data were labelled (R_x,S_y,A_z) where R_x refers to the origin of the bone within the body (e.g rib, skull,etc.); S refers to one of two possible sites within each bone; A_x gives the analysis number.

2.2.10 Experimental conditions

Table 2.1 below presents a list of the operating conditions under which all studies were carried out. The most sensitive prominent spectral lines for each respective element were studied for potential interferences. These effects on the analyte emission were evaluated by observing the recorded intensity profiles on a video display. This was done by aspiration of a standard solution, using the "restpeak" facility for viewing of the signal on the screen, then repeating the procedure for a sample solution. In this way, an immediate and overall indication was obtained of the concentration of the particular element of interest. In addition, it was established whether background correction needed to be applied. Table 2.2 lists the wavelengths selected.

TABLE 2.1 : Operating conditions of Plasma-200

Power	1.2kW
Plasma coolant gas flow	13 l/min
Sample feed rate	1 ml/min
Nebulizer driving pressure	206.8 kPa
Aerosol carrier flow rate	0.4 l/min
Pump delay	30 secs
Peak window	0.067 nm
Integration time	3 secs
Observation height	4-30 mm, varied
Number of readings	3

TABLE 2.2 : Wavelength data

Element	Wavelength (nm)	Background correction	Monochromator	Viewing height (mm)*
Ca	315.89	-	A	12
P	213.62	-	B	-
Mg	285.21	-	B	-
Na	589.59	-	A	30
Sr	407.77	-	A	14
K	766.49	-	A	4
Zn	213.86	Rhs	B	-
Fe	259.94	-	B	-

* viewing height is fixed for channel B (vacuum)

The concentrations of the various standards prepared are listed in Table 2.3 below. These were prepared from 1000mg/l stock solutions.

TABLE 2.3 : Concentrations of standards used (mg/l)

Ca	P	Mg	Na	Sr	K	Fe	Zn
1	1	0.10	0.50	0.10	0.10	0.10	0.10
10	5	0.20	1.50	0.30	0.30	0.50	0.50
20	10	0.50	3.00	0.60	0.60	1.00	1.00

2.2.11 Statistical evaluation

In order to meet some of the objectives of this section of the study, a statistical analysis was performed on the bone results obtained from the ICP measurments. This analysis involved ascertaining whether differences in elemental concentrations at different sites within the same bone were attributable to experimental errors or to inherent characteristics of the bones. In addition, the nature of differences observed between bones of different regions of the body were also examined. In order to achieve these objectives, a variance component model was used by applying the VARCOMP procedure (Rao73) as described in the SAS User's Guide (Car85). The VARCOMP procedure computes estimates of the variance components in a general linear model. The "maximum likelihood" method is used. This estimates variance components by iterating initial estimates of the components until the log-likelihood objective function converges. The presence of random and non-random effects are therewith effectively determined (the log-estimates and respective standard errors are listed in Table 5, APPENDIX 2).

2.3 INFRA-RED TECHNIQUE INTRODUCTION

Infrared spectroscopy is a well-established technique used in a wide variety of applications (Law61,Whi66,Ram78). It is based on the principle that when a beam of electromagnetic radiation (infrared) is passed through a sample, different wavelengths are absorbed to different extents. These are recorded on a chart. ~~The~~

The infrared spectrum consists of three different region (Sim66,Kno84), of which the "middle" region is of interest in this study. Fig.2.3 depicts the eletromagnetic spectrum.

Fig.2.3 - Electromagnetic spectrum

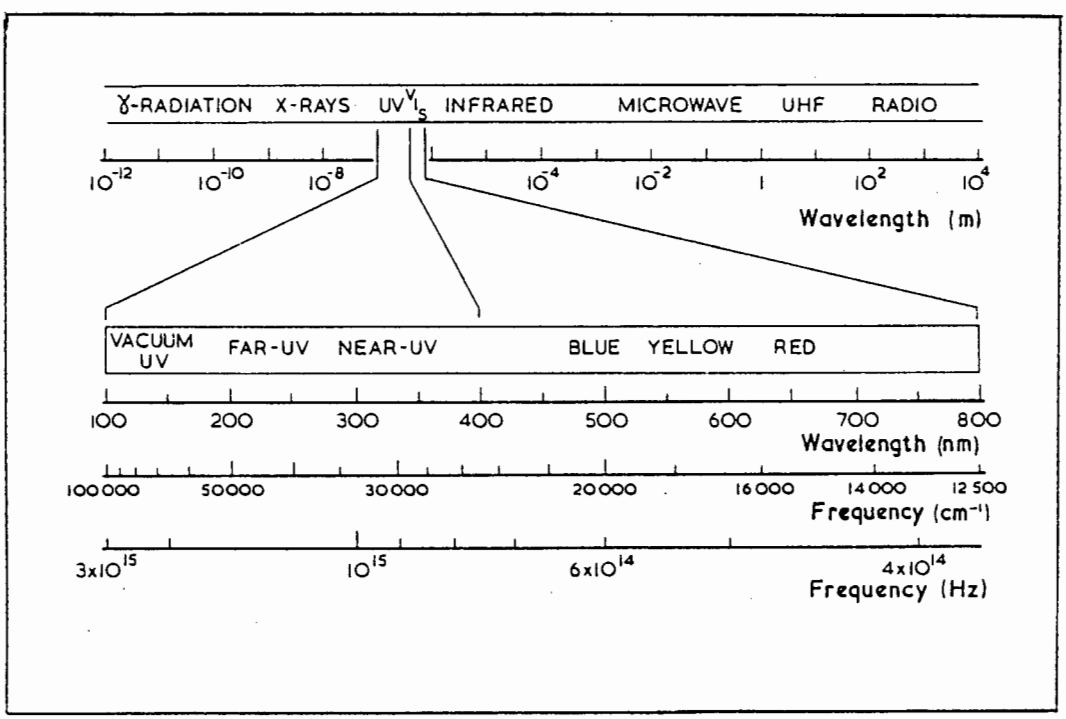

Most organic and inorganic materials show absorbtion yielding a spectrum which is characteristic of the particular substance. The infra-red spectrum is thus a fundamental property of a compound and may be regarded as its "fingerprint" in the same way as the XRD pattern.

Infrared spectroscopy has been used successfully as a tool to determine the $\%CO_3$ content of various samples such as tooth enamel, bone tissue, and synthetic apatites (HasX, Are75,Fea84). IR absorbtion spectra of apatite are characterized by vibration bands produced by OH^-, PO_4^{3-}, and CO_3^{2-} groups (HasX, Are75,LeGe81). The CO_3^{2-} vibrational modes are given the signals v_1, v_2, v_3, and v_4 (LeGe81,Nel82).

Generally, in hydroxyapatite, CO_3^{2-} occurs in three different positions (LeGe67):

i) adsorbed on the crystal surface;

ii) in OH^- sites, and

iii) in PO_4^{3-} sites.

About one third to two-thirds of the total CO_3^{2-} occurs on the surface. The remainder is distributed between PO_4- and OH-sites in the ratio of 90% to 10% respectively.

a] Carbonate determination from IR-spectra

In order to determine the $\%CO_3$ and CO_3/PO_4 ratios for a sample, the bands due to CO_3 ($875cm^{-1}$,$1415cm^{-1}$,and $1460cm^{-1}$) and PO_4 ($575cm^{-1}$, $600cm^{-1}$, and $1040cm^{-1}$) have to be examined. It is also necessary to calculate the extinction coefficient of the carbonate in-plane stretching band at about $1415cm^{-1}$ (E_{1415}). This is achieved from measurement of baseline (background) transmittance (T_2) and peak maximum transmittance (T_1) via the relationship:

$$E = \log (T_2/T_1) \qquad \text{(Are75,Fea84)}$$

The T_2 value for the above band is obtained by drawing a straight line between ~1330 and 1750cm^{-1}. Care must be taken to choose the corresponding points on each of the spectra as their shapes may differ. For the 875cm^{-1} band, a straight line is drawn between the ~820cm^{-1} and 925cm^{-1} points. Once the above extinction coefficients are obtained, values can be calculated via the relationship:

$$(\beta = E_{1415}/E_{875}) \qquad \text{(Are75)}$$

Imperative to this study is the preparation of a series of standards of varying mixtures of $BaCO_3$/calcium phosphate(tribasic). From these standards a series of E_{1415}/E_{875} values are obtained.These are then plotted against the $\%CO_3$ values and the slope of the graph so obtained yields the $\%CO_3$ value of each sample individually via the relationship

$$\%CO_3 = (\text{slope}*1.77)(E_{1415}/E_{875}) \quad \text{(Fea84)}$$

The value of 1.77 is the slope ratio and is specific for the mixture of barium carbonate/calcium phosphate tribasic (CPT) used as standards in this case (Fea84). It functions as a conversion factor in the relationship above.

This method has been reported as yielding an estimate of carbonate content to better than 10% (Fea84).

b] CO_3/PO_4 ratio

This is proportional to the ratio of the band intensities for the CO_3 and PO_4 peaks (Ble75,LeGe83,Sil86).The fact that ratios are employed as opposed to absolute figures introduces the concept of internal standardization and overcomes the need for uniform and/or known particle size (Fea84).

c] The objectives of this part of the study are:

i) to assign the various bands in the spectra to their respective groups;
ii) to determine the $\%CO_3$ contents of bones and implants; and
iii) to determine CO_3/PO_4 ratios for the above.

2.3.1 Instrumentation and operating conditions

In order to obtain accurate spectra, the samples were vacuum-pressed (7000psi) into alkali halide disks, using preheated and purified KBr. The ratio of sample to KBr used was 2:400mg. The spectra were recorded in triplicate in the range 4000-400cm^{-1} using a PERKIN-ELMER Model 983 spectrophotometer. The operating conditions are given in Table 2.4:

TABLE 2.4 : Operating variables

Scan mode	3
Pen set	65%
Slit	$0.37cm^{-1}$
Scan time	2.5 min
Resolution	$5.3\ cm^{-1}$

In order to minimise experimental errors, a newly-pressed disk was used for each run.

Before $\%CO_3$ determinations were carried out, the spectra were examined and the major bands of importance assigned (HasX,Nel82,Pos85). These are listed in Tables 3.13 and 3.14, pgs.61 and 62.

a] $\%CO_3$ Determination:

Six standards containing varying barium carbonate:calcium phosphate tribasic ratios were prepared and are listed in Table 2.5.

TABLE 2.5 : Mass ratios of standards

Ratio	masses used	$\%CO_3$
1:400	0.001:0.3994	0.25
1:300	0.001:0.3001	0.33
1:200	0.001:0.2004	0.49
1:100	0.001:0.1002	0.99
1:50	0.001:0.0504	2.18
1:40	0.001:0.0404	2.72

The reproducibility of the results was tested by preparation of two of the standards four times and calculating means with their respective standard deviations. An accuracy of 4.75% was achieved. This is described in greater detail under the section RESULTS, p.63.

As mentioned in the previous section, the bands at 1415cm^{-1} and 875cm^{-1} were examined for both the standards and the samples (implants as well as bones) (Fea84). Linear regression analysis was performed on the plot of E_{1415}/E_{875} vs $\%CO_3$ for the standards and the slope was calculated. This value was then used to calculate the respective $\%CO_3$ values for all the samples via the relationship outlined previously (p.35). Three values were obtained for each sample (one from each spectrum) and the mean was taken as the final value. Thus $\%CO_3$ values for the ten implant materials as well as the six human bone samples were obtained.

b] CO_3/PO_4 ratios:

The CO_3/PO_4 ratios were determined from the same spectra by making enlarged photocopies (three times enlargement) of the chart on which the spectra had been recorded. Thereafter the paper was cut along the traces defining the peaks at 1415 and 875cm^{-1}. Errors due to imprecise cutting were minimized by using enlarged spectra. These peak "cut-outs" were then weighed to yield integrated peak intensities. The ratio of the masses was taken as the ratio CO_3:PO_4. The procedure was repeated in triplicate.

2.4 THERMAL DECOMPOSITION

When a sample of apatite is heated, changes in its physico-chemical nature may occur, depending upon the rate of heating and the temperature attained (Cor74,Aok77,LeGe78,Bar84,Fow86). The particular temperatures at which the mass changes occur indicate the nature of the substance present and the extents of the changes indicate the amounts present (Rod85). These changes may include the conversion of a small percentage of the main crystal phase to another phase (e.g. traces of β-tricalcium phosphate have been reported after heating) (Aok77). Other changes may also include mass-losses due to liberation of water, which generally occurs at an early stage of heating (40 to 140°C)(LeGe78). Further changes which have been detected after heating are loss of protein or organic component (at ~350°C) and loss of carbonate (at ~550-800°C) (Aok77, LeGe78, Bar84). Samples that have been investigated in this manner include human bone, enamel, dentine, gallstone, urinary and salivary calculi, all of which have an apatitic nature (Cor74, Hol80, Bar84).

The objectives of this part of the study are:

i) to investigate mass losses after heating;
ii) to investigate changes in crystal phase after heating;
iii) to investigate changes in crystal dimensions after heating;and
iv) to determine differences in organic content between bones and implants.

2.4.1 Methodology

The samples were ground to a uniform fine powder (mesh size 54μ m) prior to heating. A furnace (THERMO-ACTIVE, Model ALPHA-TWO) with variable rate heating capacity was used. The temperature range covered was from ambient to 900°C and the heating rate was maintained at 10°C min^{-1}. Approximately 0.30g of each sample was used in every determination. Each sample was placed in a small porcelain crucible and heated individually. Heating took place in three stages:

i) from room temperature to 200°C
ii) from 200 to 650°C, and
ii) from 650 to 900°

Samples were weighed at 200°C, 650°C and 900°C and were subjected to XRD analysis after the 650°C and 900°C stages.

The XRD analyses involved similar parameters as previously described p.(17). The sample size used for these determinations was 0.05g.

2.5 SURFACE CHEMISTRY:

For many years chemists and biochemists have attempted to decipher the interrelationships between blood and bone, for in this lies the key to understanding bone physiology and its electrolyte metabolism, and aid understanding of apatite implants for the role as suitable substitutes. A number of ion-binding studies have been performed on cartilage and bone to determine their ion-binding properties (Fre21a,Fre21b,Neu47, Boy50,Amp52). It has been shown that the mineral phase of bone (hydroxyapatite) is able to adsorb and exchange ions from solution in quantities which are dependent on certain factors, such as pH, concentration of ion, and presence of any competing ions (Fre21a,Boy50, Chr85,Kro86). For example, early studies on animal cartilage by Freudenberg and Gyorgy (Fre21a,Fre21b) showed that several ions were capable of exchanging with calcium in bone crystal. When more than one type of ion is present, competition for calcium sites occurred. During the fifties, experiments conducted by Boyd and Neuman confirmed these results (Boy50). Since then, many complexes have been adsorbed onto the mineral phase of bone in order to study the mechanism of bone-plasma interaction and the involvement of various enzymes (Neu51,Dry60,Mun77,Chr85,Kro86).

Since the present study involves the comparison of the physicochemical properties of some implant materials with those of human bone, a series of experiments was devised in order to compare the ion-exchange capabilities in these two groups of samples. It was decided to focus attention on adsorption and exchanges of foreign ions with calcium, since the latter is the major component of apatite. Both exogenous Ca^{2+} and Na^{+} ions are expected to either adsorb and/or exchange with the Ca^{2+} ions on the surface of the apatite crystal in bone (Fre21a,Fre21b,Car46,Boy50, Amp52,Neu53,Neu58). Analysis of test samples by

atomic absorption after exposure to solutions of varying ionic strength would hopefully yield meaningful data which would permit conclusions to be drawn concerning the type of interaction which had occurred. For example, if Na^+ is "adsorbed" onto apatite crystals, raised Na levels would be expected upon analysis. On the other hand, if Na^+ "exchanges" with Ca^{2+} in the apatite lattice, progressively lower Ca levels would be expected within the samples. Similarly, if exogenous Ca^{2+} is adsorbed, it would be reflected in increasing Ca levels.

Thus, the objectives of this part of the study are to:

i) determine whether the exogenous ions used either adsorb or exchange with ions in the surface of the bone and implant samples;
ii) ascertain whether there exists a saturation concentration for each exogenous ion i.e. a maximum ionic concentration beyond which adsorption or exchange does not occur;
iii) determine whether such a maximum is the same in bones and implants.

2.5.1 Methodology

For each foreign ion studied, six portions (0.3g each) of finely ground bone and implant sample (54μm mesh size sieve) were placed in separate sealable containers. To each of the six containers was added 50ml of an aqueous solution of progressively increasing concentration of the particular ion under investigation. The pH was approximately 7. After sealing, the containers were agitated for three days (Fre21a,Fre21b, Boy50). The suspensions were then removed, filtered and washed thoroughly (using a vacuum pump) with deionised water. Once washed, the samples were dried in an oven at 40°C until constant mass was reached.

A portion of this was used for AAS analysis.

a] Details of experiments

A total of 33 experiments were performed. Of these, the first twelve dealt primarily with developing a suitable procedure and optimising various parameters. Experimental details which were resolved in these preliminary studies are discussed below.

1) Appropriate stirring procedure: during stirring, the suspension of bone powder was splashed against the inside roof of the container thereby limiting its exposure to the ionic solution; finally, gentle shaking of the solutions was found to be more efficient than stirring.

2) Suitable containers: most containers which were initially tested were not air-tight resulting in loss of water over the duration of the experiment. Various types of containers were tested:

   2.1 Erlenmeyer flasks covered with para-film were not suitable as extensive evaporation occurred.

   2.2 Plastic bottles with screw-caps were difficult to seal properly because there were insufficient windings on the cap.

   2.3 Glass bottles with plastic screw-caps were also unsuitable as the screw-caps, which were backed with a waxed cardboard layer, trapped fine sample powder and effectively removed it from solution.

   2.4 Screw-cap, all-plastic containers were found to give very satisfactory results.

3) Quantity of sample: trial and error experiments were conducted to establish sample masses that yielded detectable changes in elemental levels. The optimal mass was found to be 0.30g.

4) Appropriate flame choice: interference in the elemental determinations occurred with the calcium line when using an air/acetylene mixture. This manifested itself in final values that were subdued. Subsequent determinations were carried out using the hotter nitrous-oxide/acetylene flame.

2.6 ATOMIC ABSORPTION SPECTROSCOPY

Atomic absorption spectroscopy is the study of absorption of radiant energy by atoms (Rob66). As an analytical process, it includes the conversion of combined elements to atoms, and the absorption of radiant energy by those atoms. The radiant energy absorbed is in the form of very narrow spectral lines, generally in the visible and ultra-violet spectral regions. During its absorption, outer valence electrons are excited. Atomic absorption spectroscopy is used widely to detect elements at trace levels even in the presence of other elements at much higher concentrations. For some determinations, detection limits in the parts per billion range are well within the capabilities of modern instruments (Lav68,Rub69). Since the technique relies only on the absorption of energy by valence electrons in the ground state, the only types of interferences present are those of chemical and physical processes which inhibit the formation of ground state atoms in the flame (Whi66,Pin78,Fuw82). However, these can be rectified by careful choice of flame type. Because the intensity of the transmitted radiation can be represented by Beer's law, it means that the absorbance is proportional to the concentration at any specific wavelength for a given absorption path length (Dea75,Bar81).

a] Optimisation

As with ICP-AES, it is imperative that the instrument be properly aligned to acquire consistent, reliable data. The following parameters have to be optimised (Rub69,Kno84):

(i) Lamp Operation:

Hollow cathode lamps are used for the determinations. The lamp must be operated at the prescribed (manufacturer) current. If the signal-to-noise ratio is

high, the lamp current should be increased. However, caution must be exercised, since increasing the lamp current increases the curvature of the calibration line.

ii) Spray Chamber Assembly:

The spray chamber is designed to ensure uniform mixing of the fuel, support and sample. The flow rates and flame stoichiometry have to be optimized in order to achieve maximum precision and reliability. Of importance are the following (Rub69,Loo80):

a] the nebulizer must perform optimally and in a constant manner;

b] the optimum position of the impact bead relative to the nebulizer orifice has to be ascertained;

c] the system should be flushed with water regularly to avoid contamination of samples in the spray chamber;

d] the burner must be kept clean to ensure a steady flame. This can be achieved by using a mildly abrasive detergent.

To obtain maximum sensitivity and accuracy, and to keep interference to a minimum, the burner height and degree of rotation (lateral position) must be set optimally for each element combination tested. The lateral position of the burner must be set for maximum sensitivity, to prevent severe chemical interference and instability as a result of the lower temperatures occurring at the edges of the flame. Sometimes the burner can be rotated from the longitudinal position as a convenient means of reducing sensitivity without actually diluting the sample.

b] Flames and Gases

Use of the correct flame type is imperative to maintain accuracy and to avoid interference problems. Among the many flame types, only one is relevant to the

present work, namely nitrous oxide/acetylene. This flame has a higher temperature (3200K) than the conventional air-acetylene type (2600K) and possesses a strongly reducing character which permits a large range of elements to be determined (Lav68,Kno84). Because of the higher flame temperature, a special nitrous oxide burner has to be used which has a head of slightly smaller size than the standard air/ acetylene burner.

c] Wavelength Selection

In the process of selecting a suitable wavelength, the following factors have to be considered:

i) sensitivity must be sufficiently high to avoid excessive sample dilution;
ii) the intensity of the line should yield a reasonable signal-to-noise ratio;
iii) the wavelength should be above 220nm to minimise atomic absorption by gases and matrix (Dea75).

d] Interferences (Kno84):

Two types are commonly encountered:

i) matrix effects are often caused by precipitation of the element of interest and influences the amount of sample reaching the flame. To avoid this, it is necessary that the physical properties of sample and standard be matched as closely as possible;
ii) chemical interferences occur when incomplete dissociation of compounds takes place, resulting in the formation of refractory compounds (such as calcium phosphate). This can be overcome with the use of a higher-temperature flame such as nitrous-oxide/acetylene.

e] Advantages of flame AAS

Some of the advantages include:

i) the technique has a long history and methods for different element-analyses are well-documented;

ii) most elements can be easily atomized by an appropriate flame;

iii) the instrument is easily optimized and choice of flames, although important to the success of the analysis, is not a complicated procedure;

iv) good sensitivity and precision (0.4-2.0% RSD) can be obtained; and

v) the technique is simple and reliable;

f] Instrument description and operating conditions

The apparatus used in this study was a VARIAN-TECHTRON, Model 70. The various parameters used are listed in Table 2.6 while the wavelengths selected are given in Table 2.7.

TABLE 2.6 : Operating data for elements tested

Element	Slit-width (nm)	Lamp current (mA)	Sensitivity (g/ml)	Det.Limit (g/ml)
Ca	0.20	4	0.021	0.0005
Na	0.50	4	0.003	0.0002
Mg	0.20	3	0.003	0.0002
			0.014	

TABLE 2.7: Wavelengths selected

Element	Wavelength (nm)
Calcium	422.67
Sodium	589.00
Magnesium	285.20

For all determinations, a nitrous-oxide flame was used to prevent enhancement of readings (5 to 10% in the case of calcium) caused by metals such as Na, K, and Mg. The use of a lean flame further reduced these effects. No significant interferences were apparent when using this flame with Na and Mg and thus, there was no need to change to the air/acetylene flame for these analyses.

2.6.1 Methodology

Dilutions were made by pouring each of the dissolved sample solutions prepared for AAS into a separate 50ml volumetric flask and diluting with 18mohm water. A 1ml aliquot of each of these was placed separately into a 50ml volumetric flask and again made up to volume with 18mohm water. These were then used for the analyses.

a] Preparation of Standards

Standards were prepared from stock solutions (1000mg/l). Five standards were made for each element. The most concentrated standard for calcium was

5.0mg/l, beyond which an increase in curvature of the calibration line became apparent.

The various concentration ranges covered by the standards are given in Table 2.8.

TABLE 2.8 : Concentrations of standards (mg/l)

Ca	Na	Mg
1.0	0.10	0.10
2.0	0.20	0.20
3.0	0.40	1.00
4.0	0.50	2.00
5.0	0.60	3.00

Linear regression analysis was performed on the readings of all standards in order to obtain a best line fit. An international bone standard IAEA-H5 (International Atomic Energy Agency, Vienna, Austria) was used in each determination to monitor accuracy (Bar81,Lee83a,Wan86).

3. RESULTS

3.1 X-RAY DIFFRACTION

The crystal phase present in the implant materials as well as the bone samples was identified as hydroxyapatite using published mineral diffraction data (Joi72). No trace of β-tricalcium phosphate (whitlockite) was detected in any of the samples. Typical XRD scans and listings of d-spacings vs intensity values for the implant materials and human bones are given in APPENDIX 1.

Unit cell parameters of the implant materials are given in Table 3.1, whereas those of the human bone samples are given in Table 3.2.

TABLE 3.1 : Unit-cell parameters of the implant materials

Implant	a-axis(Å)	S.D.	c-axis(Å)	S.D.
1	9.45	-	6.89	-
2	9.45	0.021	6.88	-
3	9.44	-	6.90	-
4	9.49	-	6.89	0.024
5	9.49	-	6.88	-
6	9.45	0.014	6.90	0.048
7	9.42	-	6.89	-
8	9.43	0.014	6.89	-
9	9.42	0.028	6.88	-
10	9.42	-	6.89	-

TABLE 3.2 : Unit cell parameters of the human bones

Sample	a-axis(Å)	S.D.	c-axis(Å)	S.D.
1	9.45	-	6.86	-
2	9.45	-	6.87	0.014
3	9.45	-	6.87	0.014
4	9.45	-	6.86	-
5	9.38	-	6.86	0.014
6	9.42	-	6.87	0.028

Crystallinity values (calculated from the 002 reflections as described on p.19) for the implants as well as for the bones are given in Tables 3.3 and 3.4 respectively.

TABLE 3.3 : Crystallinity values for the implants

Implant	Crystallinity	S.D.
1	0.34	0.056
2	0.46	0.014
3	0.43	0.007
4	0.35	0.009
5	0.48	0.007
6	0.58	0.007
7	0.39	0.021
8	0.51	0.007
9	0.44	0.021
10	0.45	0.007

Units for the crystallinity values are °2θ.

TABLE 3.4 : Crystallinity values for the human bones

Sample	Crystallinity	S.D.
1	0.41	0.007
2	0.46	0.028
3	0.48	0.007
4	0.43	-
5	0.46	0.007
6	0.45	0.014

The bone samples contain both the organic and inorganic phase.

3.2 ICP

3.2.1 Implants

a) %Mass content

The mass of each implant material used for the ICP analyses is quoted in Appendix 2. The percentage mass content of the implants were calculated from the concentration values obtained from ICP data and are given in Table 3.5.

TABLE 3.5 : %Mass contents of implants

Sample	%Ca	%Mg	%P	%Na	%Sr	%K	%Fe	%Zn
1	38.92	0.505	18.55	0.53	$8.59*10^{-3}$	0.47	2.02*10-3	$5.05*10^{-4}$
	(0.32)	(0.035)	(0.05)	(0.005	$(1.55*10^{-4})$	(0.009)	$(2.11*10^{-4})$	$(6.06*10^{-5})$
2	37.29	-	18.49	1.61	$1.01*10^{-3}$	0.36	$1.01*10^{-3}$	$5.04*10^{-4}$
	(0.19)	-	(0.11)	(0.003)	$(1.21*10^{-4})$	(0.068)	$(2.11*10^{-4})$	$(1.16*10^{-5})$
3	34.31	$5.04*10^{-4}$	19.10	1.80	-	0.34	$5.04*10^{-4}$	$1.51*10^{-3}$
	(0.50)	(0.0025)	(0.07)	(0.02)	(-)	(0.017)	$(1.05*10^{-4})$	$(3.53*10^{-5})$
4	33.53	0.727	20.72	0.89	0.01	0.46	-	0.025
	(0.28)	(0.009)	(0.11)	(0.02)	$(3.88*10^{-3})$	(0.034)	(-)	$(6.01*10^{-5})$
5	36.53	0.492	19.67	0.55	0.01	0.40	-	0.014
	(0.44)	(0.003)	(0.11)	(0.005)	$(1.51*10^{-3})$	(0.045)	(-)	$(3.53*10^{-4})$
6	35.49	0.315	18.66	0.54	$9.63*10^{-3}$	0.37	$1.01*10^{-3}$	0.033
	(0.21)	(0.003)	(0.09)	(0.002)	$(2.59*10^{-4})$	(0.052)	$(2.68*10^{-4})$	$6.08*10^{-5}$

7	37.22	0.0015	18.91	0.02	0.01	0.33	-	-
	(0.35)	(0.0015)	(0.07)	(0.001)	($4.45*10^{-3}$)	(0.002)	(-)	(-)
8	39.58	$2.00*10^{-3}$	19.44	0.03	0.01	0.35	-	-
	(0.15)	($3.5*10^{-3}$)	(0.05)	(0.001)	($1.82*10^{-4}$)	(0.006)	(-)	(-)
9	38.11	0.088	18.71	0.19	0.45	0.30	-	-
	(0.26)	($1.0*10^{-3}$)	(0.05)	($2.0*10^{-3}$)	(0.089)	(0.052)	(-)	(-)
10	38.81	0.078	18.69	0.13	0.50	0.41	-	-
	(0.11)	($7.56*10^{-4}$)	(0.14)	($7.50*10^{-4}$)	(0.012)	(0.05)	(-)	(-)

b) Ca/P and Mg/Ca ratios

These were calculated for both implants and bones and are given in Tables 3.6 and 3.7 respectively. For the latter, values were calculated from the final average values of the %mass contents given on p.60.

TABLE 3.6 : Ca/P and Mg/Ca ratios of implant materials

Implant	Ca/P	S.D.	Mg/Ca	S.D.
1	2.10	0.006	0.013	-
2	2.01	0.010	-	-
3	1.79	0.012	$1.46x10^{-5}$	-
4	1.62	0.006	0.022	$6.0x10^{-4}$
5	1.86	0.010	0.015	-
6	1.90	0.012	$8.87x10^{-3}$	$1.0x10^{-4}$
7	1.96	0.006	$4.06x10^{-5}$	-
8	2.03	0.006	$5.05x10^{-5}$	-
9	2.03	0.006	$2.31x10^{-3}$	$2.52x10^{-5}$
10	2.07	0.010	$2.01x10^{-3}$	$2.52x10^{-5}$

Table 3.6 : Ca/P and Mg/Ca molar ratios of implant materials

Implant	Ca/P	S.D	Mg/Ca	S.D.
1	1.63	0.007	0.021	-
2	1.58	0.005	-	-
3	1.38	0.011	2.41*10(-5)	-
4	1.27	0.008	0.036	3.5*10(-4)
5	1.46	0.009	0.014	-
6	1.50	0.010	0.014	2.5*10(-4)
7	1.51	0.005	6.68*10(-5)	-
8	1.59	0.007	8.40*10(-5)	-
9	1.63	0.012	3.68*10(-3)	1.60*10(-4)
10	1.59	0.010	3.25*10(-3)	1.70*10(-5)

TABLE 3.7 : Ca/P and Mg/Ca ratios for the bones

Rx	Ca/P	S.D.	Mg/Ca	S.D.
1.	2.71	0.035	0.013	0.004
2.	2.22	0.071	0.012	0.003
3.	2.29	0.007	0.012	0.001
4.	2.22	0.042	0.016	0.007
5.	2.18	0.042	0.008	-
6.	2.20	0.014	0.009	-

3.2.2 Bones

a] %Mass contents

The %mass contents of the six bone samples as determined by ICP are given in Tables 3.8 to 3.11. The masses used for the analyses are listed in APPENDIX 2. Two sites on each bone sample were analysed and these were done in duplicate.

Corrected

Table 3.7 : Ca/P and Mg/Ca molar ratios of the bones

Rx	Ca/P	S.D.	Mg/Ca	S.D.
1	1.67	0.021	0.021	0.006
2	1.71	0.086	0.019	0.002
3	1.77	0.010	0.021	0.002
4	1.71	0.035	0.028	0.005
5	1.68	0.025	0.014	-
6	1.69	0.009	0.015	-

TABLE 3.10 : %Mass contents (site 2,anal 1)

Rx	%Ca	%Mg	%P	%Na	%Sr	%K	%Fe	%Zn
1.	25.03 (0.15)	0.246 (0.021)	11.54 (0.048)	0.440 (-)	1.22×10^{-3} (2.10×10^{-5})	0.044 (-)	0.44 (6.14×10^{-4})	0.0019
2.	25.13 (0.09)	0.277 (0.028)	11.35 (0.07)	0.509 (-)	2.56×10^{-3} (1.35×10^{-5})	0.033 (0.007)	0.028 (3.78×10^{-4})	0.0008
3.	22.57 (0.18)	0.254 (0.015)	9.73 (0.01)	0.495 (-)	3.95×10^{-3} (1.59×10^{-5})	0.064 (0.007)	6.21×10^{-3} (1.97×10^{-4})	0.0056
4.	23.48 (0.22)	0.684 (0.021)	10.79 (0.05)	0.647 (0.011)	1.52×10^{-3} (-)	0.099 (0.007)	.023 (-)	0.0055
5.	22.64 (0.12)	0.174 (0.033)	10.55 (0.03)	0.538 (0.004)	1.74×10^{-3} (1.21×10^{-4})	- (-)	0.024 (6.54×10^{-4})	0.0050
6.	23.36 (0.14)	0.202 (0.027)	10.43 (0.02)	0.504 (0.008)	1.61×10^{-3} (-)	0.108 (0.014)	0.036 (8.48×10^{-4})	0.0006

TABLE 3.11 : %Mass contents (site 2,anal 2)

Rx	%Ca	%Mg	%P	%Na	%Sr	%K	%Fe	%Zn
1.	23.48 (0.27)	0.246 (-)	11.05 (0.04)	0.487 (0.019)	0.004 (1.21×10^{-4})	0.051 (0.002)	0.039 (9.21×10^{-4})	0.0005
2.	23.46 (0.18)	0.265 (-)	10.97 (0.06)	0.620 (0.012)	0.005 (-)	0.021 (-)	0.026 (5.67×10^{-4})	0.0024
3.	21.50 (0.20)	0.254 (-)	9.42 (0.03)	0.636 (0.006)	0.006 (1.97×10^{-4})	0.052 (0.008)	0.005 (1.94×10^{-4})	0.0060
4.	22.72 (0.27)	0.303 (-)	10.26 (0.08)	0.523 (0.009)	0.004 (5.31×10^{-4})	0.089 (0.007)	0.019 (5.32×10^{-4})	0.0059
5.	23.08 (0.44)	0.218 (-)	10.12 (0.05)	0.539 (0.003)	0.004 (3.51×10^{-4})	0.010 (-)	0.022 (8.37×10^{-4})	0.0089
6.	22.15 (0.58)	0.202 (-)	10.19 (0.04)	0.489 (0.008)	0.004 (-)	0.110 (0.021)	0.036 (8.48×10^{-4})	0.0010

TABLE 3.8 : %Mass contents (site 1,anal 1)

	%Ca	%Mg	%P	%Na	%Sr	%K	%Fe	%Zn
1.	22.03 (0.28)	0.289 (-)	10.05 (0.02)	0.440 (0.012)	9.98×10^{-3} (3.86×10^{-4})	0.194 (0.034)	0.065 (2.73×10^{-3})	0.0006
2.	22.35 (0.28)	0.317 (-)	10.13 (0.03)	0.532 (0.006)	4.59×10^{-3} (1.98×10^{-4})	0.191 (0.016)	0.032 (1.23×10^{-3})	0.0002
3.	22.18 (0.31)	0.310 (-)	9.76 (0.04)	0.561 (0.005)	5.53×10^{-3} (1.55×10^{-4})	0.091 (0.028)	0.038 (8.85×10^{-4})	0.0074
4.	18.48 (0.17)	0.198 (-)	8.43 (0.02)	0.328 (0.005)	2.34×10^{-3} (2.15×10^{-5})	0.098 (0.026)	0.033 (9.19×10^{-4})	0.0002
5.	18.72 (0.27)	0.153 (-)	8.96 (0.03)	0.337 (0.003)	2.62×10^{-3} (-)	0.068 (0.031)	0.078 (1.33×10^{-3})	0.0005
6.	21.11 (0.56)	0.200 (-)	9.97 (0.02)	0.369 (0.002)	3.14×10^{-3} (-)	0.163 (0.072)	0.058 (1.03×10^{-3})	0.0001

TABLE 3.9 : %Mass contents (site 1,anal 2)

Rx	%Ca	%Mg	%P	%Na	%Sr	%K	%Fe	%Zn
1.	23.14 (1.58)	0.301 (0.08)	10.65 (0.92)	0.406 (-)	0.008 (1.22×10^{-4})	0.119 (0.099)	0.048 (0.008)	8×10^{-4} (6×10^{-5})
2.	23.54 (1.06)	0.282 (0.05)	10.62 (0.78)	0.571 (0.008)	0.005 (1.51×10^{-4})	0.109 (0.116)	0.027 (1×10^{-4})	0.0011 (8×10^{-4})
3.	22.08 (0.05)	0.282 (0.04)	9.62 (0.06)	0.579 (0.018)	0.006 (1.83×10^{-5})	0.076 (0.026)	0.024 (0.011)	0.0048 (0.0015)
4.	20.96 (3.03)	0.351 (0.20)	9.44 (1.54)	0.461 (0.176)	0.003 (2.18×10^{-4})	0.098 (0.005)	0.017 (0.005)	0.0049 (5×10^{-4})
5.	20.99 (2.64)	0.175 (0.03)	9.61 (1.03)	0.442 (0.134)	0.003 (1.54×10^{-4})	0.036 (0.044)	0.043 (0.018)	0.0050 (-)
6.	22.16 (0.86)	0.201 (-)	10.07 (0.34)	0.449 (0.068)	0.004 (1.21×10^{-4})	0.137 (0.039)	0.042 (0.008)	6×10^{-4} (4×10^{-4})

TABLE 3.12 : Ave. of %mass contents of site 1 and site 2

Rx	%Ca	%Mg	%P	%Na	%Sr	%K	%Fe	%Zn
1.	22.00 (0.48)	0.420 (0.022)	9.95 (0.03)	0.372 (8.86×10^{-3})	0.185 (0.028)	0.185 (0.028)	0.042 (6.40×10^{-4})	0.0002
2.	23.23 (0.07)	0.317 (0.025)	9.99 (0.04)	0.622 (0.007)	0.007 (1.51×10^{-5})	0.190 (0.017)	0.019 (3.53×10^{-4})	0.0008
3.	22.03 (0.03)	0.310 (-)	9.56 (0.03)	0.620 (0.008)	0.008 (-)	0.097 (0.031)	0.026 (5.53×10^{-4})	0.0019
4.	19.16 (0.11)	0.216 (-)	8.26 (0.02)	0.343 (0.006)	0.004 (1.26×10^{-4})	0.104 (0.018)	0.021 (3.60×10^{-4})	0.0090
5.	19.51 (0.09)	0.153 (-)	8.80 (0.02)	0.351 (0.003)	0.004 (-)	0.066 (0.036)	0.046 (1.07×10^{-3})	0.0036
6.	22.00 (0.13)	0.200 (-)	9.68 (0.02)	0.432 (0.003)	0.005 (1.07×10^{-5})	0.164 (0.068)	0.036 (5.71×10^{-4})	0.0005

3.3 INFRARED SPECTROSCOPY

3.3.1 Frequency assignments

The frequency assignments for the implant materials and the bone samples are given in Tables 3.13 and 3.14 respectively.

Typical IR spectra for implants and bones are included in APPENDIX 3.

TABLE 3.13 : Frequency assignments for the implants (cm^{-1})

(*) See next page

Vibrating gp.	Mode	S1	S2	S3	S4	S5	S6	S7	S8	S9	S10
OH		3422	3431	3418	3424	3416	3422	3426	3421	3433	3429
		1625	1631	1640	1645	1644	1658	1635	1631	1644	1640
PO^4	υ_2	1089	1088	1087	1088	1089	1088	1088	1089	1087	1087
		1043	1039	1037	1042	1041	1040	1042	1037	1040	1041
	υ_4	631	630	628	630	629	630	628	630	630	628
		602	601	601	601	602	602	600	601	601	601
		568	566	566	569	567	567	569	567	567	567
CO_3	υ_2	960	958	961	960	962	961	960	961	961	961
	υ_3	1458	1459	1459	1459	1459	1458	1460	1457	1459	1459

Frequency assignments for implants (cm^{-1})

Vibrating gp.	Mode	S1	S2	S3	S4	S5	S6
OH		3422	3431	3418	3416	3416	3422
		631	630	628	630	629	630
OH(H2O)		1625	1631	1640	1645	1644	1658
PO4	v1	960	958	961	960	962	961
	v2	1089	1088	1087	1088	1089	1088
		1043	1039	1037	1042	1041	1040
	v4	602	601	601	601	602	602
		568	566	566	569	567	567
CO3	v2	871	870	871	871	872	870
	v3	1458	1459	1459	1459	1459	1458
		1412	1415	1418	1413	1415	1415

Vibrating gp.	Mode	S7	S8	S9	S10
OH		3426	3421	3433	3429
		628	630	630	628
OH(H2O)		1635	1631	1644	1640
PO4	v1	960	961	961	961
	v2	1088	1089	1087	1087
		1042	1037	1040	1041
	v4	600	601	601	601
		569	567	567	567
CO3	v2	872	871	871	871
	v3	1460	1457	1459	1459
		1417	1415	1415	1415

TABLE 3.14 : Frequency assignments for the human bones (cm^{-1})

Vibrating gp.	Mode	S1	S2	S3	S4	S5	S6
OH		3567	3566	3566	3568	3394	3418
PO_4	υ_1	960	960	960	960	960	960
	υ_2	1088	-	-	1088	-	-
		1040	1033	1029	1029	1037	1040
	υ_4	632	629	629	631	-	-
		601	602	601	601	602	602
		569	564	564	569	567	567
CO_3	υ_2	875	871	878	891	871	871
	υ_3	1457	1459	1459	1460	1457	1459

3.3.2 %CO_3 Values

The values of E_{1415}/E_{875} for the six standards are given in Table 3.15 under the heading "β".

Corrected

Vibrating gp.	Mode	S1	S2	S3	S4	S5	S6
OH		3567	3566	3566	3568	3394	3418

TABLE 3.15 : Average β values for standards

Standard	$\%CO_3$	ave.β
1	0.25	3.04
2	0.33	3.29
3	0.49	3.49
4	0.99	3.53
5	2.18	4.51
6	2.72	4.54

In order to check the reproducibility of these values, the entire procedure involving pellet pressing and infrared scanning was repeated four times for standards 2 and 5. The average values are given in Table 3.16.

TABLE 3.16 : Average β of four scans and their errors

Standard	ave.β	S.D.	%R.S.D
2	3.15	0.18	5.71
5	4.66	0.21	4.51

There is thus a percentage relative standard deviation of 4-5% associated with this method.

The slope of the calibration curve of $\%CO_3$ vs β is 0.5938.

β-Values and their corresponding $\%CO_3$ figures for the ten implant materials are given in Table 3.17, while those for the human bone samples are given in Table 3.18.

TABLE 3.17 : List of β, $\%CO_3$ and ave.$\%CO_3$ values of implants

Implant	1	2	3	%CO3	%CO3	%CO3	ave.%CO3	S.D.
1	2.26	1.83	2.50	2.37	1.92	2.62	2.30	0.35
2	2.49	2.10	2.03	2.62	2.21	2.13	2.32	0.26
3	0.55	0.40	0.45	0.57	0.42	0.47	2.49	0.18
4	3.45	3.05	3.51	3.63	3.21	3.69	3.51	0.26
5	2.73	2.67	2.62	2.87	2.81	2.46	2.71	0.22
6	2.86	3.11	3.15	3.01	3.26	3.31	3.19	0.16
7	2.46	2.33	2.59	2.58	2.34	2.72	2.55	0.19
8	1.52	1.80	1.75	1.59	1.89	1.84	1.77	0.16
9	1.76	1.70	2.05	1.85	1.70	2.15	1.90	0.23
10	2.01	1.97	2.33	2.11	2.07	2.45	2.21	0.21

Due to the linearity of the calibration curve, it was deemed sufficient to extend the %CO3 range to the value of 2.72, since the value of the slope obtained would be accurate enough even for values of carbonate content up to the maximum of 6% obtained for some samples.

TABLE 3.18 : List of β, $\%CO_3$ and ave. $\%CO_3$ values of bones

Sample	1	2	3	%CO3	%CO3	%CO3	ave.%CO3	S.D.
1	4.95	4.50	4.91	5.20	4.73	5.16	5.03	0.26
2	4.07	4.33	4.61	4.91	4.55	4.84	4.77	0.19
3	3.98	4.59	4.14	4.18	4.82	4.35	4.45	0.33
4	5.25	5.05	5.65	5.52	5.31	5.94	5.32	0.31
5	5.56	5.01	5.42	5.84	5.26	5.69	5.33	0.29
6	3.82	3.95	3.75	4.01	4.15	3.94	3.84	0.16

3.3.3 CO_3/PO_4 Ratios

The CO_3/PO_4 ratios for the ten implant materials as calculated from the spectra are given in Table 3.19, while those for the human bone samples are given in Table 3.20.

TABLE 3.19 : CO_3/PO_4 ratios of the implant materials

Implant	CO_3/PO_4	S.D.
1	0.338	0.093
2	0.333	0.111
3	0.328	0.070
4	0.295	0.058
5	0.285	0.053
6	0.267	0.021
7	0.353	0.078
8	0.271	0.065
9	0.209	0.048
10	0.254	0.041

TABLE 3.20 : CO_3/PO_4 ratios of the bones

Sample	CO_3/PO_4	S.D.
1	0.310	0.010
2	0.311	0.011
3	0.349	0.020
4	0.309	0.015
5	0.318	0.035
6	0.287	0.013

3.4 THERMAL DECOMPOSITION

3.4.1 Mass losses

The total mass-loss incurred by each sample after heating to 900°C, is recorded in Table 3.21.

TABLE 3.21 : Total %mass-loss for each sample tested

Implant	%mass lost
1	5.84
2	3.56
3	3.60
4	3.65
5	3.98
6	4.03
7	3.13
8	3.66
9	3.54
10	2.75

Bones	%mass lost
1	40.61
2	[illegible]

3.4.2 XRD analysis

Unit cell parameters,crystallinity and crystal phase identification data for implants and bone samples during heating are given in Tables 3.22 to 3.25.

TABLE 3.22 : XRD parameters of implants - after heating to 650°C

Implant	a-(Å)	S.D.	c-(Å)	S.D.	crystallinity	S.D.	crystal phase
1	9.42	0.0146	6.90	0.014	0.29	0.007	HA
2	9.42	0.007	6.89	-	0.33	0.009	HA
3	9.42	-	6.90	-	0.28	0.007	HA
4	9.44	0.028	6.90	-	0.24	0.007	HA
5	9.42	0.007	6.91	0.028	0.45	0.014	HA
6	9.42	-	6.89	-	0.50	0.007	HA
7	9.39	0.010	6.88	0.007	0.24	0.007	HA
8	9.42	-	6.90	-	0.23	0.021	HA
9	9.42	-	6.88	0.014	0.23	0.014	HA
10	9.42	-	6.89	-	0.25	0.014	HA

TABLE 3.23 : XRD parameters of implants - after heating to 900°C

Implant	a-(Å)	S.D.	c-(Å)	S.D.	crystallinity	S.D.	crystal phase
1	9.44	0.014	6.86	-	0.25	0.007	HA
2	9.42	0.007	6.86	-	0.26	0.021	HA + β-TCP + Cao
3	9.42	-	6.86	0.007	0.22	0.014	HA + β-TCP + Cao
4	9.42	-	6.86	-	0.20	0.014	HA
5	9.42	-	6.86	0.007	0.19	0.007	HA
6	9.42	0.007	6.86	-	0.40	0.020	HA
7	9.39	0.014	6.86	-	0.19	0.007	HA
8	9.42	-	6.86	-	0.21	0.007	HA
9	9.42	0.014	6.86	0.007	0.18	0.014	HA + CaO
10	9.44	-	6.86	-	0.25	0.007	HA + CaO

TABLE 3.24 : XRD parameters of human bones- after heating to 650°C

Sample	a- (Å)	S.D.	c-(Å)	S.D.	crystallinity	S.D.	crystal phase
1	9.45	-	6.88	-	0.45	0.014	HA
2	9.45	-	6.89	-	0.46	0.007	HA
3	9.45	0.007	6.90	0.007	0.43	0.014	HA
4	9.43	-	6.88	0.014	0.44	0.007	HA
5	9.40	0.014	6.88	-	0.44	0.007	HA
6	9.42	0.014	6.89	0.007	0.45	0.007	HA

TABLE 3.25: XRD parameters of human bones - after heating to 900°C

Sample	a-(Å)	S.D.	c-(Å)	S.D.	crystallinity	S.D.	crystal phase
1	9.46	0.007	6.90	0.007	0.31	0.007	HA + CaO
2	9.46	0.014	6.89	-	0.27	0.014	HA
3	9.45	0.007	6.88	-	0.26	0.014	HA + CaO
4	9.44	-	6.89	0.014	0.28	0.007	HA + CaO
5	9.42	0.007	6.88	0.007	0.27	0.014	HA + CaO
6	9.44	0.014	6.88	-	0.24	0.007	HA + CaO

Typical XRD scans and lists of d-spacings vs intensity taken after each heating stage for the implants and the bones are given in APPENDIX 4.

3.5 SURFACE REACTIONS (AAS RESULTS)

Linear regression analysis was performed on the values obtained for the calibration curves used in every experiment.

3.5.1 Experiment 13

In this experiment, samples of human forearm bone (radius) were exposed to aqueous NaCl solutions of varying concentration (Table 3.26). The %mass contents for both Ca and Na were determined.

TABLE 3.26 : Ca and Na levels after exposure to NaCl solutions

Solution	NaCl(M)	%Ca	S.D.	%Na	S.D.
1	0.011	20.11	0.18	0.310	0.035
2	0.019	20.02	0.29	0.318	0.024
3	0.100	20.08	0.31	0.330	0.017
4	0.153	19.52	0.20	0.352	0.026
5	0.322	18.48	0.14	0.486	0.009
6	4.967	18.07	0.19	0.530	0.034

3.5.2 Experiment 14

Since the NaCl concentration range between 0.1 and 0.322M produced the most notable effect in Experiment 13 (as observed by changes in the %Ca and %Na in

the samples), it was decided to explore the effect further by exposing the samples to several NaCl solutions within this range (Table 3.27). As in the previous experiment, the levels of Ca and Na in the samples after exposure were determined.

TABLE 3.27 : Ca and Na levels in bone after exposure to NaCl solutions

Solution	NaCl(M)	%Ca	S.D.	%Na	S.D.
1	0.03	19.54	0.26	0.309	0.051
2	0.10	19.41	0.12	0.318	0.029
3	0.15	19.28	0.36	0.348	0.015
4	0.20	18.79	0.30	0.364	0.031
5	0.25	18.85	0.14	0.389	0.027
6	0.30	18.32	0.26	0.456	0.018
7	0.40	18.38	0.27	0.504	0.030
8	1.44	18.25	0.42	0.568	0.017

3.5.3 Experiment 15

Bone samples were placed in aqueous solutions of $CaCl_2$ of varying concentrations (Table 3.28). Only Ca levels were determined in each sample after exposure.

TABLE 3.28 : Ca levels in bone after exposure to $CaCl_2$ solutions

Solution	$CaCl_2$(M)	Ca	S.D.
1	0.01	24.87	0.32
2	0.05	24.21	0.15
3	0.10	24.59	0.26
4	0.20	24.64	0.42
5	0.30	23.91	0.30
6	0.51	24.26	0.18
7	1.70	24.63	0.26

3.5.4 Experiment 16

Since experiment 15 appeared to indicate "saturation", it was decided to repeat the experiment in a lower $CaCl_2$ concentration range (Table 3.29).

TABLE 3.29 : Ca levels after exposure

Solution	$CaCl_2$(M)	%Ca	S.D.
1	$6x10^{-5}$	21.31	0.29
2	$2x10^{-4}$	21.80	0.48
3	$6x10^{-4}$	22.89	0.32
4	$1x10^{-3}$	23.68	0.13
5	$3x10^{-3}$	24.25	0.37
6	$8x10^{-3}$	24.52	0.30

3.5.5 Experiment 17:

In this experiment, implant 1 was exposed to three different $CaCl_2$ solutions and three different NaCl solutions. The levels of Ca and Na are given in Table 3.30.

TABLE 3.30 : Ca and Na levels in implant 1 after exposure to $CaCl_2$ and NaCl solutions

Solution	$CaCl_2$(M)	NaCl(M)	%Ca	S.D.	%Na	S.D.
1	0.0003		37.83	0.14	0.491	0.035
2	0.0007		37.11	0.39	0.436	0.041
3	0.0065		37.15	0.28	0.485	0.022
4		0.20	37.52	0.41	0.476	0.033
5		0.40	37.77	0.28	0.423	0.028
6		1.41	37.42	0.13	0.468	0.016

IAEA-H5 standard and untreated implant (i.e. implant prior to exposure to aqueous solution) were analysed to determine the precision of the results. The Ca and Na levels obtained are given in Table 3.31.

TABLE 3.31: Ca and Na levels in IAEA-H5 std

	%Ca	S.D.	%Na	S.D.
IAEA-H5	21.36	0.38	0.411	0.015
implant	37.75	0.24	0.468	0.031

The reference (literature) values for this standard are given in Table 3.32 (Mah83).

TABLE 3.32 : IAEA-H5 standard reference values

%Ca	S.D.	%Na	S.D.
21.17	2.40	0.477	0.097

3.5.6 Experiment 18

In this experiment, implant 2 was treated as described in Expt.17. The Ca and Na levels are given in Table 3.33.

TABLE 3.33 : Ca and Na levels in implant 2 after exposure to $CaCl_2$ and NaCl solutions

Solution	$CaCl_2$(M)	NaCl(M)	%Ca	S.D.	%Na	S.D.
1	0.0003		36.95	0.48	1.301	0.011
2	0.0007		36.11	0.15	1.306	0.039
3	0.0061		36.07	0.22	1.365	0.029
4		0.20	35.89	0.42	1.392	0.019
5		0.40	36.02	0.26	1.345	0.035
6		1.41	36.14	0.31	1.350	0.022

To monitor precision, the IAEA-H5 standard and untreated implant were also analysed.

Ca and Na levels are given in Table 3.34.

TABLE 3.34 : Ca and Na levels in IAEA-H5 std.

	%Ca	S.D.	%Na	S.D.
IAEA-H5	21.55	0.41	0.455	0.026
implant	37.51	0.25	1.381	0.033

3.5.7 Experiment 19

In this experiment implant 3 was treated as described in the previous experiments.

TABLE 3.35 : Ca and Na levels in implant 3 after exposure to $CaCl_2$ and NaCl solutions

Solution	$CaCl_2$(M)	NaCl(M)	%Ca	S.D.	%Na	S.D.
1	0.0003		32.19	0.26	1.551	0.045
2	0.0007		31.95	0.41	1.496	0.030
3	0.0065		32.15	0.37	1.554	0.041
4		0.20	33.01	0.49	1.520	0.016
5		0.40	32.24	0.31	1.499	0.026
6		1.43	32.56	0.18	1.512	0.025

TABLE 3.36 : Ca and Na levels in IAEA-H5 and untreated implant 3

Sample	%Ca	S.D.	%Na	S.D.
IAEA-H5	21.24	0.22	0.418	0.049
Implant	32.58	0.36	1.531	0.034

3.5.8 Experiment 20:

In this experiment, implant 4 was treated as described in the previous experiments. Table 3.37 gives the Ca and Na levels after exposure to $CaCl_2$ and NaCl solutions.

TABLE 3.37 : Ca and Na levels in implant 4 after exposure to $CaCl_2$ and NaCl solutions

Solution	$CaCl_2$(M)	NaCl(M)	%Ca	S.D.	%Na	S.D.
1	0.0003		31.79	0.35	0.629	0.019
2	0.0007		31.51	0.18	0.678	0.028
3	0.0065		31.42	0.19	0.691	0.025
4		0.20	31.03	0.33	0.618	0.035
5		0.40	31.42	0.31	0.654	0.022
6		1.41	31.89	0.24	0.626	0.013

As previously, precision was monitored by analysis of IAEA-H5 standard and untreated implant 4. The Ca and Na levels are given in Table 3.38.

TABLE 3.38 : Ca and Na levels in IAEA-H5 standard and untreated implant

Sample	%Ca	S.D.	%Na	S.D.
IAEA-H5	21.08	0.28	0.421	0.022
Implant	31.53	0.42	0.695	0.034

3.5.9 Experiment 21:

Implant 5 was used in this experiment. Table 3.39 gives the Ca and Na levels obtained after exposure.

TABLE 3.39 : Ca and Na levels in implant 5 after exposure to $CaCl_2$ and NaCl solutions

Solution	$CaCl_2$(M)	NaCl(M)	%Ca	S.D	%Na	S.D.
1	0.0003		35.92	0.16	0.487	0.021
2	0.0007		35.28	0.39	0.521	0.029
3	0.0065		35.16	0.42	0.533	0.038
4		0.20	36.05	0.25	0.499	0.037
5		0.40	35.63	0.28	0.475	0.031
6		1.41	35.89	0.40	0.509	0.044

TABLE 3.40 : Ca and Na levels in IAEA-H5 and untreated implant 5

Sample	%Ca	S.D.	%Na	S.D.
IAEA-H5	20.96	0.35	0.395	0.026
Implant	36.11	0.38	0.512	0.039

3.5.10 Experiment 22

Implant 6 was used in this experiment.

TABLE 3.41 : Ca and Na levels in implant 6 after exposure to $CaCl_2$ and NaCl solutions

Sample	$CaCl_2$(M)	NaCl(M)	%Ca	S.D.	%Na	S.D.
1	0.0003		33.83	0.44	0.312	0.022
2	0.0007		34.21	0.16	0.331	0.021
3	0.0065		34.15	0.38	0.311	0.034
4		0.20	33.98	0.36	0.342	0.029
5		0.40	34.31	0.40	0.328	0.013
6		1.41	34.10	0.19	0.313	0.027

TABLE 3.42 : Ca and Na levels in IAEA-H5 and untreated implant 6

Sample	%Ca	S.D.	%Na	S.D.
IAEA-H5	21.12	0.34	0.435	0.018
Implant	34.55	0.26	0.341	0.026

Due to insufficient material, no experiments could be performed using implants 7,8, and 9.

3.5.11 Experiment 23

This experiment involved implant 10.

TABLE 3.43 : Ca and Na levels in implant 10 after exposure to $CaCl_2$ and NaCl solutions

Solution	$CaCl_2$(M)	NaCl(M)	%Ca	S.D.	%Na	S.D.
1	0.0003		37.21	0.48	0.095	0.031
2	0.0007		37.39	0.33	0.110	0.050
3	0.0065		37.92	0.24	0.128	0.024
4		0.20	37.11	0.29	0.085	0.039
5		0.40	37.55	0.16	0.112	0.036
6		1.41	36.98	0.34	0.108	0.029

TABLE 3.44 : Ca and Na levels in IAEA-H5 and untreated implant 10

Sample	%Ca	S.D.	%Na	S.D.
IAEA-H5	21.39	0.21	0.418	0.030
Implant	36.71	0.15	0.106	0.024

4. DISCUSSION

4.1 X-RAY DIFFRACTOMETRY

4.1.1 Implant samples

A] Crystal phase

As mentioned in the RESULTS section, all the implants were found to be hydroxyapatite. The possible presence of β-TCP, otherwise known as whitlockite, was investigated as other workers have reported its presence in lower concentrations alongside the hydroxyapatite phase (Sob49,Wan86). However, no traces of this phase were found in any of the samples. The spectra were also inspected for the presence of intensity enhancements due to the possible inclusion of calcite (Sil86,SilX). Common reflections in the calcite and hydroxyapatite spectra are given in Table 4.1.

TABLE 4.1 : Common reflections in calcite and hydroxyapatite

d	Calcite intensity(%)	d	HA intensity(%)
3.04	100	3.08	18
2.50	18	2.53	6
2.28	23	2.26	20
2.09	20	-	-

It is seen that the presence of calcite might be detected by enhancement of the reflection in the apatite spectrum at a d-spacing of 3.08Å. The relative intensities of this reflection in the ten implant samples are given in Table 4.2.

TABLE 4.2 : Intensities of reflection at d=3.08Å of the implant materials

1	2	3	4	5	6	7	8	9	10
19.20	28.95	25.85	18.00	25.55	22.90	21.70	22.40	18.77	18.25

Although implants 2,3 and 5 appear to show an increased intensity, caution must be exercised in interpreting this as being indicative of calcite inclusion as no mention is made in the literature of the extent to which intensity enhancement might be expected. Moreover, none of the samples displayed a peak at d=2.09Å, which is exclusive to calcite (Blu75,Sil86), relative to HA. Thus, if calcite is indeed present in the samples mentioned, it can only be in very low quantities.

B] Cell parameters and crystallinity

The inorganic portion of teeth and bones is basically "impure" calcium phosphate occurring predominantly in crystalline form as "biological apatite" (LeGeX,You75). The inorganic component of bones comprises 75% of the entire structure. Various substitutions may take place within this structure which can be manifested by changes in the lattice parameters (a- and c-axes) of the apatite

depending on the size of the substituting cation or anion (Tra55, Pos63, Mco65, LeGe69, LeGe80, Tra85). The incorporation of one such cation, namely carbonate, has been the subject of study and speculation for more than three decades (LeGe57,Mco60,LeGe65,LeGe67, LeGe69,LeGe83). Despite this, uncertainty still prevails over the mode of incorporation of carbonate into the apatite structure. For example, Eitel first proposed a CO_3-for-OH substitution in the apatite structure (LeGe69). In such a substitution, the planar CO_3 group is larger than the OH group and an expansion of the unit cell of the apatite would be expected (Meo65,LeGe69,LeGe80,LeGe81). However, LeGeros and Trautz (LeGe67,LeGe68) have presented evidence showing that CO_3 substitutes for PO_4 in the apatite structure. If this is indeed the case, then such substitution would be accompanied by a contraction of the unit-cell, since the planar carbonate is smaller than the tetrahedral PO_4 group it replaces. This is because the O-O distance in a CO_3 group is 15% smaller than the O-O distance in a regular PO_4 group (LeGe67). McConnell (Mco65) also supports the theory of carbonate for phosphate substitution in the apatite structure of both the mineral carbonate apatites (e.g. Dahllite, Staffelite, and Fancolite) as well as in the calcified tissues of teeth and bone. According to McConnell, four flat CO_3 groups replace three tetrahedral PO_4 groups, so that one CO_3 group is located on the trigonal axis of the crystal, while the other three CO_3 groups are located vertically around the axis (Mco65,Tra85). This is said to occur in hexagonal structures (LeGe67,LeGe68,Tra85), of which all the samples tested in this study are an example. Furthermore, when carbonate is included in the apatite structure, a corresponding decrease in the amount of phosphate has been observed (LeGe65,LeGe67,LeGe68). This has been shown to occur even when all OH-groups were replaced by F^- in the structure, rendering OH sites unavailable for CO_3 substitution (LeGe67). A recent report by LeGeros (LeGe81) presents a final compilation of the mode of carbonate substitution: In synthetic apatites, there can occur either, CO_3-for-OH substitution (in which case there is an expansion of the

a-cell parameter), or CO_3-for-PO_4 substitution, which is accompanied by cell size changes already discussed. The former mechanism has been observed in apatites obtained from non-aqueous systems (at temperatures around 1000°C), and the latter from aqueous systems (temperatures around 100°C) (LeGe69,LeGe81). In apatites of natural origin, however, it seems that CO_3-for-PO_4 substitution is the favoured mechanism (Hir47, LeGe57, LeGe68, Blu81, LeGe81).

To determine which type of substitution is prevalent in the implant materials tested in this work, the unit cell parameters were calculated according to the method outlined on p.18 of this study. Measurements determined by Elliott et al (Ell73) will be used as reference values. His studies were performed on Holly Springs hydroxyapatite, which is considered to be "carbonate-free". These cell dimensions are as follows:

a = 9.4214(8) Å and

c = 6.8814(7) Å

(The values in brackets are the standard deviations).

These values may be compared with those obtained in the present study for the ten implant materials. Values of these parameters are given in Table 3.1, p.52. Implants 1 to 6 have a-cell parameters which are greater (maximum difference 0.21%) than that of HA tested by Elliott while samples 7 to 10 lie close to the reference value. The c-cell parameters do not differ significantly from the reference value, and this is to be expected, since according to McConnell (Mco65), effects of substitutions manifest themselves more in terms of a-cell sizes than c-cell sizes. Perhaps then, implants 1 to 6 have a CO_3-for-PO_4 mode of substitution, while samples 7 to 10 favour a CO_3-for-OH mode of substitution.

In retrospect, it may be said that the scanning speed used (2°/min) was perhaps somewhat too fast to ensure accurate lattice parameter and crystallinity measurements.

However,this is a very tentative suggestion, since according to studies performed by R.Z. Le Geros et al (LeGe65,LeGe67,LeGe81), the increase in a-cell sizes can also be attributed to the possible presence of chlorine ions substituting for OH, as well as HPO_4^{2-} substituting for PO_4^{3-} in these structures. These substitutions cause a lengthening of the a-cell parameters, overriding any shortening effects that may be prevalent due to CO_3-for-PO_4 substitution also present in the structure.

Other substituents and their influences have been reported. These include:

i) incorporation of fluoride substituting for OH groups causes a shrinkage in a-cell size, and no change in c-cell size (Pos63,Mco65,LeGe87);

ii) cations larger than Ca^{2+}, such as Sr^{2+}, Pb^{2+}, and Ba^{2+}, can be incorporated in the apatite structure to a greater extent than those which are similar or smaller in size, such as Na^{+}, Mg^{2+}, and Zn^{2+} (LeGe80,LeGe84). If the cation is larger than Ca^{2+}, then the lattice parameters expand after incorporation, and vice versa with the smaller cations.

iii) substitution of H_2O-for-OH groups causes an expansion of the a-cell parameter. This incorporation may be accompanied by the substitution of H_4O_4-for-PO_4, also causing an expansion in the a-cell parameter (Mco65,LeGe78,LeGe84).

Unfortunately, the simultaneous or concerted substitutions of different ions in apatites cause additive or conflicting effects on the physico-chemical properties of the apatite (LeGe84). Therefore, it cannot be ascertained merely from the cell-parameters which mode of substitution is present.

The question of whether any CO_3-for-PO_4 substitution occurs in the implant materials, can be further addressed, albeit tentatively, from the separation of the peak intensities of the 112 and 211 maxima (LeGe65, LeGe67,LeGe69,LeGe80). According to LeGeros (LeGe65,LeGe67), the higher the % mass content of CO_3 in the apatite, the less is this peak separation. Fig.4.1 shows the 112 and 211 separations for the ten implant materials.

Fig 4.1 - Separations between the d_{112} and d_{211} peaks

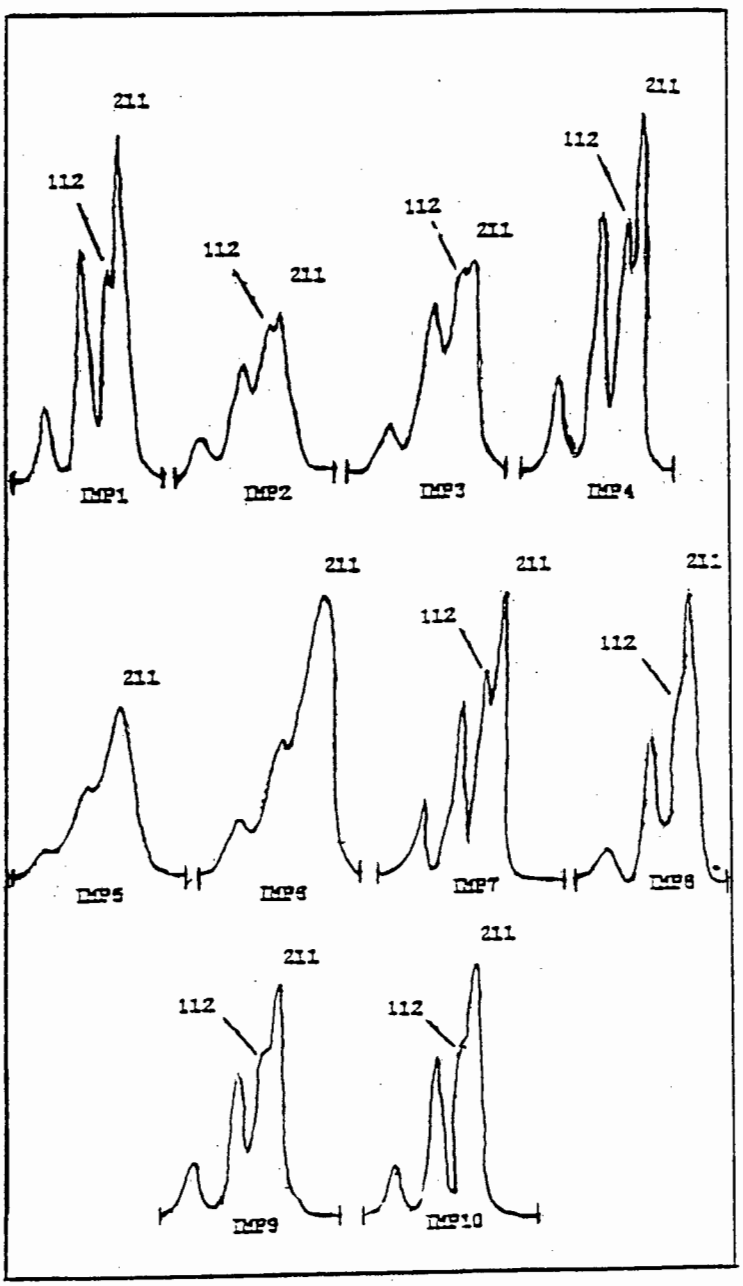

From Fig. 4.1, it is seen that samples 4 and 7 display the most marked separations of the 112 and 211 peaks. Samples 5, 6 and 8 do not display such separations i.e. their 112 and 211 peaks have become superimposed. This occurs as a result of broadening of the diffraction maxima, (i.e. a decrease in degree of crystallinity) which could be caused by the presence of carbonate (Sob49,Mco65,LGe68,LeGe80,Blu81,LeGe81). Both McConnell (Mco65) and LeGeros (LeGe68) state that once CO_3^{2-} is incorporated, the degree of crystallinity of the sample decreases. Therefore, the higher the suspected carbonate content of a sample, the lower will be its relative degree of crystallinity. Accordingly, implants 5, 6 and 8 are expected to have the highest carbonate content which would be reflected by their relatively low crystallinity values. On the other hand, implants 1, 4 and 7 (all of which displayed marked separations of the 112 and 211 reflections) are expected to have the lowest carbonate content which would be reflected by relatively high crystallinity values. Inspection of Table 3.3, p.53, indicates that the results of the present study confirm this prediction. It is seen that samples 1,4 and 7 do indeed display relatively small peak widths (0.34, 0.35 and 0.39 respectively) indicating a high degree of crystallinity, while samples 5,6 and 8 display relatively large peak widths (0.48, 0.58 and 0.51 respectively) indicating a low degree of crystallinity.

The other implant samples are in an intermediate range, as expected. It seems that on a relative basis, the samples differ with respect to their degree of crystallinity, and that this might be attributed to possible differences in carbonate contents. However, carbonate is only one of the many substituents which can influence the crystallinity of a sample. For example, the presence of magnesium, potassium or fluoride can have conflicting influences upon the crystallinity of the apatite, depending upon the quantity incorporated (LeGe84). Thus, a correlation between the crystallinity values obtained by the above technique and $\%CO_3$

values obtained from infrared data could lead to a meaningful conclusion. This will be discussed later in this chapter (p.104).

4.1.2 Bone samples

A] Crystal phase

As with the implant materials, the bone samples were found to be hydroxyapatite. According to Hirschman et al (Hir47), bone containing normal levels of PO_4 have HA as the main crystal phase present, with no traces of β-TCP. The spectra of the present study were inspected in the 2 region around 31,35 and 37 degrees, where β-TCP gives rise to high intensity peaks (100, 55 and 25% respectively) (Joi72,LeGe81). However, no β-TCP was detected. the spectra were also examined for CaO since this substance has been previously identified in bone (LeGe81,Sil86). Indeed, a peak at d=2.34Å was found in each of the bone samples, their intensities varying around the 10% value, thus suggesting traces of CaO in the bone samples.

Finally, an investigation for the presence of $CaCO_3$ was performed as for the implant materials. The intensity of the peak at d=3.08Å was studied (Table 4.3).

TABLE 4.3 : List of intensity at d=3.08Å of bone samples

1	2	3	4	5	6
22.13	23.23	22.64	26.62	25.33	20.71

The enhanced intensities would suggest that $CaCO_3$ might be present, but as with the implants, no trace of a peak at d=2.09 (which is exclusive to calcite) was detectable. Hence, only very low quantities of $CaCO_3$ can be expected in these bone samples, if at all.

B] Cell parameters and crystallinity

The cell parameters of the six bone samples were calculated using the same relationships as those for the implant materials and are listed in Table 3.2,p.53.

Comparison of these values to those of "pure" HA, shows that the a-cell parameters are larger in the bone samples. This may be attributed to CO_3-for-OH substitution or otherwise a CO_3-for-PO_4 substitution (shortening of a-axis) is being masked by the effects of "lattice H_2O" present, Cl-for-OH and other concerted substitutions of larger cations (LeGe78,LeGe81).

c-Cell parameters in some of the bones are slightly smaller than that of Holly Springs HA (Mac72,Ell73). However, both CO_3-for-OH substitution and the concerted substitutions which may accompany a CO_3-for-PO_4 substitution cause c-cell parameter reduction, so that again, no conclusion can be made as to which mode is favoured here.

Crystallinity values, (Table 3.4, p.54), show that the bones displayed lower degrees of crystallinity (i.e. broader peak-widths of 002 reflection) than the implant materials. Closer examination reveals that samples 1 and 4 have the narrowest 002 peak widths, indicating highest crystallinty relative to the other bone samples. Yet, even though these are the narrowest peak widths found among the bones, the narrowest values found for the implants were in the region of 0.35 °2θ . This is expected, as results reported by LeGeros (LeGe81) noted the tendency of bone

to display very much broader peaks than those displayed by apatite in enamel or dentine. As before, this can be substantiated by addressing the peak separation between the 112 and 211 reflections. Fig.4.2 presents the relevant peaks for each sample.

Fig.4.2 - d_{112} and d_{211} separations for bone samples

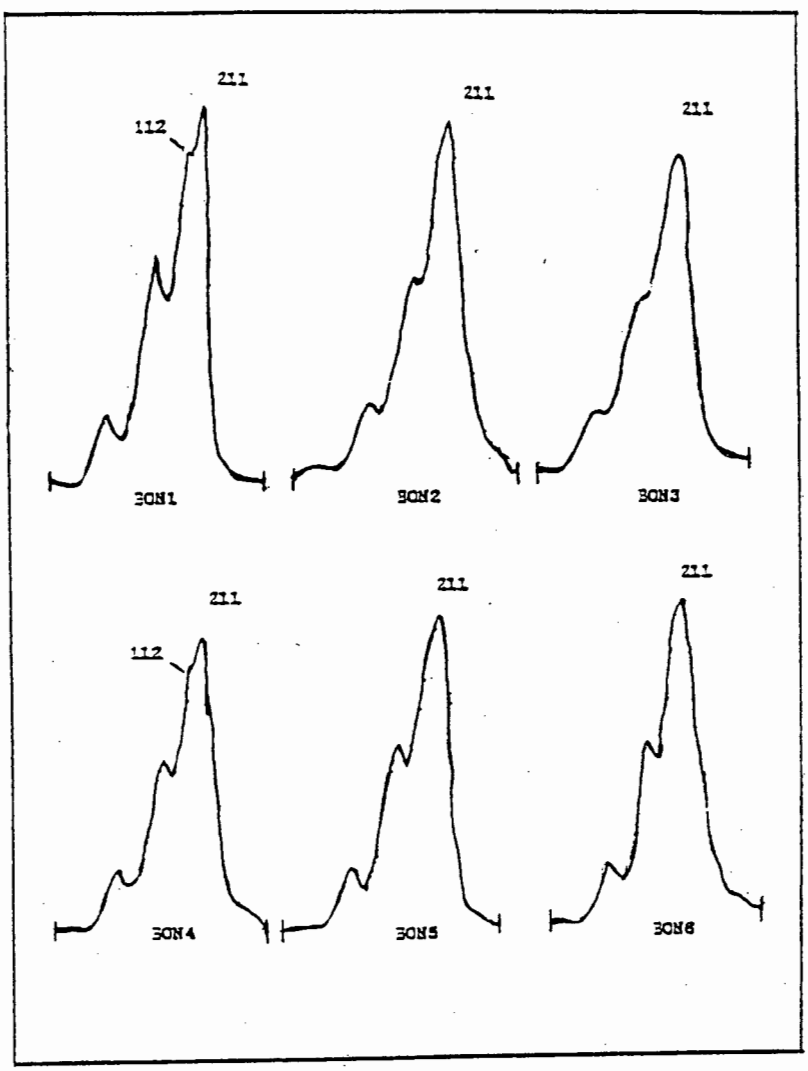

From these spectra it can be seen that only samples 1 and 4 display small shoulders on the 211 peaks due to the 112 reflections. The other samples have no trace of a peak due to 112 reflection at all. If the principles of CO_3 contents, already outlined in the discussion of the implant materials, are applied, then it would seem that samples 1 and 4 have slightly lower CO_3 content than that of the others. Generally, however, the peaks of the bone samples seem to be slightly broader and less separated than those of the implant materials, which would confirm a lower degree of crystallinity for the bone samples. Whether this could indeed be attributed to a higher content of CO_3 or not, will perhaps become more apparent when the results of the infra-red studies are considered.

4.1.3 Summary

It seems as if both the implants and the bone samples are composed of hydroxyapatite crystals, with the difference being that the bones have trace amounts of CaO present. In both groups of samples, no trace of calcite appears to be present. When compared to Holly Springs hydroxyapatite, the a-cell parameters of some of the implants were found to be 0.21% greater. However, only bone sample number 4 had its a-cell parameter equal to that of Holly Springs apatite; the remainder all displayed slightly increased a-cell sizes. It appears that the c-cell parameters of implants and bones are similar to those of the reference material. Because the manifested changes in a-cell sizes of most implants and bones are not very great, it is assumed that if any impurities are present, they occur in very small quantities.

Generally, the relative degree of crystallinity of the implant materials was found to be higher than that of the bones, reflecting a decreased crystallite size and/or

increased crystallite strain for the bone (LeGe81), partly attributable perhaps, to a higher CO_3 content in the latter.

4.2 ICP

4.2.1 Implant materials

In natural hydroxyapatite, the Ca/P ratio has been found to be 1.67 (Mco65,Sil86). Any departure from this value may be assigned to substitutions occurring, amongst others, for either Ca or PO_4 in the structure. For example, if there is CO_3 substituting for PO_4, the ratio will increase. On the other hand, if there are ions such as Na^+ or Mg^{2+} substituting for Ca^{2+}, then the ratio will decrease. The Ca/P ratios can then be compared with powder diffraction results, since crystallinity may be regarded as an indication of the extent of CO_3 in the structure.

Consideration of the Ca/P ratios for the implants in the present study (Table 3.6, p.56), reveals that only sample 4 has a value below that of hydroxyapatite. While this may be due to CO_3 substituting for PO_4, other substitutions might explain this. For example, Table3.5, p.55 shows that sample 4 has the highest level of Mg^{2+}, and a relatively high level of Na^+. Thus, these elements may be substituted for some of the Ca^{2+} in the crystal, thereby decreasing the Ca/P ratio of the sample.

Implant number 3 has a Ca/P ratio (1.79 ± 0.03) which is below the average for all the samples (1.94 ± 0.14). Although the Mg level in this implant is relatively low ($5.04 \times 10^{-4} \pm 0.0025\%$), the value for Na ($1.80 \pm 0.017\%$) is the highest of all. Thus implant 3 might be exhibiting a greater extent of Na-for-Ca substitution than the other implants, thereby reducing the Ca/P ratio below the average. However, CO_3-for-PO_4 substitution might well be present, as in implant 4, which would explain its inflated Ca/P ratio relative to natural hydroxyapatite.

The remainder of the implants have Ca/P ratios which are similar to each other. These values are above 1.67 and could thus possibly be attributed to CO_3-for-PO_4 substitution, as indicated by the XRD findings, p.84.

Sr^{2+} has been found to substitute for Ca^{2+} in synthetic apatites causing an expansion in both c- and a-axis dimensions (LeGe80,LeGe84,Sil86). In the present study, samples 9 and 10, which are of synthetic nature, were found to have the highest Sr^{2+} levels of all the implants, but have very small a-axis dimensions. This demonstrates that there may be several substitutions occurring each with overriding effects and that no one effect can be clearly identified.

From the above argument, it may be stated that the values of %mass contents for the remaining minor elements obtained in this study merely serve the purpose of identifying their presence within the apatites, and conclusions as to their effects on cell parameters cannot be argued.

Comparison of the published reference values for the animal bone standard IAEA-H5 (Mah83) with those obtained for the standard in this study (Table 2, APPENDIX 2), shows that there is good agreement, thereby lending confidence to all of the above findings.

Finally, Mg/Ca ratios were calculated for the implants and are listed in Table 3.6, p.56. Values for all samples are very low again as a result of the high Ca levels (all implants) and in some cases very low Mg levels (implants 2,3,7 and 8). Comparison of these values with the Mg/Ca ratio obtained for the IAEA-H5 standard of Mahanti and Barnes (0.013 as calculated from Table 2, APPENDIX 2), shows that only samples 1 and 4 approximate this value while the remainder are

much lower. This further serves to illustrate an apparent fundamental chemical difference between the implants and the reference bone.

4.2.2 Bone samples

In order to determine whether there is any variation in the chemical composition of bones originating in different regions of the body, as well as within any one individual bone itself, statistical analyses were performed. A variance component model was used in which the regions, sites and analyses were considered as random choices from a population, and are thus considered as random effects with a certain distribution.

The model may thus be regarded as a three factor experiment with the region factor used at 6 levels, a site factor used at 2 levels, an analysis factor at 2 levels and 3 repeated measurements (made on the 6*2*2 combination of region, site and analysis).

The observations may be represented by:

Y_{ijkl} where i = 1 to 6
j = 1, 2
k = 1, 2
and l = 1, 2 ,3

Thus, "i" denotes the level of the region, "j" the level of the site, "k" the level of the analysis, and "l" used for the repeated measurements.
The final model is as follows:

$$Y_{ijkl} = \mu + \alpha_i + \beta_j + \delta_k + \gamma_{ij} + \nu_{ik} + \xi_{jk} + \vartheta_{ikj} + \epsilon_{ikjl}$$

where α_i, β_j, δ_k, γ_{ij}, ν_{ik}, ξ_{jk}, ϑ_{ijk}, ϵ_{ijkl} are all uncorrelated and

$\alpha_i \sim (0, 6^2 \text{ region})$ $\beta_j \sim (0, 6^2 \text{ site})$ $\delta_k \sim (0, 6^2 \text{ anal})$

$\gamma_{ij} \sim (0, 6^2 \text{ region x site})$ $\nu_{ik} \sim (0, 6^2 \text{ region x anal})$ $\xi_{jk} \sim (0, 6^2 \text{ site x anal})$

$\vartheta_{ijk} \sim (0, 6^2 \text{ region x site x anal})$ $\epsilon_{ijkl} \sim (0, 6^2_e)$

The parameters represent the variances due to the main effects of region, site and analysis, the two-way interaction between the main effects and the three-way interaction between the main effects. Thus a figure was obtained for the variation component, which simply is the percentage variation between the effects specified respectively. In other words, if the "varcomponent" value for a specific set of main effects is low, it signifies low variance in values between the two effects. The results for the various effects are given in Table 4.4:

TABLE 4.4 : Varcomponent percentages

Effect	Ca	P	Mg
Region	12.5	14.0	0.0
Site	27.6	34.2	0.0
Region*site	43.2	46.1	37.0
Analysis	0.0	4.0	0.0
Region*analysis	1.4	0.0	0.0
Site*analysis	8.6	1.0	0.0
Region*site*analysis	4.5	0.5	62.0
Reading	2.2	0.2	1.0

Only the major elements were used in the model since far greater variations were expected to occur in the values of the minor elements as a result of these being present in quantities close to the detection limits of the instrument. Moreover, for simplicity sake, it seemed wiser to study only the main elements, since much of the discussions in texts have centered around these.

It can be seen from Table 4.4 above, that the varcomponent% value of the reading effect is very small in all three elements. However, the same is not true for the region, site, and region*site effects, which in calcium and phosphorus contribute 83.3% and 94.3% respectively towards variation in the measurements in those elements. This implies that calcium and phosphorus levels vary to a large extent from one site to the next within the same bone, but that this variation is not significant since the error (Table 5, APPENDIX 2) is larger than the variance component itself. Ideally, one would need a larger sample size to decrease the error component to a value below that of the variance component and determine whether site-to-site variation is then still insignificant. However, in the present study it is assumed that technique error causes the site-to-site variation to be insignificant.

In magnesium, the three-way interaction percentage (Region*site*analysis, Table 4.4) is very high and the one outlier in the results of Mg levels (Table 4, APPENDIX 2) could well be the cause.

The second part of the statistical evaluation involved combining the two sites of each bone into one average reading. The aim of this was to determine the degree of variation within bones from different regions of the (same) body without the variation of the sites interfering and distorting the results. The model used in this case was as follows:

$$Y_{ijk} = \mu + \alpha_i + \beta_j + \gamma_{ij} + \epsilon_{ijk}$$

i=1,...,12 (11 for Mg as outlier ignored)

j=1,2

k=1,2,3

where

μ is the overall mean effect

α_i the effect of the i-th sample, β_j the effect of the j-th analysis, and γ_{ij} the effect of the i-level and j-level of the sample and analysis. E_{ijk} represents the error of the readings.

Table 4.5 lists the findings.

TABLE 4.5 : Varcomponent percentages

Effect	Ca	P	Mg
Sample	83.1	94.5	72.0
Analysis	0	4.1	5.6
Sample*analysis	14.7	1.2	20.0
Reading	2.2	0.2	2.4

For all three elements there is a significant variation component, calculated at 95% confidence level (Est $\pm$1.96 Std.Error). In Ca the analysis component is estimated as zero and in P and Mg it is not significantly higher. However, the interaction of the analysis and sample components shows that there is a significant variation, comprising 14.7% of the total variation in Ca, only 1.2% in P, and 20% in Mg. It is thus concluded that only phosphorus seems to yield very consistent estimates of the element concentration over a number of samples. The variations of 20% in Mg and 14.7% in Ca are substantial components that will cause inconsistencies in the element concentration determinations. The error throughout the three readings taken for each element is small, with P again the most consistent.

These analyses indicate that the error component found within bones from different regions of the body is high but only partly (12%) attributable to experimental error. Also, the error component from one analysis of a specific site on a bone to the next (Table 4.4) is high and greatly attributable to experimental error. This would imply that concentrations of the elements tested across the surface of a bone do not differ significantly, but that concentrations in bones from different regions do. This is the reason for having combined values of the two sites per bone sampled and merely compared the bones of the different regions to one another (Table 4.5), and having found them to differ significantly.

While these results are of great interest, it must be mentioned that other factors such as nutrition and degre of exercise, for example, play a significant role in the nature of bone. To have sampled bones from several bodies was outside the scope of this study, but would have made the statistical evaluation far more meaningful. The fact that there are indeed significant differences in the chemical constitution of bones from different parts of the body of the one cadaver studied, would certainly warrant future investigation into this area.

The final values for each bone (taken from an average of the values of the two sites) are listed in Table 3.12, on p.60. Based on the above findings, it is therefore not surprising that the Ca levels in the various bones are different to that given by Mahanti and Barnes (Mah83) of 27.10% (±0.30%) (Table 3, APPENDIX 2). However, the Ca value for the reference standard IAEA-H5 animal bone was found to be 19.72% (±0.34%), which compares favourably with the published value (Mah83) of 21.17% (±2.40%).

The difference between the Ca value in this study and that obtained by the authors mentioned, might be attributed to the factors already mentioned which influence the chemical constitution of bones from one individual to the next. The fact that the Ca value of the standard determined in this study agrees well with the published value lends confidence to the results.

4.2.3 Final comparison

Consideration of Ca/P ratios of implants and bones, it is seen that the latter exhibit much higher values, even though the implants have higher Ca levels. As already mentioned, the reason for this could be that there is CO_3^{2-} substituting for PO_4^{3-} in the bones, depressing the phosphorus levels and causing higher Ca/P ratios. It has already been established from powder diffractometry and infra-red studies that the bones do have higher carbonate contents than the implants, and this latest finding serves to substantiate those results.

The Mg/Ca ratios of the bones also appear to be higher than those of the implants, perhaps signifying greater substitution of Mg^{2+} for Ca^{2+} in the former. However, if this were true, decreasing levels of Ca^{2+} in the bones should be observed. Since this is not the case, it is suggested that the amount of CO_3^{2-}

substituting for PO_4^{3-} is so great in the bones that it offsets any decreases of calcium in the structures. This would further confirm the other results obtained in the present study where the bone samples were found to have greater amounts of included carbonate. Moreover, it would also explain the lower Ca^{2+} levels in the bones when compared to the implants.

Another factor which emerges from the comparison of the %mass content values for the implants and the bones, is that the levels of strontium are higher in the former. This is especially true for implants 9 and 10, which exhibit the highest levels of all. However, this seems to be a feature of synthetic implant materials (LeGe84), which these two samples indeed are.

Thus, it can be said that the bones seem to differ significantly in chemical make-up from region to region in the body (for the one subject studied) and that they also differ from the implants with respect to characteristics such as Ca/P and Mg/Ca ratios.

4.3 INFRA-RED SPECTROSCOPY

4.3.1 Spectra assignments

Infrared absorbtion spectra of hydroxyapatites are characterized by vibration bands produced by OH, PO_4, and CO_3 groups (HasX,LeGe69, LeGe81). The vibrational band due to the OH group was found to occur around 3400cm^{-1} (with a smaller peak at ~1640cm^{-1}) for the implants as well as for the bone samples and was a very prominent feature on all the spectra. This compared favourably with reported results of hydroxyapatite infrared studies (Bad66,LeGe68,LeGe81).

The CO_3 vibrational modes are given the symbols v_1,v_2,v_3, and v_4, according to LeGeros (LeGe81).

Two features were immediately obvious in implant- and bone-spectra:

i) the band at 1495cm^{-1} v_4, which is attributed to surface and amorphous carbonate (HasX), was not detectable; and

ii) the asymmetric stretching mode in the region 1450 to 1500cm^{-1} was split into two bands for implants and bones.

According to LeGeros and Trautz, the greater the carbonate content of a sample, the stronger and more resolved will be the doublet at 1450cm^{-1} (LeGe68,LeGe81). The fact that this doublet is present in both the implants and the bones would imply that both contain CO_3. However, in the bone spectra, the bands are wider and generally more prominent than in the implant spectra, possibly implying a higher content of carbonate for the bone samples. Comparison of this band's shape as obtained in bone and implant spectra with

those published in the literature (Fig 4.3), (LeGe68), shows that the bone spectra of the present study resemble those of biological apatite (spectrum C in Fig.4.3) more than do those of the implants, while the latter resemble the spectrum obtained for synthetic apatite. Since the latter contain CO_3-for-OH substitutions, it seems reasonable to suggest that the same substitutions may be present in some of the samples of the present study. This would explain the increase in a-cell size in implants 1 to 6 Table 3.1, p.52.

Fig 4.3 - Published spectra for apatites

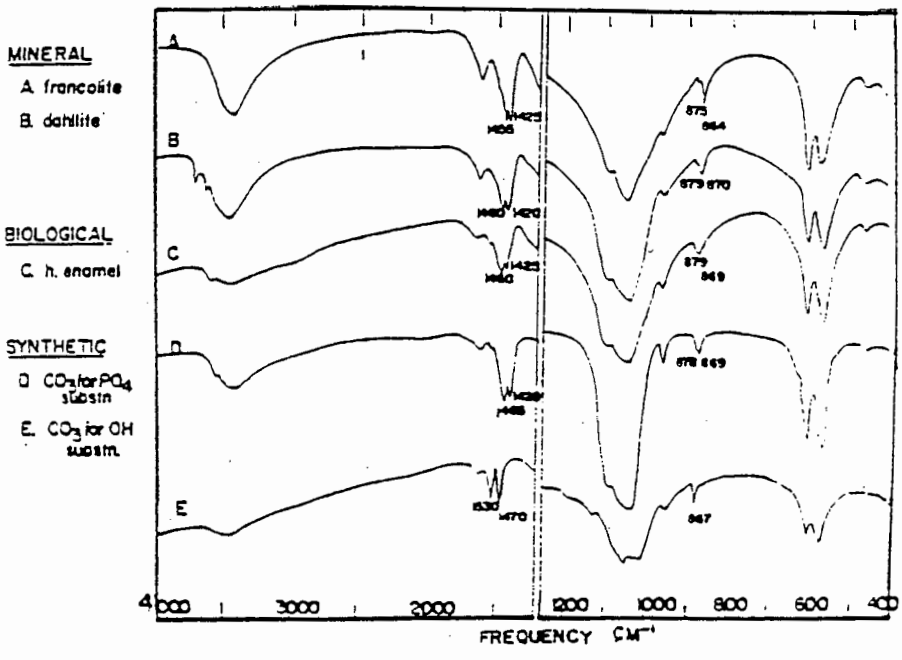

Another interesting aspect of all the spectra is the band, v_2, for CO_3 in the region 860 to 880cm^{-1}. According to LeGeros(LeGe81), the appearance of such a band is usually in the form of an anomalous doublet for apatites and indicates the presence of CO_3^{2-} in two different environments. These environments, as already outlined in the introduction, p.34, are defined as carbonate partially adsorbed and partially in the lattice as a substituent for either OH^- and/or PO_4^{3-}. Under the experimental conditions, the doublet was not actually resolved, the maximum absorbtions only being visible at ~875cm^{-1}.

However, it should be stated that if the organic phase of bone is present, as in this case, the absorption bands due to N-H group overlaps with the CO3 absorption. Thus a certain element of error might be present in the results of the bone samples.

The amount of carbonate incorporated in the structures is said to be directly in relation to the loss of resolution of the PO_4^{3-} absorbtion bands, v_4, in the region 560 to 600cm^{-1} (HasX,LeGe68,LeGe81). However, inclusion of carbonate also has an effect on the crystallite size of the sample (LeGe81) and this will influence the spectra in a similar manner. Nevertheless, it can be seen from the spectra that the bones have less well-resolved PO_4^{3-} bands than do the implants. In some implants a band occuring as a shoulder (at ~630cm^{-1} on the PO_4^{3-} bands can be identified.

According to LeGeros and Trautz (LeGe68), this band is assigned to the OH group and only occurs in more crystallized samples. This band seems to be absent in most bone samples of the present study, with only one or two displaying a broadening of the base of the PO_4^{3-} band. This would be a factor confirming that implants have less carbonate within their structures than do the bones, since less carbonate causes higher crystallinity, resulting in the appearance of this OH band.

It appears, from the spectra for both implants and bones, that the band in the region 900 to 1200cm^{-1} due to PO_4^{3-} group mirrors any spectral shape changes imposed on the PO_4^{3-} bands at around 600cm^{-1} when crystallinities are altered. Therefore both these bands appear to be useful in determining qualitative contents of carbonate in the samples.

For the implants, samples 1 and 9 have the sharpest PO_4^{3-} bands, (i.e. those at around 600cm^{-1} as well as around 1100cm^{-1}). Similarly for the bones, it is sample 6 which has the sharpest PO_4 bands, perhaps signifying lowest carbonate contents for all of these.

Therefore, as a result of the difference in resolution of the PO_4^{3-} bands and the fact that carbonate bands are present in all the spectra, it would seem that there are varying amounts of CO_3^{2-} within the implants and bones. The fact that the PO_4^{3-} bands at around 600cm^{-1} and around 1100cm^{-1} are less well-resolved for the bones than for the implants, suggests possible higher levels of carbonate in the former. Furthermore, the appearance of the OH band at around 630cm^{-1} for the implants would further substantiate the hypothesis that the implants contain less carbonate than the bone counterparts.

4.3.2 $\%CO_3$ Levels

From Tables 3.17 and 3.18 on p.64 and 65, it is immediately obvious that the carbonate levels of the bones appear to be higher than those of the implants.

Consideration of the implants individually, reveals that $\%CO_3$ values appear to be similar except for numbers 8 and 9, where lower values are manifested by sharper PO_4^{3-} bands. Similarly bone sample 6 appears to display lowest $\%CO_3$ levels, again confirmed by the sharpest PO_4^{3-} bands. Thus it would appear that the theory concerning the resolution of the PO_4^{3-} bands (HasX,LeGe68,Sil86) in the spectra of both types of samples agrees well with the findings of carbonate levels, thus lending confidence to the technique of carbonate-determination by the use of standards as outlined by Featherstone and LeGeros (Fea84).

4.3.3 CO_3/PO_4 Ratios

These are given for the implants and the bones in Tables 3.19 and 3.20 respectively on p.66.

Other bands in the bone samples shown in Appendix 3 were not assigned but some of these are due to the organic component.

Consideration of CO_3/PO_4 ratios shows that large errors are involved which lends a degree of uncertainty to the results. These errors might have emerged as a result of possible inaccurate estimation of the base of the relevant absorbtion band.

The CO_3/PO_4 ratios for the bones and implants did not differ as much as might have been expected on the basis of their different CO_3 contents. However, the values obtained for both sample-types appear to be in the correct "range" when compared with published values (Are75), Table 4.4. Therefore, the results of this part of the study should not be viewed as absolute but rather as indicative of *trends* concerning carbonate contents. The CO_3/PO_4 ratio study thus confirms a trend towards lower carbonate contents in the implants relative to the bones, thereby lending the bones a less crystalline nature.

TABLE 4.4 : Values of CO_3/PO_4 from reference experiments(Are75)

CO_3/PO_4	S.D.	$\%CO_3$ by mass	S.D.
0.300	0.006	4.43	0.05

The values given in Table 4.4 were obtained for sound bovine enamel pooled from four teeth.

The Infra-red technique was found to be successful as it met the objectives of this part of the study:

i) bands were assigned to their respective groups;

ii) the $\%CO_3$ contents were calculated for the implants as well as the bones;

iii) CO_3/PO_4 ratios were calculated and trends correlated with $\%CO_3$ results; and

iv) the findings were found to correlate well with results of XRD.

4.4 THERMAL DECOMPOSITION

In discussing the results of this experiment, reference will be made to the tables of diffraction maxima obtained after heating (APPENDIX 4).

4.4.1 Water loss

When heating a sample such as apatite, the first component to be eliminated from the structure is water (LeGe78,Bar84). Recent studies have demonstrated that there are two types of water present (LeGe78,Hol80, LeGe81,Bar84):

i) "adsorbed H_2O";
ii) "lattice H_2O".

The adsorbed water is reversible, that is, once lost due to heat, it can readsorb upon cooling (e.g. from atmosphere). The loss of this water has no effect upon the cell parameters (LeGe81). However, lattice water, which is due to H_2O-for-OH and/or HPO_4-for-PO_4 substitution, when lost, does influence the cell parameters by causing a contraction in a-axis dimension (LeGe78,Hol80).

Inspection of the masses lost upon heating (Table 3.21, p.67), shows that for the implants, the %losses up to 200°C were of the order of 1.50%. This would suggest the presence of adsorbed water. Figs.4.4 and 4.5 demonstrate typical curves of mass loss vs temperature for implants and bones respectively. There was only slight variation in the amount of water lost from implant to implant, with the notable exceptions of implants 7 and 10, which exhibited the lowest losses. It would seem thus, that the implants are relatively similar with respect to their capacity to hold

water on the crystal surface, with samples 7 and 10 having the lowest such capacity.

Fig.4.4 - Typical %mass loss vs temperature curve for the implants

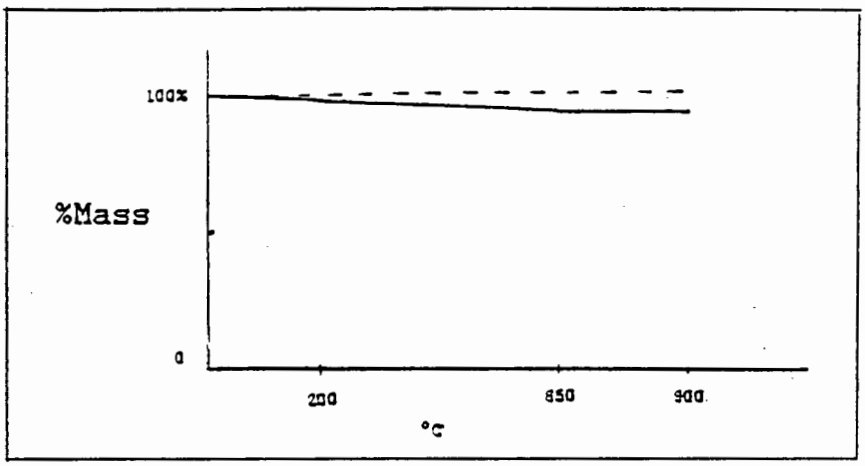

Fig.4.5 - Typical %mass loss vs temperature curve for the bones

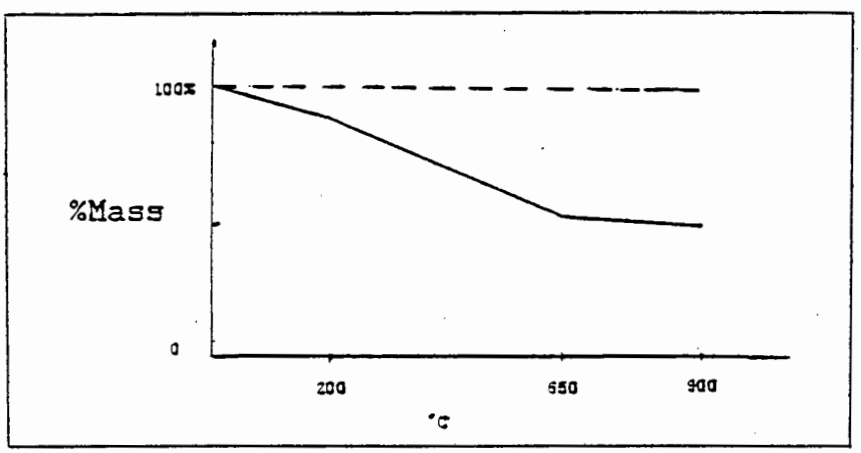

In the bones, however (Fig.4.5), the %losses at 200°C were of the order of 10%, suggesting a much higher adsorbed water content for these samples. Again, only small variations of the amount of water lost occurred from sample to sample, except for sample 4, which exhibited a 6.14% loss. It can be concluded from these findings that the presence of adsorbed water in both the implants as well as the bones is confirmed, but that the amount held by the implants is far less.

The following stage in the experiment involved heating to 650°C. Any losses observed in this range are due to decomposition of the organic phase (if present) and elimination of lattice water (Aok77,Hol80, Bar81).The Tables of mass-losses show that the implants exhibit losses in the range of 0.6 to 1.50%, with the exception of sample 1, which lost 3.95%. These figures are rather low when compared to those of bone, which are in the 30 to 40% range. This would suggest an expected organic phase (collagen) present in the bones, whereas none can be found for the implants. The slight losses exhibited by the implants could possibly be attributed to some lattice water having been present. Lattice water is probably also present in the bones but the organic losses would have overridden these effects.

Since we have these losses occuring, changes in the lattice parameters as well as altered crystallinity values are envisaged (LeGe78).

4.4.2 Cell parameters and crystallinity

Table 3.22, p.68 lists the lattice parameters and crystallinities of the implants as found after heating to 650°C. A slight shrinkage of the a-cell sizes can be observed when compared to original values listed in Table 3.1, p.52, while the c-cell sizes have not altered. The shrinkage in the a-lattice parameter can possibly be ascribed to the loss of lattice water (LeGe78,LeGe81). Another feature which can be observed from Table 3.22, is that the crystallinity of the samples increased (i.e. d_{002} peak widths decreased). Perhaps this might be attributed to possible losses of traces of carbonate (as CO_2 gas). According to reports, a loss of carbonate from the structure results in an expansion of the a-cell parameter (LeGe78,LeGe81), and would increase the crystallinity of the sample. The observation of increased crystallinity correlates well with this, but perhaps the loss

of lattice water influences the effect of carbonate loss on the a-cell size to such an extent, that it masks it. Hence the slight contraction can be explained in this manner. For the bones, a somewhat different scenario arises. It has already been suggested that the high mass-losses observed here are due to the decomposition of the organic phase and that lattice water is probably being lost as well. However, no significant changes in cell parameters can be observed (Table3.24, p.69). Even the crystallinity values have not altered. This would suggest that the loss of 30-40% mass observed in the bones is mainly due to the loss of organic material, which might possibly be accompanied by minimal (and thus undetected) loss of lattice water. Little or no carbonate has been lost at this stage. This would imply an inherent difference between the bones and the implants in that some carbonate seems to have been lost when heating the implants to 650°C, as manifested by the increased crystallinity.

The final stage of the experiment involved heating to 900°C. The implants exhibit mass losses in the range of 0.6 to 1.5% after completion of heating (Fig.4.4). The losses may be attributed to the elimination of carbonate from the crystal structures (LeGe78,Hol80,LeGe81). However, the increase in a-cell parameter which would accompany such a loss is not detected here, a possible reason being that it is so small that the error margin masks it. This would suggest very small amounts of carbonate lost during this stage. Crystallinity values show that although the widths of the 002 peaks have decreased, implying increased crystallinity, these have not occurred to a great extent. This would confirm the fact that although some carbonate may have been lost during the heating from 650 to 900°C most of it had been eliminated in the previous stage.

The bone samples also exhibited only small changes in a-cell parameters, but a rather noticeable increase in crystallinity. Perhaps this would suggest loss of carbonate, but that it did not manifest itself appreciably in the cell-dimension.

A study undertaken by Holcomb and Young (Hol80) on tooth enamel, reported a contraction of a-cell size of 0.012Å after heating to 400°C, and a subsequent expansion of the a-unit size of 0.013Å after heating to 800°C. In the present study, the former was observed in the implants. For the bones, however, any changes that might have occurred were within the error margin and consequently, could not be detected.

Hence, the fact that crystallinities for both the implants and the bones have increased after heating to 900°C, suggests carbonate losses from their structures. However, the temperatures at which these losses occur differ from implants to bone, with most of the carbonate being released from the implants at temperatures below 650°C (confirmed by crystallinities), and at temperatures above 650°C for the bones. Both types of sample exhibited loss of surface water below 200°C. A major portion of the final mass lost in the bones was due to the decomposition of the organic phase, which was found (as expected) to be inherently absent in the implants.

4.4.3 Crystal phase

Attempts were made to identify the crystal phases prevalent after each heating stage. According to LeGeros, when carbonate substitutes into the apatite structure, it does so in the place of HPO_4^{2-} (LeGe81). The appearance of tricalcium phosphate in biological apatites which have been heated to 700°C has been attributed to the original HPO_4^{2-} content of the material. Therefore, the greater the extent of substitution of CO_3-for-HPO_4 in the structure, the less will be

Another possible explanation would be that whole bone (i.e. containing the organic phase) gives poorly resolved X-ray diffraction peaks and that accurate measurements of the a-axis from the 300 peak are made difficult, a factor compounded by the fast scan speed used.

the extent to which β-TCP is present. Since in the present study infra-red spectroscopy and X-ray powder diffractometry have shown that such a substitution occurrs to a much greater extent in the bones than the implants, it would be expected that the spectra of the bones (after heating to 900°C) would bear less evidence of β-TCP than the implants.

Inspection of the spectra recorded for the implants after they were heated to 650° C (APPENDIX 4), shows that the crystal phase is hydroxyapatite, except for samples 9 and 10, which display traces of whitlockite in addition to hydroxyapatite.

~~traces of β-TCP are apparent~~. However, the spectra recorded after heating the implant samples to 900°C, revealed different results. The XRD spectra of some of the implants (2 and 3) revealed the following incriminatory features:

i) a maximum intensity peak at d=2.87Å; this is closer to the maximum intensity peak of β-TCP (d=2.84Å) than of HA (d=2.81Å);

ii) an enhanced peak at d=3.17Å of relative intensity 63%; for pure HA this peak is expected to have a relative intensity of 10% while for β-TCP it is expected to have a relative intensity of 40%;

iii) a peak at d=2.61Å with a relative intensity of 70%; peaks occur in the HA spectrum at d=2.53Å and d=2.63Å with respective relative intensities of 5% and 31% while β-TCP has a peak at d=2.58Å with a relative intensity of 55%.

Therefore, implants 2 and 3 probably contain traces of β-TCP.

Finally, the presence of CaO was investigated. A peak at d=2.40Å with a relative intensity of 13% is characteristic (LeGe81) of this substance. Accordingly, implants 2,3,9 and 10 were found to contain traces of CaO.

The bone spectra were inspected in a similar manner. In all bone samples, HA was found to be the only crystal phase prevalent after heating to 650°C. However, the spectra obtained after heating to 900°C revealed traces of CaO in all the samples except number 2. No traces of β-TCP were found.

Thus, the results of this part of the study have confirmed that the presence of CO_3^{2-} as a substituent for HPO_4^{2-}, reduces the extent to which β-TCP phase forms after heating above 700°C. This correlates well with the initial findings of this study (XRD and IR) that the implants have lower CO_3^{2-} contents than the bones.

In experiment 14, the specific range in which this critical point is suspected, was explored. This showed that a turning point occurs in the range 0.3 to 0.4M NaCl solution (Fig.4.7).

Fig.4.7 - %Ca vs NaCl molarity

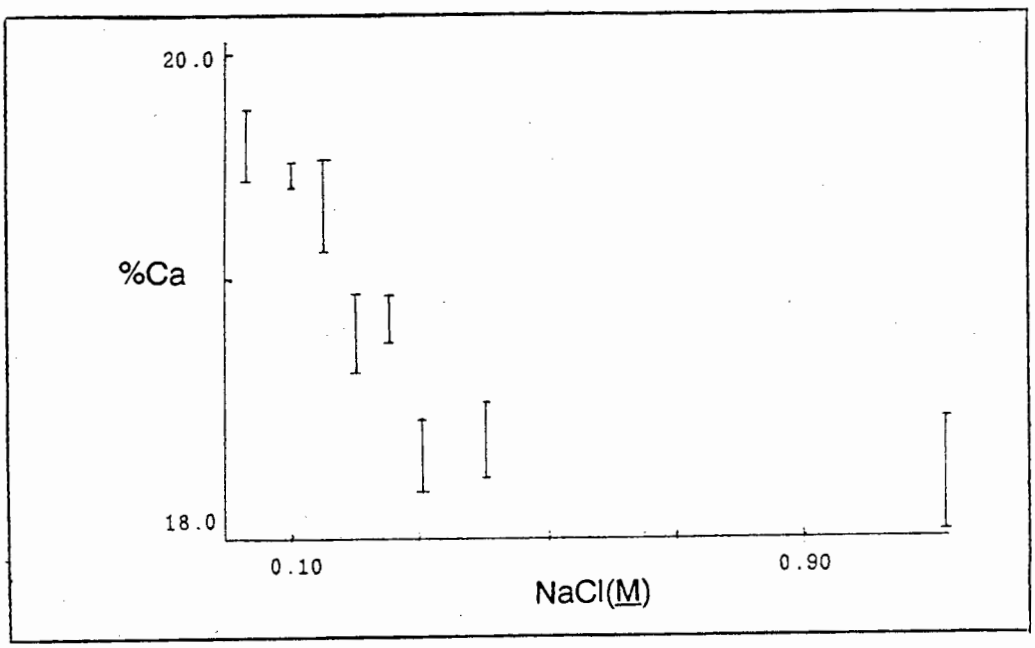

When $CaCl_2$ was used as the ionic medium (Experiment 15), the initial concentrations of the exogenous $Ca^{2+}(aq)$ solutions ranged from 0.01M to 1.70M. From Table 3.28, p.73, it can be seen that the percentage calcium content detected in all the samples after exposure to the latter solutions are about 24%. Since this exceeds the normal expected value of 20.84%($\pm$0.25%) in untreated bone (as determined in this study) it is suggested that exogenous Ca^{2+} has been included in the lattice, but that the threshold level was attained even with the solution of concentration 0.01M. Hence, experiment 16 was set up to explore a lower concentration range. Table 3.29, p.74 lists the concentration range used and the %Ca levels attained in the samples after exposure. The first two samples exhibited a "normal" level of Ca. Thereafter, a definite increase in the Ca content is observable, up to maximum of about 24% for the final two solutions. This trend is illustrated in Fig. 4.8.

Fig 4.8- %Ca vs $CaCl_2$ molarity

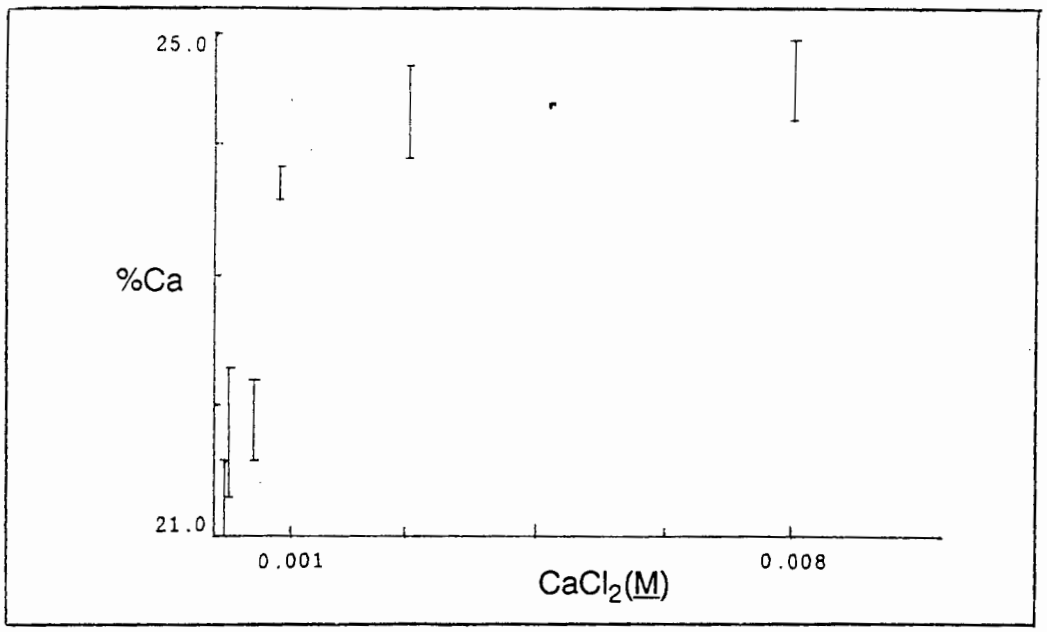

A turning-point at about 0.001M exogenous concentration is clearly visible. Saturation is achieved where the exogenous Ca^{2+} concentration is about twice that at the turning point. Therefore, the surface-reaction with $CaCl_2$ occurs within a narrow band of exogenous calcium con-centrations, and exhibits a characteristic turning-point as well as a saturation level.

4.5.2 Implant materials

Having established the turning-points and saturation levels produced by the different ionic solutions for the bone samples, implants 1,2,3,4,5,6, and 10 were studied individually. The results (pgs.74-82) show that no changes occurred in Ca or Na content of the implants after exposure to the ionic solutions. Thus, although surface exchange or adsorption processes may occur at higher exogenous concentrations than those tested, the results nevertheless have illustrated a fundamental difference in the chemical nature of bone and the implants.

This observed difference between bone samples and implants could be due to differences in crystallinity (crystal size) and therefore surface area. The organic phase in the bone samples may also be a factor.

5. CONCLUSION

Biocompatibility is a crucial factor in determining whether a given implant is likely to function correctly. The present study has shown that inherent physico-chemical differences prevail between implant materials and human bone. Moreover, these differences are not limited to an implant vs bone comparison since the properties of implants themselves vary depending upon whether they are of natural or synthetic origin and variations also exist between different types of bone. The problem of matching an implant substance with the bone in which it is to be embedded is thus a formidable one. It is recognised that it would be impractical to perform physico-chemical experiments such as those described in this project whenever implantation is required. However, this thesis has demonstrated that many such properties can be successfully determined. The techniques and experiments which have been described enabled the objectives of the project to be fulfilled. Hence they can be utilised by other investigators who might wish to address some of the important questions which were raised but which were beyond the scope of this study. For example, an intriguing result of the present study is the finding that physico-chemical properties seem to vary between bones originating in different regions of the human body. Since only one skeleton was studied in this work, this aspect of bone composition needs to be explored further. An obvious follow-up question is whether similar variations occur between the same bone types but from different individuals. Such questions are of importance as biocompatibilty is dependent on these factors.

The present thesis has provided a firm foundation upon which further studies can be based. It is suggested that the techniques and experiments which have been described might be used to answer the above-mentioned questions concerning bone composition and that, in addition, a large series of different

implant materials of both natural and synthetic origin might be subjected to physicochemical characterization. In this way, researchers might be able to draw firm conclusions and perhaps provide a set of definitive guidelines for the selection of appropriate implant materials for specific bone types.

REFERENCES

All M — Allied Analytical Systems,
ICP Emission Spectrometry, Allied operator's manual,
IL Plasma 200

Amp 52 — R. Amprino,
Autoradiographic Analysis of the Distribution of labelled Ca and P in bones,
Experientia 1952, VOL.VIII/1,20

Aok 77 — H. Aoki, T. Ban, M. Akao, K. Kato, S.Iwai,
Thermal Analysis of Calcified Tissues,
Reports for the Institute for Medical & Dental Engineering, 1977, **11**, pp.27-31

Are 75 — J. Arends, C.L. Davidson,
HPO_4^{2-} Content in Enamel and Artificial Carious Lesions,
Calcif. Tiss. Res. 1975, **18**, pp.65-79

Bad 66 — C.B. Baddiel, E.E. Berry,
Spectra Structure Correlations in Hydroxy and Fluorapatite,
Spectrochim. Acta. 1966, **22**, pp.1407-1416

Bar 81 — R. Barnes,
Developments in Atomic Plasma Spectrochemical Analysis,
2nd Edition, Heyden,Longmans Green and Co, London, 1981, p.713

Bar 84 — S. Baravelli, A. Bigi, A. Ripamonti, N. Roveri, E. Foresti,
Thermal Behaviour of Bone and Synthetic Hydroxyapatites Submitted to Magnesium Interaction in Aqueous Medium,
J. Inorg. Biochem. 1984,**20**, app.1-12

Blu 75 — N.C. Blumenthal, F. Betts, A.S. Posner,
Effect of Carbonate and Biological Macromolecules on Formation and Properties of Hydroxyapatite,
Calcif. Tiss. Res. 1975, **18**, pp.81-90

Blu 81 — N.C. Blumenthal, F. Betts, A.S. Posner,
Bone Mineralization,
J. Cryst. Growth 1981, **53**, pp.63-73

Bon 83 L.C. Bonar, A.H. Roufosse, W.K. Sabine, M.D. Grynpas, M.J. Glimcher,
X-ray Diffraction Studies of the Crystallinity of Bone Mineral in Newly Synthesized and Density Fractionated Bone,
Calcif. Tiss. Int. 1983, **35**, pp.202-209

Boy 50 E.S. Boyd, W.F. Neuman,
The Surface Chemistry of Bone - v.The Ion-Binding Properties of Cartilage,
J. Biol. Chem. 1950, **185**, pp.243-251

Bra 83 P. Bratter, K.P. Berthold, P.E. Gardiner,
The Use of Reference Materials as Standards in the Simultaneous Multielement Analysis of Biological Materials Using Inductively Coupled Plasma Spectrometry,
Spectrochim. Acta 1983, **38B**, Nos.1/2, pp.221-228

Cal 84 Calcitek Inc.,
Calcium Phosphates for Implants in Bone,
Information Brochure from Calcitek Inc, 1984

Car 46 H. Carpenter, E. Gavett, I. Thomas,
The Adsorbtion of Strontium at Forty Degrees by Enamel, Dentine, Bone, and Hydroxyapatite as shown by the Radioactive Isotope.
J. Biol. Chem. 1946, **163**, pp.1-6

Car 85 SAS Institute Inc.,
SAS User's Guide : Statistics, Version 5 Edition, Carey, NC:SAS Institute Inc., 1985, 956pp.

Chr 85 M.R. Christoffersen, J. Christoffersen,
The Effect of Aluminum on the Rate of Dissolution of Calcium Hydroxyapatite - A Contribution to the Understanding of Aluminum-Induced Bone Diseases,
Calcif. Tiss. Int. 1985, **37**, pp.673-676

Cor 74 J.T. Corcia, W.E. Moody,
Thermal Analysis of Human Dental Enamel,
J. Dent. Res. 1974, **53**, pp.571-580

Cur 62 J.D. Currey,
Strength of Bone,
Nature 1962, **195**, No.4840, pp.513-514

Dac 90 G. Daculsi, R.Z. LeGeros, M. Heughebaert, I. Barbieux, Formation of Carbonate-Apatite Crystals After Implanatation of Calcium Phosphate Ceramics, *Calcif. Tiss. Int.* 1990, **46**, pp.20-27

Dav 68 J.C. Davila, E.V. Lautsch, T.E. Palmer, Some Physical Factors Affecting the Acceptance of Synthetic Materials as Tissue Implants, *Ann. N.Y. Acad. Sci.* 1968, **146**, pp.138-147

Dea 75 J.A. Dean, T.C. Rains *Flame Emission and Atomic Absorbtion Spectrometry*, Vol.3, 3rd Edition, Marcel Dekker, New York, 1975

Don 69 G. Donnay, X-ray Diffraction Studies of Echinoderm Plates, *Science* 1969, **166**, pp.1147-1150

Dry 60 M.E. Dry, R.A. Beebe, Adsorbtion Studies on Bone Mineral and Synthetic Hydroxyapatite, *J. Phys. Chem.* 1960, **64**, pp.1300-1304

Ell 69 J.C. Elliott, Recent Progress in the Chemistry, Crystal Chemistry and Structure of the Apatites, *Calcif. Tiss. Res.* 1969, **3**, pp.293-307

Ell 73 J.C. Elliott, P.E. Mackie, R.A. Young, Monoclinic Hydroxyapatite, *Science* 1973, **180**, pp.1055-1057

Fea 84 J.D.B. Featherstone, S. Pearson, R.Z. LeGeros, An Infrared Method for Quantification in Carbonate Apatites, *Caries Res.* 1984, **18**, pp.63-66

For 87 J.M. Forrester *A Companion to Medical Studies - Anatomy, Biochemistry and Physiology*, 3rd Edition, Blackwell Scientific Publications, London, 1987

Fow 86 B.O. Fowler, S. Kuroda, Changes in Heated and in Laser-Irradiated Human Tooth Enamel and their Probable Effects on Solubility, *Calcif. Tiss. Int.* 1986, **38**, pp.197-208

Fre 21a — E. Freudenberg, P. Gyorgy,
Uber Kalkbindung durch Tierische Gewebe II,
Bioch. Z. 1921, pp.115-116

Fre 21b — E. Freudenberg, P. Gyorgy,
Uber Kalkbindung durch Tierische Gewebe III,
Bioch. Z. 1921, pp.118-119

Fuw 82 — K. Fuwer,
Recent Advances in Analytical Spectroscopy, 2nd Edition,
Pergamon Press, Great Britain, 1982

Gan 89 — W.F. Ganong,
Review of Medical Physiology, 14th Edition,
Prentice Hall, U.S.A., 1989

Geh 83 — R.C. Gehringer, G.J. McCarthy, R.G. Garvey,
X-ray Diffraction Intensity of Oxide Solid Solutions;
Application to Qualitative and Quantitative Phase Analysis,
Adv. X-ray Anal. 1983, **26**, pp.119-128

Gro 66 — H.J. Grover,
Metal Fatigue in Some Orthopedic Implants,
J. Mat. 1966, **2**, pp.413-424

Gru 60 — J.W.Gruner, D.McConnell, W.D.Armstrong,
Recent Adavances in the Investigation of the Crystal Chemistry of Dental Enamel,
Arch. Oral Biol. 1960, **3**, pp.28-34

Has X — A.A. Hassan,
Geochemical and Mineralogical Studies on Bone Material and their Implications for Radiocarbon Dating,
Phd. thesis, in press

Heu 88 — M. Heughebaert, R.Z. LeGeros, M. Gineste, A. Guilhem, G. Bonel
Physicochemical Characterization of Deposits Associated with HA Ceramics Implanted in Nonosseous Sites,
J. Biomed. Mater. Res. : Applied Biomaterials 1988, **22**, pp.257-268

Hir 47 — A. Hirschman, A.E. Sobel, B. Kramer, I. Fankuchen,
An X-ray Diffraction Study of High Phosphate Bones,
J. Biol. Chem. 1947, **171**, pp.285-291

Hol 80 D.W. Holcomb, R.A. Young,
Clinical Investigation: Thermal Decomposition of Human Tooth Enamel,
Calcif. Tiss. Int. 1980, **31**, pp.189-201

Int 85 Interpore Inc.,
A Unique Biomatrix for Bone Regenration,
The Nature of Interpore 1985, Information Brochure

Jen 81 R. Jenkins,
JCPDS - International Centre for Diffraction Data:
Sample Preparation Methods in X-ray Powder Diffraction,
Powder Diffraction 1981, **1**, No.2, pp.51-63

Joi 72 Joint Committee on Powder Diffraction Standards,
Selected Powder Diffraction Data for Minerals, 1st Edition,
Publication DBM-1-23, 1972

Kno 84 A. Knowks, C. Burgess,
Practical Absorption Spectrometry, 8th Edition, UV Spectrometry Group, Editors, Chapman Hall, London, 1984

Kro 86 J. Kroesbergen, A.M.P. Van Steijn, W.J. Gelsema, C.L. De Ligny,
^{99m}Tc Bone Scanning Agents-II.
Adsorption of $^{99m}TcO_4^{6c}$ Pyrophosphate Complexes on the Mineral Phase of Bone,
Int. J. Nucl. Med. Biol. 1986, **12**, No.6, pp.411-417

Lav 68 W. Lavin,
Atomic Absorption Spectrometry, 7th Edition, L.E.Early, Editor, Interscience Publishers, New York, 1968

Law 61 K.E. Lawson,
Infrared Absorption - of Inorganic Substances, 12th Edition,
S.R. Barnes, F. Rails, Editors, Reinhold Publishing Co., New York, 1961

Lee 83a J. Lee,
Calcium Matrix Effects in Multi-Element Analysis of Animal Bone by Inductively-Coupled Plasma Emission Spectrometry,
Analytica Chim. Acta 1983, **152**, pp.141-147

Lee 83b J. Lee,
Multi-Element Analysis of Animal Tissue by Inductively-Coupled Plasma Emission Spectrometry,
ICP Inf. Newsletter 1983, **8**, No.10, pp.553-561

LeGe 65 R.Z. LeGeros,
Effect of Carbonate on the Lattice Parameters of Apatite,
Nature 1965, **206**, pp.403-404

LeGe 67 R.Z. LeGeros, O.R. Trautz, J.P. LeGeros, E. Klein,
Apatite Crystallites: Effects of Carbonate on Morphology,
Science 1967, **155**, pp.1409-1411

LeGe 68 R.Z. LeGeros, O.R. Trautz, J.P. LeGeros, E. Klein,
Carbonate Substitution in the Apatite Structure (1),
Bulletin de la Societe Chimique de France, (no special) 1972,
pp.1712-1718

LeGe 69 R.Z. LeGeros, O.R. Trautz, E. Klein, J.P. LeGeros,
Two Types of Carbonate Substitution in the Apatite Structure,
Experienta 1969, **25/1**, pp.5-7

LeGe 71 R.Z. LeGeros, J.P. LeGeros, O.R. Trautz, W.P. Shirra,
Conversion of Monetite, $CaHPO_4$, to Apatites: Effect of Carbonate on the Crystallinity and the Morphology of the Apatite Crystallites,
Advs. X-ray Anal. 1971, **14**, pp.57-67

LeGe 73 R.Z. LeGeros, W.P. Shirra, M.A. Miravite, J.P. LeGeros,
Amorphous Calcium Phosphates: Synthetic and Biological,
Coll. Internationaux C.N.R.S. 1973, **No.230**, pp.105-115

LeGe 78 R.Z. LeGeros, G. Bonel, R. Legros,
Types of "H_2O" in Human Enamel and in Precipitated Apatites,
Calcif. Tiss. Res. 1978, **26**, pp.111-118

LeGe 80 R.Z. LeGeros, M.H. Taheri, G.B. Quirolgico, J.P. LeGeros,
Formation and Stability of Apatites: Effects of some Cationic Substituents,
Proc. 2nd Int. Congr. Phosphorus Comp. 1980, Boston, Imphos (Paris), pp.89-103

LeGe 81 R.Z. LeGeros,
Apatites in Biological Systems,
Prog. Crystal Growth Chart. 1981, **4**, pp.1-45

LeGe 83 R.Z. LeGeros, M.S. Tung,
Chemical Stability of Carbonate- and Fluoride-Containing Apatites,
Caries Res. 1983, **17**, pp.419-429

LeGe 84 R.Z. Legeros, J.P. LeGeros,
Phosphate Minerals, J. Nriagu, P. Moore, Editors, Springer Verlag, Berlin, 1984, pp.351-385

LeGe 87 R.Z. LeGeros, R. Kijkowska, W. Jia, J.P. LeGeros,
Fluoride-Cation Interactions in the Formation and Stability of Apatites,
XVI Conf. Int. Soc. Fluoride Res. 1987, Nyon, Switzerland

LeGe 88a R.Z. LeGeros,
Calcium Phosphate Materials in Restorative Dentistry: A Review,
Adv. Dent. Res. 1988, **2(1)**, pp.164-180

LeGe 88b R.Z. LeGeros, J.R. Parsons, G. Daculsi,
Significance of the Porosity and Physical Chemistry of Calcium Phosphate Ceramics: Biodegradation-Bioresorption,
Ann. N.Y. Acad. Sci. 1988, **Position paper 3**, pp.268-271

LeGe 90 R.Z. LeGeros, G. Daculsi, I. Orly, J.P. LeGeros,
Bone Augmentation and Implant Coating Materials,
Proc. 1st Int. Conf. Oral Implant Dent. 1990, pp.27-36

Lev 69 G.E. Levitt, P.H. Crayton, E.A. Monroe, R.A. Condrate,
Forming Methods for Apatite Prsthesis,
J. Biomed. Mater. Res. 1969,**3**, pp.683-685

Loo 80 J.C. Van Loon,
Analytical Atomic Absorption Spectroscopy - Selected Methods, 5th Edition, K.Larsen, Editor, Academic Press, New York, 1980

Mac 72 P.E. Mackie, J.C. Elliott, R.A. Young,
Natural and Synthetic Apatites and their Molecular Structure,
Acta Cryst. Sect. B 1972, **28**, pp.840-852

Mah 83 H.S. Mahanti, R.M. Barnes,
Determinations of Major, Minor and Trace Elements in Bone by Inductively-Coupled PLasma Emission Spectrometry,
Anal. Chim. Acta 1983, **151**, pp.409-417

Mat 86 N. Matsushima, M. Tokita, K. Hikichi,
X-Ray Determination of the Crystallinity in Bone Mineral,
Biochim. Biophys. Acta 1986, **883**, pp.574-579

Mco 60 D. McConnell,
The Crystal Chemistry of Dahllite,
Amer. Min. 1960, **45**, pp.209-216

Mco 65 D. McConnell,
Crystal Chemistry of Hydroxyapatite - Its Relation to Bone Mineral,
Arch. Oral Biol. 1965, **10**, pp.421-431

Mon 71 Z.A. Monroe, W. Votawa, D.B. Bass, J. McMullen,
New Calcium Phosphate Ceramic Material for Bone and Tooth Implants,
J. Dent. Res. 1971, **50**, pp.860-862

Mon 87 A. Montaseu, D.W. Golightly,
Inductively Coupled Plasmas in Analytical Atomic Spectrometry, 3rd Edition, G.R. Walsh, Editor, VCH Publishers, London, 1987

Mor 66 F.R. Morral,
Cobalt Alloys as Implants in Humans,
J. Materials 1966, **1**, No.2, pp.384-411

Mun 77 G.R. Mundy, A.J. Altman, M.D. Gonder, J.G. Bandelin,
Direct Resorbtion of Bone by Human Monocytes,
Science 1977, **196**, pp.1109-1110

Nel 82 D.G.A. Nelson, J.D.B. Featherstone,
Preparation, Analysis, and Characterization of Carbonated Apatites,
Calcif. Tiss. Int. 1982, **34**, pp.69-81

Neu 47 W.F. Neuman, R.F. Riley,
The Uptake of Radioactive Phosphorus by the Calcified Tissues of Normal and Choline-Deficient Rats,
J. Biol. Chem. 1947, **168**, pp.545-554

Neu 51 W.F. Neuman, V. DiStefano, B.J. Mulryan,
The Surface Chemistry of Bone: III.Observations on the Role of Phosphatase,
J. Biol. Chem. 1951, **193**, pp.227-235

Neu 53 W.F. Neuman, M.W. Neuman,
The Nature of the Mineral Phase of Bone,
Chem. Rev. 1953, **53**, pp.1-45

Neu 58 W.F. Neuman, M.W. Neuman,
The Chemical Dynamics of Bone Mineral, 2nd Edition,
University of Chicago Press, Chicago, 1958, pp.1-181

Pin 78 M. Pinta,
Modern Methods for Trace Element Analysis, 3rd Edition,
A.J.Thompson, Editor, Ann Arbor Science Publishers, London,
1978

Pos 63 A.S. Posner, E.D. Eans, R.A. Harper, I. Zipkin,
X-Ray Diffraction Analysis of the Effect of Fluoride on
Human Bone Aapatite,
Arch Oral Biol. 1963, **8**, pp.549-570

Pos 85 A.S. Posner,
The Mineral of Bone,
Clin. Orth. Rel. Res. 1985, No.200, pp.92-99

Rah 84 H.V.R. Von Rahden, M.J.E. Von Rahden,
Some Practical Aspects of Quantitative X-Ray Diffraction,
Trans. Geol. S. Afr. 1984, **87**, pp.297-302

Ram 78 W. Ramsay, F.G. Donnan,
Spectroscopy, 3rd Edition, Vol.1, F.D. Lawson, Editor,
Longmans Green and Company, London, 1978

Rao 73 C. Rao,
Varcomp : Linear Statistical Inference and its Applications,
2nd Edition, John Wiley and Sons, New York, 1973

Rob 66 J.W. Robinson,
Atomic Absorption Spectroscopy, 5th Edition, Richard Arnold
Publishers Ltd., London, 1966

Rod 85 A.L. Rodgers,
The Application of Physico-Chemical Procedures in the
Analysis of Urinary Calculi,
Scanning Electron Microscopy 1985, **II**, pp.745-758

Roy 74 D.M. Roy, S.K. Linnehan,
Hydroxyapatite formed from Coral Skeletal Carbonate by
Hydrothermal Exchange,
Nature 1974, **247**, pp.220-222

Rob 66 J.W. Robinson,
Atomic Absorption Spectroscopy, Edward Arnold Publishers
Ltd., London, 1966

Rub 69 — I. Rubeka, B. Moldan,
Atomic Absorption Spectrophotometry, 9th Edition, |
Iliffe Books, Czechoslovakia, 1969

Sar 86 — D.J. Sartoris, D.H. Gershuni, W.H. Akeson, R.E. Holmes, D. Resnick,
Coralline Hydroxyapatite Bone Graft Substitutes: Preliminary Report of Radiographic Evaluation,
Radiology 1986, **159**, No.1, pp.133-137

Sch 68 — G. Schmeisser, Jr.,
Progress in Metallic Surgical Implants,
J. Materials 1968, **3**, No.4, pp.951-976

Sel 88 — E.E. Selkurt,
Basic Physiology for the Health Sciences, 2nd Edition,
Little, Brown and Co., Boston, U.S.A., 1988

Sil 86 — A. Sillen,
Biogenic and Diagenic Sr/Ca in Plio-Pleistocene Fossils of the Omo Shungura Formation,
Paleobiology 1986, **12(3)**, pp.311-323

Sil X — A. Sillen,
Diagenesis of the Inorganic Phase of Cortical Bone,
in press

Sim 66 — I. Simon,
Infrared Radiation, W.C. Michele, Editor, D. Van Nostrand Company, New York, 1966

Smi 83 — S.B. Smith Jr., R.G. Schleicher, A.G. Dennison, G.A. McLean,
Consideration in the Design of a Sample Introduction and Plasma Generation System for ICP Spectroscopy,
Spectrochim. Acta 1983, **38B**, Nos.1/2, pp.157-163

Sob 49 — A.E. Sobel, A. Hanok, H.A. Kirshner, I. Fankuchen,
Calcification of Teeth: III. X-Ray Diffraction Patterns in Relation to Changes in Composition,
J. Biol. Chem. 1949, **179**, pp.205-211

Tho 83 — M. Thompson, J.N. Walsh,
A Handbook of Inductively Coupled Plasma Spectrometry
E.R. Brown, Editor, Blackie and Son, London, 1983

Tra 55 O.R. Trautz,
X-Ray Diffraction of Biological and Synthetic Apatites,
Ann. N.Y. Acad. Sci. 1955, **60(S)**, pp.696-711

Tra 60 O.R. Trautz,
Crystallographic Studies of Calcium Carbonate Phosphate,
Ann. N.Y. Acad. Sci. 1960, **85**, pp.145-160

Wan 86 M.A.E. Wandt, M.A.B. Pougnet,
Simultaneous Determination of Major and Trace Elements in Urinary Calculi by Microwave-assisted Digestion and Inductively Coupled Plasma Atomic Emission Spectrometric Analysis,
Analyst 1986, **Vol.III**, pp.1249-1253

Web 71 J.N. Weber, E.W. White,, J. Lebiedzik,
New Porous Biomaterials by Replication of Echinoderm Skeletal Microstructures,
Nature 1971, **233**, pp.337-339

Web 73 J.N. Weber, E.W. White,
Carbonate Minerals as Precursors of New Ceramic, Metal, and Polymer Materials for Biomedical Applications,
Miner. Sci. Engng. 1973, **5**, No.2, pp.151-165

Wei 68 S. Weisman,
Metals For Implantation in the Human Body,
Ann. N.Y. Acad. Sci. 1968, **146**, Art.1, pp.80-95

Whi 66 D.H. Whiffen,
Spectroscopy, 4th Edition, E.R. Fulwer, T.R.Manning, Editors,
Longmans, Green and Co., London, 1966

Wic 66 J.K. Wickstrom,
Surgical Implants - Their Mechanical and Environmental Problems,
J.Materials 1966, **1**, No.2, pp.366-372

You 75 R.A. Young,
Biological Apatite vs Hydroxyapatite at the Atomic Level,
Clin. Orth. Rel. Res. 1975, No.113, pp.249-262

APPENDIX 1

Typical XRD scan for the implants

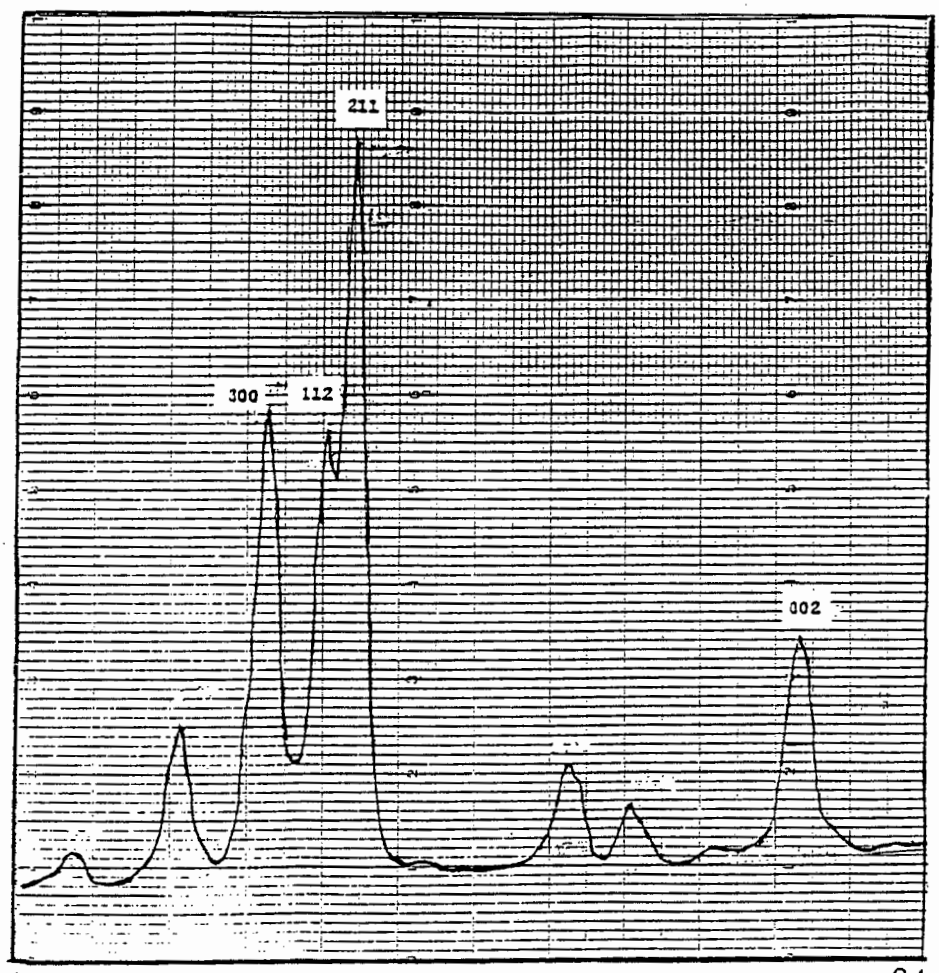

Typical XRD scan for the bones

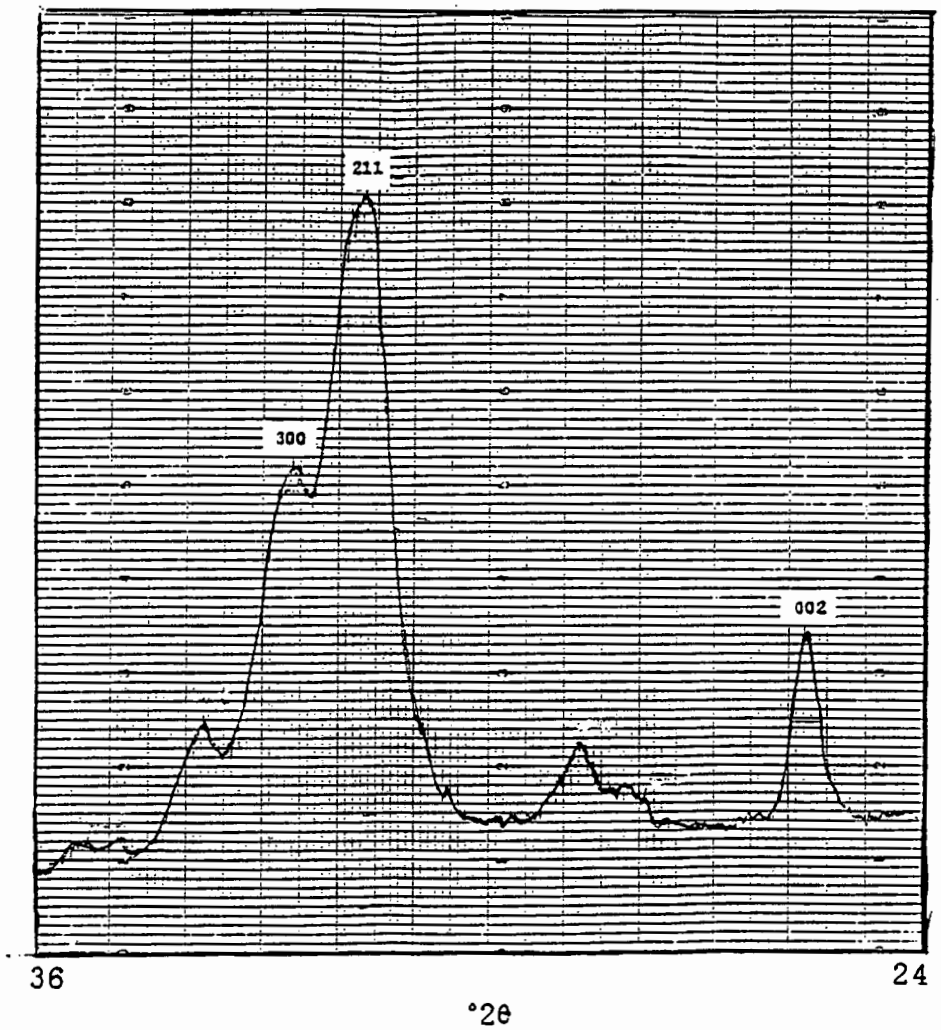

Listing of d-spacings vs intensities for the bones

1		2		3		4		5		6	
d	I	d	I	d	I	d	I	d	I	d	I
4.09	21.62	4.07	15.68	4.07	16.73	4.05	22.62	4.03	19.73	4.07	15.81
3.90	18.15	3.90	16.77	3.89	17.74	3.88	23.94	3.88	19.86	3.84	16.67
-		-		-		3.72	18.31	3.75	16.13	3.74	12.87
3.45	10.01	3.46	40.72	3.46	38.99	3.43	42.25	3.43	19.99	3.42	34.56
3.18	18.27	3.17	17.36	3.17	18.24	3.15	19.72	3.16	18.67	3.16	15.81
3.09	24.36	3.09	23.23	3.08	27.64	3.07	26.62	3.07	25.33	3.07	20.71
2.82	100	2.82	100	2.81	100	2.81	100	2.82	100	2.81	100
2.80	90.13	-		-		2.78	91.27	2.76	87.33	-	
2.73	60.58	2.73	58.08	2.73	59.62	2.72	61.97	2.71	63.20	2.72	56.74
2.64	26.46	2.64	25.75	2.64	27.55	2.62	27.46	2.61	26.00	2.62	24.38
2.54	9.89	2.54	9.82	2.54	10.18	2.54	10.98	2.51	11.87	2.53	9.68
2.36	11.17	2.35	9.58	2.35	13.33	2.34	11.27	2.34	9.20	2.34	8.33
2.28	20.85	2.26	22.16	2.26	21.07	2.26	21.08	2.26	23.33	2.26	20.58
2.16	8.72	2.15	8.50	2.15	8.80	2.15	10.98	2.14	9.20	2.14	7.84
2.07	8.03	2.07	7.78	2.07	8.17	2.06	9.15	2.06	8.00	2.06	7.10
2.03	12.61	2.03	13.29	2.03	21.38	2.03	12.53	2.03	14.80	2.03	13.48
2.00	7.55	2.00	7.40	2.01	7.81	-		-		-	
1.95	23.21	1.95	23.95	1.95	22.54	1.94	25.49	1.94	26.00	1.94	22.18
1.89	16.44	1.89	15.09	1.89	14.91	1.89	15.56	1.88	16.67	1.89	14.34
1.84	22.32	1.84	25.39	1.85	24.96	1.83	25.53	1.83	17.33	1.83	22.14
1.81	17.58	1.81	16.76	1.81	16.35	1.80	16.90	1.80	17.60	1.80	15.29
1.78	15.11	1.78	14.55	1.78	15.09	1.78	16.19	1.77	13.60	1.77	12.97
1.76	12.68	1.76	12.69	1.76	14.46	1.76	13.23	1.75	12.67	1.76	11.62
1.72	11.54	1.72	14.37	1.72	12.58	1.72	12.76	1.72	12.80	1.72	11.44

APPENDIX 2

Table1 : Masses used for the ICP determinations

Implant	Mass (g)	Bone	Mass (g)
1	0.0989	1	0.0985
2	0.0992	2	0.0990
3	0.0991	3	0.0991
4	0.0999	4	0.0995
5	0.0991	5	0.0988
6	0.0986	6	0.0992
7	0.0994		
8	0.0998		
9	0.0997		
10	0.0992		

Mass of IAEA-H5 standard analysed was 0.096g.

Table 2 : Published (Mah83) and found (this study) values for IAEA-H5 standard

	Published values		Own values	
Element	%Content	S.D.	%Content	S.D.
Ca	21.17	2.40	19.72	0.34
P	9.578	0.69	9.01	0.35
Mg	0.353	0.0025	0.311	0.012
Na	0.477	0.097	0.455	0.033
Sr	104.85	17.61 µg/g	0.0098	$1.21*10^{-4}$
Fe	80.65	11.00 "	0.085	$1.85*10^{-4}$
Zn	89.91	15.39	$6.11*10^{-5}$	$2.26*10^{-5}$

Table 3 : Reference values for human bone (Mah83)

Element	%Content	S.D.
Ca	27.10	0.30
P	13.80	0.20
Mg	0.226	0.004
Na	1.066	0.02
Sr	149.0	2.0 lg/g
Fe	29.40	0.60 "
Zn	102.0	1.00 "

See next page for Table 4 (raw data for statistical evaluation).

Table 5 : Log-estimates and respective standard errors for the bones

	Ca		P		Mg	
	Est.	S.D.	Est.	S.D.	Est.	S.D.
Region	3767.9	8079.2	960.2	1912.9	0	0
Site	8342.3	12286.6	2419.6	3070.6	0	0
Region*Site	13024.8	9116.0	3239.5	2135.5	4355.3	3562.4
Analysis	0	0	273.3	416.8	0	0
Region*Analysis	416.2	906.3	0	0	0	0
Site*analysis	2604.7	2889.9	75.6	118.7	0	0
Region*Site*Analysis	1373.2	1019.1	39.1	19.8	7159.5	2935.7
Reading	634.4	129.5	15.7	3.2	94.5	19.3

VARIABLE	N	MEAN	STANDARD DEVIATION	MINIMUM VALUE	MAXIMUM VALUE	STD ERROR OF MEAN	SUM	VARIANCE	C.V.
REGION=1 SITE=1 ANAL=1									
CA	3	2203.33333333	27.64657905	2184.0000000	2235.0000000	15.96175986	6610.0000000	764.33333333	1.255
P	3	1006.00000000	1.73205081	1005.0000000	1008.0000000	1.00000000	3018.0000000	3.00000000	0.172
MG	3	293.00000000	2.00000000	291.0000000	295.0000000	1.15470054	879.0000000	4.00000000	0.683
LOGC	3	7.69767439	0.01250609	7.6889133	7.7119965	0.00722039	23.0930232	0.00015640	0.162
LOGP	3	6.91373636	0.00172087	6.9127428	6.9157234	0.00099354	20.7412091	0.00000296	0.025
LOGMG	3	5.68015708	0.00682606	5.6733233	5.6869754	0.00394103	17.0404712	0.00004660	0.120
REGION=1 SITE=1 ANAL=2									
CA	3	2202.66666667	5.13160144	2197.0000000	2207.0000000	2.96273147	6608.0000000	26.33333333	0.233
P	3	995.33333333	3.51188458	992.0000000	999.0000000	2.02758751	2986.0000000	12.33333333	0.353
MG	3	429.00000000	19.05255888	418.0000000	451.0000000	11.00000000	1287.0000000	363.00000000	4.441
LOGC	3	7.69742222	0.00233071	7.6948481	7.6993894	0.00134564	23.0922666	0.00000543	0.030
LOGP	3	6.90307354	0.00352749	6.8997231	6.9067548	0.00203660	20.7092206	0.00001244	0.051
LOGMG	3	6.06081007	0.04387048	6.0354814	6.1114673	0.02532864	18.1824302	0.00192462	0.724
REGION=1 SITE=2 ANAL=1									
CA	3	2503.33333333	13.31665624	2492.0000000	2518.0000000	7.68837506	7510.0000000	177.33333333	0.532
P	3	1135.00000000	3.46410162	1131.0000000	1137.0000000	2.00000000	3405.0000000	12.00000000	0.305
MG	3	241.00000000	0.00000000	241.0000000	241.0000000	0.00000000	723.0000000	0.00000000	0.000
LOGC	3	7.82536904	0.00531464	7.8208409	7.8312202	0.00306841	23.4761071	0.00002825	0.068
LOGP	3	7.03438482	0.00305477	7.0308575	7.0361485	0.00176367	21.1031545	0.00000933	0.043
LOGMG	3	5.48479693	0.00000000	5.4847969	5.4847969	0.00000000	16.4543908	0.00000000	0.000
REGION=1 SITE=2 ANAL=2									
CA	3	2348.33333333	27.57414248	2322.0000000	2377.0000000	15.91993858	7045.0000000	760.33333333	1.174
P	3	1109.00000000	3.46410162	1105.0000000	1111.0000000	2.00000000	3327.0000000	12.00000000	0.312
MG	3	246.00000000	0.00000000	246.0000000	246.0000000	0.00000000	738.0000000	0.00000000	0.000
LOGC	3	7.76141522	0.01173392	7.7501842	7.7735945	0.00677458	23.2842457	0.00013768	0.151
LOGP	3	7.01121073	0.00312645	7.0076006	7.0130158	0.00180506	21.0336322	0.00000977	0.045
LOGMG	3	5.50533154	0.00000000	5.5053315	5.5053315	0.00000000	16.5159946	0.00000000	0.000
REGION=2 SITE=1 ANAL=1									
CA	3	2237.33333333	28.57154762	2210.0000000	2267.0000000	16.49579071	6712.0000000	816.33333333	1.277
P	3	1013.00000000	4.00000000	1009.0000000	1017.0000000	2.30940108	3039.0000000	16.00000000	0.395
MG	3	272.66666667	4.04145188	269.0000000	277.0000000	2.33333333	818.0000000	16.33333333	1.482
LOGC	3	7.71298565	0.01276121	7.7007478	7.7262127	0.00736769	23.1389570	0.00016285	0.165
LOGP	3	6.92066631	0.00394869	6.9167150	6.9246124	0.00227978	20.7619989	0.00001559	0.057
LOGMG	3	5.60817698	0.01479670	5.5947114	5.6240175	0.00854288	16.8245310	0.00021894	0.264
REGION=2 SITE=1 ANAL=2									
CA	3	2323.00000000	7.00000000	2316.0000000	2330.0000000	4.04145188	6969.0000000	49.00000000	0.301
P	3	1001.33333333	4.04145188	999.0000000	1006.0000000	2.33333333	3004.0000000	16.33333333	0.404
MG	3	340.33333333	20.20725942	317.0000000	352.0000000	11.66666667	1021.0000000	408.33333333	5.937
LOGC	3	7.75061171	0.00301336	7.7475968	7.7536235	0.00173976	23.2518351	0.00000908	0.039
LOGP	3	6.90908230	0.00403139	6.9067548	6.9137374	0.00232752	20.7272469	0.00001625	0.058
LOGMG	3	5.82872138	0.06046555	5.7589018	5.8636312	0.03490980	17.4861641	0.00365608	1.037

VARIABLE	N	MEAN	STANDARD DEVIATION	MINIMUM VALUE	MAXIMUM VALUE	STD ERROR OF MEAN	SUM	VARIANCE	C.V.
REGION=2 SITE=2 ANAL=1									
CA	3	2512.00000000	5.56776436	2506.0000000	2517.0000000	3.21455025	7536.0000000	31.00000000	0.222
P	3	1131.66666667	7.50555350	1124.0000000	1139.0000000	4.33333333	3395.0000000	56.33333333	0.663
MG	3	227.00000000	0.00000000	227.0000000	227.0000000	0.00000000	681.0000000	0.00000000	0.000
LOGC	3	7.82883289	0.00221711	7.8264431	7.8308230	0.00128005	23.4864987	0.00000492	0.028
LOGP	3	7.03143208	0.00663387	7.0246490	7.0379060	0.00383007	21.0942963	0.00004401	0.094
LOGMG	3	5.42495002	0.00000000	5.4249500	5.4249500	0.00000000	16.2748501	0.00000000	0.000
REGION=2 SITE=2 ANAL=2									
CA	3	2348.00000000	19.07878403	2328.0000000	2366.0000000	11.01514109	7044.0000000	364.00000000	0.813
P	3	1098.33333333	6.11010093	1093.0000000	1105.0000000	3.52766841	3295.0000000	37.33333333	0.556
MG	3	265.00000000	0.00000000	265.0000000	265.0000000	0.00000000	795.0000000	0.00000000	0.000
LOGC	3	7.76129715	0.00813088	7.7527648	7.7689560	0.00469437	23.2838915	0.00006611	0.105
LOGP	3	7.00153885	0.00555830	6.9966815	7.0076006	0.00320909	21.0046166	0.00003089	0.079
LOGMG	3	5.57972983	0.00000000	5.5797298	5.5797298	0.00000000	16.7391895	0.00000000	0.000
REGION=3 SITE=1 ANAL=1									
CA	3	2219.33333333	30.89228598	2186.0000000	2247.0000000	17.83566963	6658.0000000	954.33333333	1.392
P	3	977.66666667	4.72581563	974.0000000	983.0000000	2.72845092	2933.0000000	22.33333333	0.483
MG	3	310.00000000	0.00000000	310.0000000	310.0000000	0.00000000	930.0000000	0.00000000	0.000
LOGC	3	7.70489738	0.01394637	7.6898287	7.7173513	0.00805194	23.1146921	0.00019450	0.181
LOGP	3	6.88516100	0.00482840	6.8814113	6.8906091	0.00278768	20.6554830	0.00002331	0.070
LOGMG	3	5.73657230	0.00000000	5.7365723	5.7365723	0.00000000	17.2097169	0.00000000	0.000
REGION=3 SITE=1 ANAL=2									
CA	3	2204.33333333	3.05505046	2201.0000000	2207.0000000	1.76383421	6613.0000000	9.33333333	0.139
P	3	957.00000000	3.60555128	954.0000000	961.0000000	2.08166600	2871.0000000	13.00000000	0.377
MG	3	310.00000000	0.00000000	310.0000000	310.0000000	0.00000000	930.0000000	0.00000000	0.000
LOGC	3	7.69817976	0.00138623	7.6966671	7.6993894	0.00080034	23.0945393	0.00000192	0.018
LOGP	3	6.86379866	0.00376485	6.8606637	6.8679744	0.00217364	20.5913960	0.00001417	0.055
LOGMG	3	5.73657230	0.00000000	5.7365723	5.7365723	0.00000000	17.2097169	0.00000000	0.000
REGION=3 SITE=2 ANAL=1									
CA	3	2250.33333333	10.01665280	2240.0000000	2260.0000000	5.78311719	6751.0000000	100.33333333	0.445
P	3	971.00000000	1.73205081	970.0000000	973.0000000	1.00000000	2913.0000000	3.00000000	0.178
MG	3	254.00000000	0.00000000	254.0000000	254.0000000	0.00000000	762.0000000	0.00000000	0.000
LOGC	3	7.71882703	0.00445220	7.7142311	7.7231201	0.00257048	23.1564811	0.00001982	0.058
LOGP	3	6.87832541	0.00178286	6.8772961	6.8803841	0.00102934	20.6349762	0.00000318	0.026
LOGMG	3	5.53733427	0.00000000	5.5373343	5.5373343	0.00000000	16.6120028	0.00000000	0.000
REGION=3 SITE=2 ANAL=2									
CA	3	2151.33333333	20.59935274	2128.0000000	2167.0000000	11.89304185	6454.0000000	424.33333333	0.958
P	3	942.00000000	3.00000000	939.0000000	945.0000000	1.73205081	2826.0000000	9.00000000	0.318
MG	3	263.33333333	16.16580754	254.0000000	282.0000000	9.33333333	790.0000000	261.33333333	6.139
LOGC	3	7.67381243	0.00959751	7.6629379	7.6810990	0.00554112	23.0214373	0.00009211	0.125
LOGP	3	6.84800189	0.00318473	6.8448155	6.8511849	0.00183870	20.5440057	0.00001014	0.047
LOGMG	3	5.57219187	0.06037514	5.5373343	5.6419071	0.03485760	16.7165756	0.00364516	1.084

VARIABLE	N	MEAN	STANDARD DEVIATION	MINIMUM VALUE	MAXIMUM VALUE	STD ERROR OF MEAN	SUM	VARIANCE	C.V.
REGION=4 SITE=1 ANAL=1									
CA	3	1850.66666667	16.50252506	1837.0000000	1869.0000000	9.52773729	5552.0000000	272.33333333	0.892
P	3	843.66666667	2.30940108	841.0000000	845.0000000	1.33333333	2531.0000000	5.33333333	0.274
MG	3	198.00000000	0.00000000	198.0000000	198.0000000	0.00000000	594.0000000	0.00000000	0.000
LOGC	3	7.52327477	0.00890181	7.5158891	7.5331588	0.00513946	22.5698243	0.00007924	0.118
LOGP	3	6.73775497	0.00273951	6.7345917	6.7393366	0.00158166	20.2132649	0.00000750	0.041
LOGMG	3	5.28826703	0.00000000	5.2882670	5.2882670	0.00000000	15.8648011	0.00000000	0.000
REGION=4 SITE=1 ANAL=2									
CA	3	1916.00000000	6.24499800	1909.0000000	1921.0000000	3.60555128	5748.0000000	39.00000000	0.326
P	3	826.00000000	0.00000000	826.0000000	826.0000000	0.00000000	2478.0000000	0.00000000	0.000
MG	3	216.00000000	0.00000000	216.0000000	216.0000000	0.00000000	648.0000000	0.00000000	0.000
LOGC	3	7.55799141	0.00326170	7.5543348	7.5606012	0.00188314	22.6739742	0.00001064	0.043
LOGP	3	6.71659477	0.00000000	6.7165948	6.7165948	0.00000000	20.1497843	0.00000000	0.000
LOGMG	3	5.37527841	0.00000000	5.3752784	5.3752784	0.00000000	16.1258352	0.00000000	0.000
REGION=4 SITE=2 ANAL=1									
CA	3	2342.66666667	9.23760431	2332.0000000	2348.0000000	5.33333333	7028.0000000	85.33333333	0.394
P	3	1081.33333333	4.04145188	1079.0000000	1086.0000000	2.33333333	3244.0000000	16.33333333	0.374
MG	3	684.00000000	0.00000000	684.0000000	684.0000000	0.00000000	2052.0000000	0.00000000	0.000
LOGC	3	7.75903997	0.00394771	7.7544815	7.7613192	0.00227921	23.2771199	0.00001558	0.051
LOGP	3	6.98594548	0.00373346	6.9837900	6.9902565	0.00215551	20.9578364	0.00001394	0.053
LOGMG	3	6.52795792	0.00000000	6.5279579	6.5279579	0.00000000	19.5838738	0.00000000	0.000
REGION=4 SITE=2 ANAL=2									
CA	3	2271.66666667	27.73685875	2241.0000000	2295.0000000	16.01388287	6815.0000000	769.33333333	1.221
P	3	1025.66666667	7.50555350	1018.0000000	1033.0000000	4.33333333	3077.0000000	56.33333333	0.732
MG	3	303.00000000	0.00000000	303.0000000	303.0000000	0.00000000	909.0000000	0.00000000	0.000
LOGC	3	7.72821921	0.01223807	7.7146775	7.7384881	0.00706565	23.1846576	0.00014977	0.158
LOGP	3	6.93308023	0.00731966	6.9255952	6.9402225	0.00422601	20.7992407	0.00005358	0.106
LOGMG	3	5.71373281	0.00000000	5.7137328	5.7137328	0.00000000	17.1411984	0.00000000	0.000
REGION=5 SITE=1 ANAL=1									
CA	3	1872.00000000	27.62245463	1841.0000000	1894.0000000	15.94783162	5616.0000000	763.00000000	1.476
P	3	896.33333333	3.05505046	893.0000000	899.0000000	1.76383421	2689.0000000	9.33333333	0.341
MG	3	152.00000000	0.00000000	152.0000000	152.0000000	0.00000000	456.0000000	0.00000000	0.000
LOGC	3	7.53468976	0.01480428	7.5180642	7.5464463	0.00854725	22.6040693	0.00021917	0.196
LOGP	3	6.79830849	0.00341021	6.7945866	6.8012830	0.00196889	20.3949255	0.00001163	0.050
LOGMG	3	5.02388052	0.00000000	5.0238805	5.0238805	0.00000000	15.0716416	0.00000000	0.000
REGION=5 SITE=1 ANAL=2									
CA	3	1952.00000000	8.66025404	1942.0000000	1957.0000000	5.00000000	5856.0000000	75.00000000	0.444
P	3	881.33333333	1.15470054	880.0000000	882.0000000	0.66666667	2644.0000000	1.33333333	0.131
MG	3	153.00000000	0.00000000	153.0000000	153.0000000	0.00000000	459.0000000	0.00000000	0.000
LOGC	3	7.57660319	0.00444232	7.5714736	7.5791680	0.00256477	22.7298096	0.00001973	0.059
LOGP	3	6.78143534	0.00131067	6.7799219	6.7821921	0.00075672	20.3443060	0.00000172	0.019
LOGMG	3	5.03043792	0.00000000	5.0304379	5.0304379	0.00000000	15.0913138	0.00000000	0.000

VARIABLE	N	MEAN	STANDARD DEVIATION	MINIMUM VALUE	MAXIMUM VALUE	STD ERROR OF MEAN	SUM	VARIANCE	C.V.
REGION=5 SITE=2 ANAL=1									
CA	3	2262.33333333	6.65832812	2255.0000000	2268.0000000	3.84418753	6787.0000000	44.3333333	0.294
P	3	1055.66666667	4.50924975	1051.0000000	1060.0000000	2.60341656	3167.0000000	20.3333333	0.427
MG	3	168.33333333	34.84728588	131.0000000	200.0000000	20.11908988	505.0000000	1214.3333333	20.701
LOGC	3	7.72414912	0.00294466	7.7209053	7.7266537	0.00170010	23.1724474	0.0000087	0.038
LOGP	3	6.96192167	0.00427251	6.9574974	6.9660242	0.00246673	20.8857650	0.0000183	0.061
LOGMG	3	5.11085666	0.21563853	4.8751973	5.2983174	0.12449896	15.3325700	0.0465000	4.219
REGION=5 SITE=2 ANAL=2									
CA	3	2309.33333333	44.43347087	2277.0000000	2360.0000000	25.65367637	6928.0000000	1974.3333333	1.924
P	3	1013.33333333	4.61880215	1008.0000000	1016.0000000	2.66666667	3040.0000000	21.3333333	0.456
MG	3	218.00000000	0.00000000	218.0000000	218.0000000	0.00000000	654.0000000	0.0000000	0.000
LOGC	3	7.74459155	0.01914817	7.7306141	7.7664169	0.01105520	23.2337746	0.0003667	0.247
LOGP	3	6.92099357	0.00456406	6.9157234	6.9236286	0.00263506	20.7629807	0.0000208	0.066
LOGMG	3	5.38449506	0.00000000	5.3844951	5.3844951	0.00000000	16.1534852	0.0000000	0.000
REGION=6 SITE=1 ANAL=1									
CA	3	2113.33333333	55.77036250	2049.0000000	2148.0000000	32.19903380	6340.0000000	3110.3333333	2.639
P	3	997.00000000	0.00000000	997.0000000	997.0000000	0.00000000	2991.0000000	0.0000000	0.000
MG	3	200.00000000	0.00000000	200.0000000	200.0000000	0.00000000	600.0000000	0.0000000	0.000
LOGC	3	7.65578720	0.02659524	7.6251071	7.6722925	0.01535477	22.9673616	0.0007073	0.347
LOGP	3	6.90475077	0.00000000	6.9047508	6.9047508	0.00000000	20.7142523	0.0000000	0.000
LOGMG	3	5.29831737	0.00000000	5.2983174	5.2983174	0.00000000	15.8949521	0.0000000	0.000
REGION=6 SITE=1 ANAL=2									
CA	3	2201.66666667	13.05118130	2188.0000000	2214.0000000	7.53510304	6605.0000000	170.33333333	0.593
P	3	970.00000000	1.73205081	968.0000000	971.0000000	1.00000000	2910.0000000	3.00000000	0.179
MG	3	200.00000000	0.00000000	200.0000000	200.0000000	0.00000000	600.0000000	0.00000000	0.000
LOGC	3	7.69695821	0.00593061	7.6907432	7.7025561	0.00342404	23.0908746	0.00003517	0.077
LOGP	3	6.87729501	0.00178654	6.8752321	6.8783265	0.00103146	20.6318850	0.00000319	0.026
LOGMG	3	5.29831737	0.00000000	5.2983174	5.2983174	0.00000000	15.8949521	0.00000000	0.000
REGION=6 SITE=2 ANAL=1									
CA	3	2336.00000000	10.58300524	2324.0000000	2344.0000000	6.11010093	7008.0000000	112.00000000	0.453
P	3	1043.00000000	4.00000000	1039.0000000	1047.0000000	2.30940108	3129.0000000	16.00000000	0.384
MG	3	202.00000000	0.00000000	202.0000000	202.0000000	0.00000000	606.0000000	0.00000000	0.000
LOGC	3	7.75618849	0.00453542	7.7510451	7.7596142	0.00261852	23.2685655	0.00002057	0.058
LOGP	3	6.94985155	0.00383511	6.9460140	6.9536842	0.00221420	20.8495547	0.00001471	0.055
LOGMG	3	5.30826770	0.00000000	5.3082677	5.3082677	0.00000000	15.9248031	0.00000000	0.000
REGION=6 SITE=2 ANAL=2									
CA	3	2217.33333333	57.72636602	2154.0000000	2267.0000000	33.32833296	6652.0000000	3332.3333333	2.603
P	3	1018.00000000	4.00000000	1014.0000000	1022.0000000	2.30940108	3054.0000000	16.0000000	0.393
MG	3	202.00000000	0.00000000	202.0000000	202.0000000	0.00000000	606.0000000	0.0000000	0.000
LOGC	3	7.70383323	0.02615418	7.6750819	7.7262127	0.01510012	23.1114997	0.0006840	0.339
LOGP	3	6.92559005	0.00392930	6.9216582	6.9295168	0.00226858	20.7767702	0.0000154	0.057
LOGMG	3	5.30826770	0.00000000	5.3082677	5.3082677	0.00000000	15.9248031	0.0000000	0.000

APPENDIX 3

Typical IR scan of the natural implants

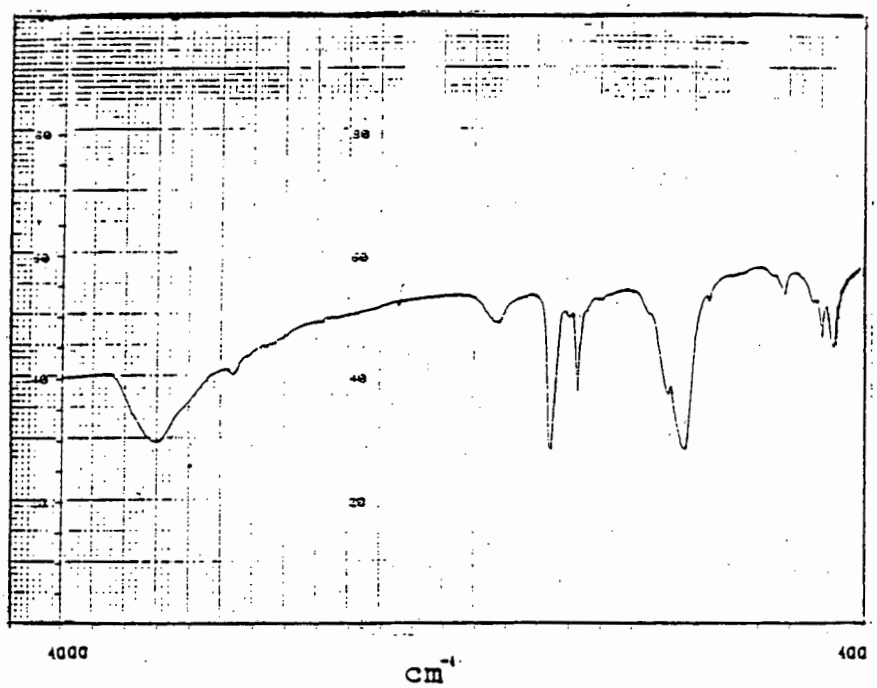

Typical IR scan of the synthetic implants

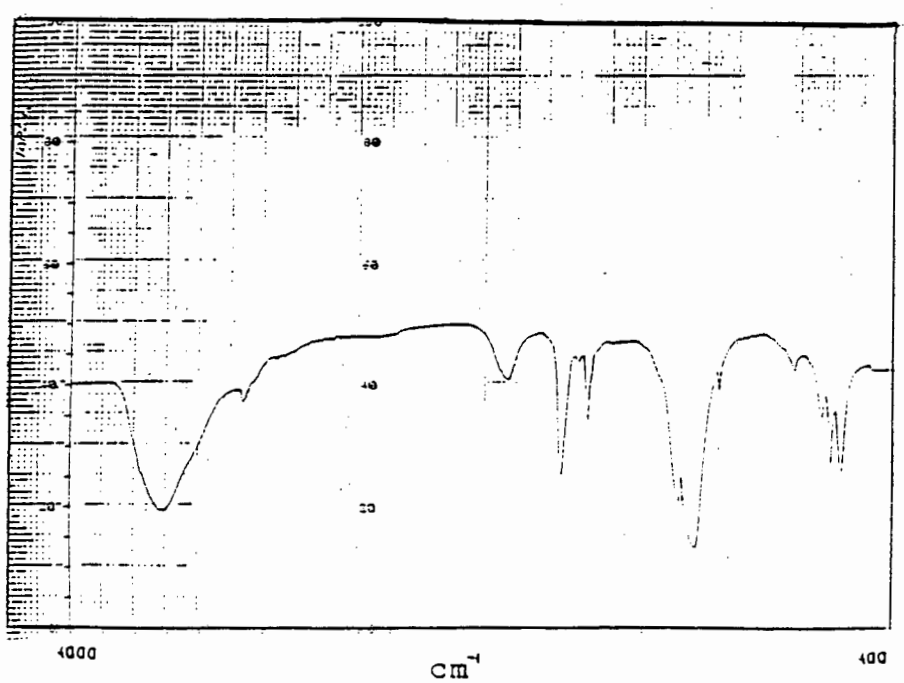

Typical IR scan of the bones

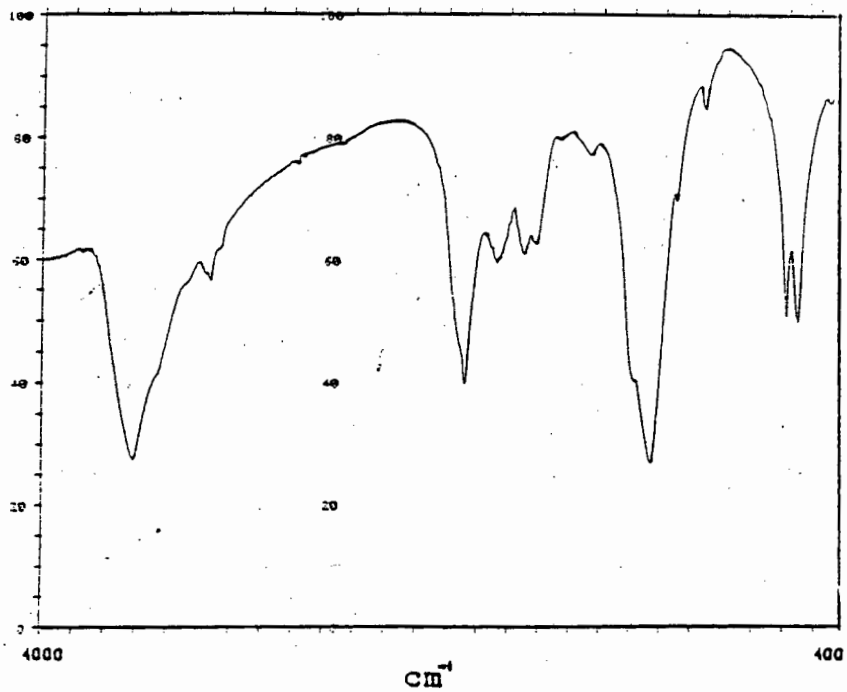

APPENDIX 4

Typical XRD scans of the implants after each heating stage

0-650 °C

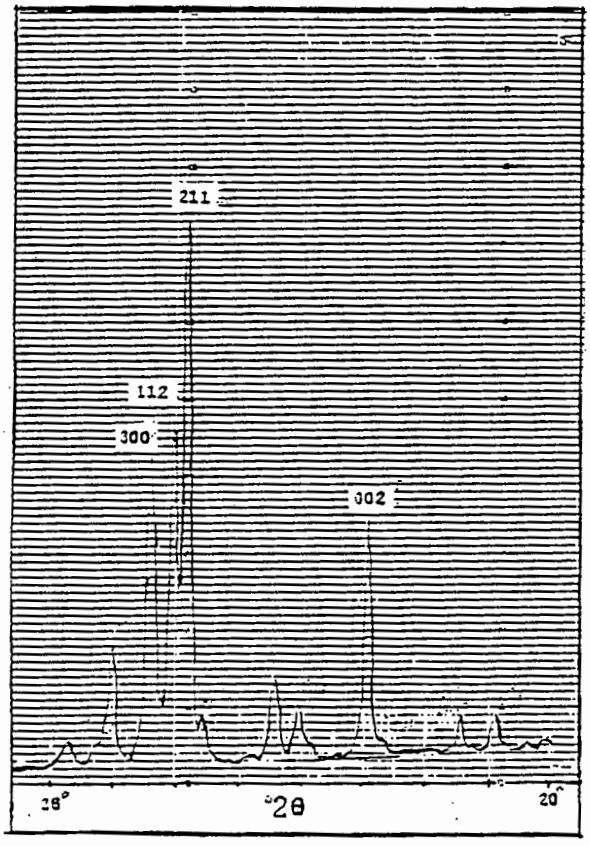

650-900 °C

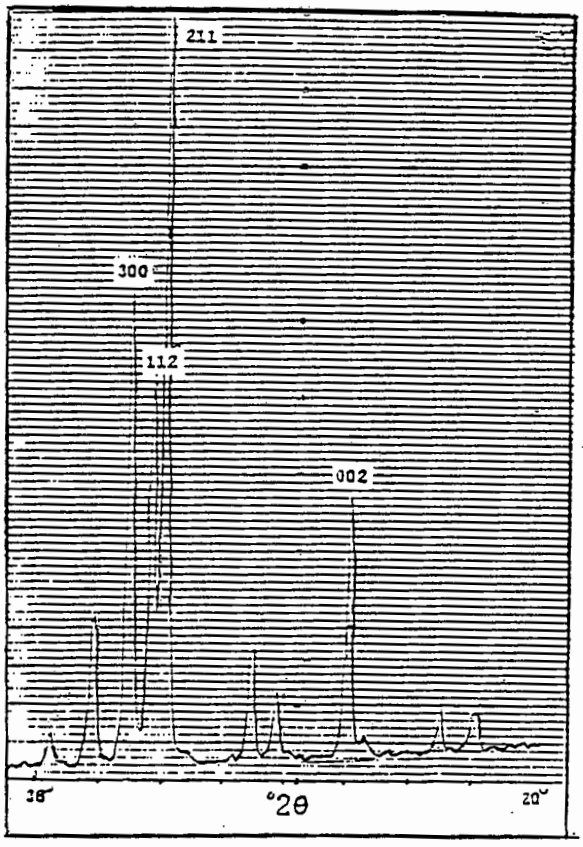

Typical XRD scans of the bones after each heating stage

0-650 °C

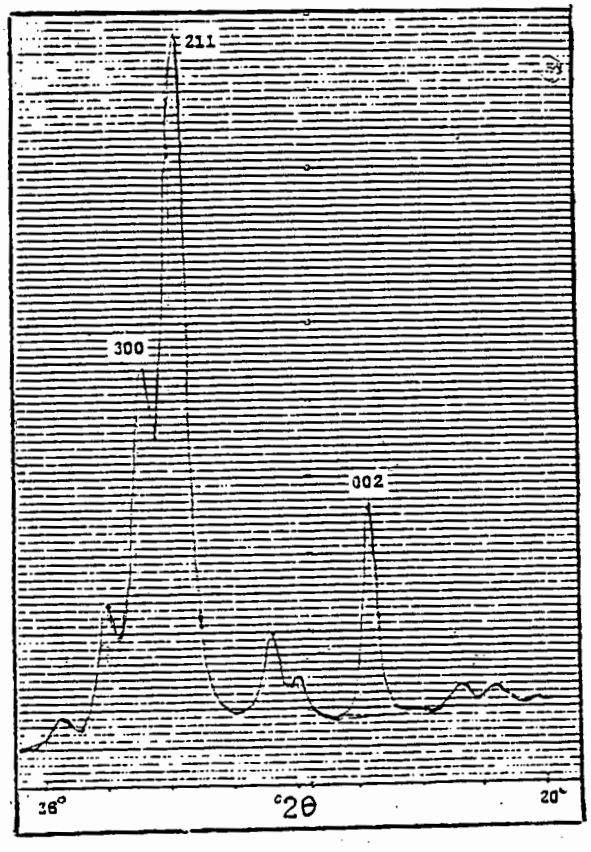

650-900 °C

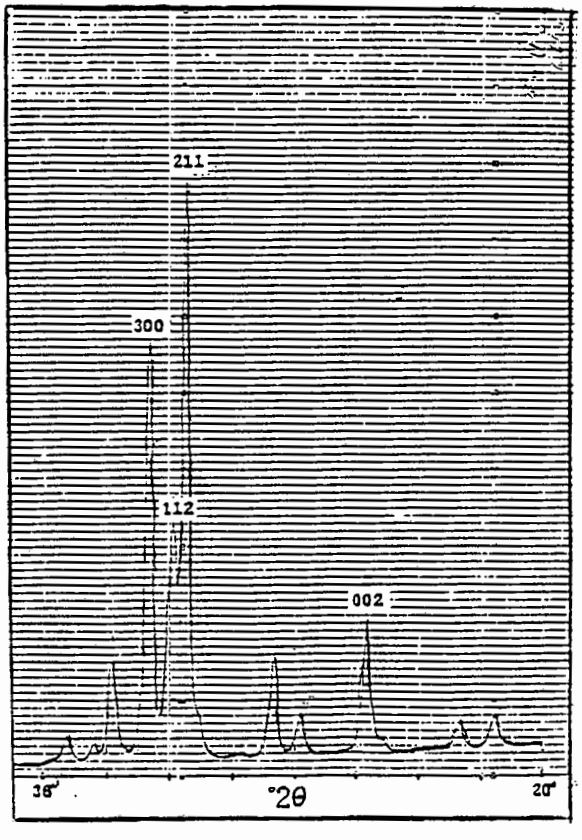

Listing of d-spacings vs intensities for the implants after heating to 650 °C

1		2		3		4		5	
d	I	d	I	d	I	d	I	d	I
4.07	11.83	4.09	17.31	4.07	10.92	4.07	8.92	4.07	6.52
4.00	11.31	3.89	19.02	3.88	30.74	3.88	9.12	3.88	7.55
3.61	10.28	3.60	19.75	3.61	6.29	3.50	5.25	-	
3.45	33.54	3.45	44.39	3.45	51.11	3.45	35.51	3.46	35.53
3.19	11.95	3.19	18.78	3.29	11.85				
3.10	19.92	3.10	27.56	3.14	13.15	3.16	10.11	3.16	10.33
3.03	9.76	3.02	24.63	3.06	28.05	3.08	17.86	3.07	16.05
2.95	21.98	2.94	36.58	2.99	14.81			3.00	7.47
2.84	100	2.82	100	2.90	15.00	2.82	100		
2.81	52.95	2.80	73.90	2.80	100	2.79	52.57	2.80	100
2.72	61.18	2.72	58.78	2.72	65.00	2.73	64.48	2.72	51.51
2.64	22.75	2.64	27.07	2.63	37.96	2.64	23.41	2.62	10.83
				2.61	32.59				
2.54	7.45	2.53	11.71	2.52	10.00	2.54	6.44	2.52	6.36
				2.40	6.29				
2.37	6.68	2.34	10.97	2.33	12.59	2.35	3.79	2.34	6.20
2.29	9.12	2.30	13.41	2.29	11.01	2.30	7.14		
2.26	24.68	2.26	24.39	2.25	26.38	2.27	24.40	2.25	20.27
2.23	4.37	2.23	10.24	2.18	9.25	2.23	3.17		
						2.20	2.57		
2.16	9.25	2.15	14.63	2.13	10.45	2.15	7.44	2.15	7.55
						2.11	2.97		
2.07	7.71	2.06	12.92	2.06	7.40	2.06	5.95	2.06	7.47
2.03	8.48	2.04	20.00	2.03	21.48	2.03	7.04	2.03	11.88
2.00	7.77	2.00	12.44	1.99	9.26	2.00	5.35	1.99	6.83
1.94	31.88	1.95	33.65	1.94	40.46	1.95	29.36	1.93	24.00
1.89	16.71	1.89	21.71	1.88	16.48	1.89	13.49		
1.87	8.74					1.87	5.05	1.87	14.15
1.83	32.00	1.84	36.34	1.83	34.16	1.84	32.24	1.83	28.22
1.80	20.56	1.80	20.00	1.79	19.44	1.80	17.06		
1.77	13.11			1.77	16.48	1.78	12.89	1.79	15.89
								1.76	14.22
1.75	13.13	1.75	15.12	1.74	15.27	1.75	12.99	1.74	12.32
1.72	14.13	1.72	19.02	1.71	18.51	1.72	14.58	1.72	14.22

cont'd

6		7		8		9		10	
d	I	d	I	d	I	d	I	d	I
4.09	10.81	4.07	8.58	4.09	10.59	4.07	12.21	4.09	9.26
3.88	8 .95	3.88	8.57	3.89	10.59	3.88	12.35	3.88	9.03
3.50	5.37	3.50	5.28	3.51	6.56	3.50	8.14	3.47	5.04
3.45	33.95	3.44	34.97	3.45	37.71	3.44	47.48	3.45	59.48
				3.34	6.99				
		3.16	10.57	3.17	12.71	3.16	14.24	3.17	15.66
3.17	11.02	3.07	17.90	3.08	19.27	3.08	19.67	3.08	23.64
3.08	18.16					2.86	12.21		
				2.82	100	2.82	100	2.81	100
2.81	100	2.80	100						
2.77	51.88	2.76	53.40	2.77	55.08	2.78	65.81	2.78	62.75
2.72	64.31	2.71	62.82	2.72	61.86	2.72	59.02	2.72	60.23
2.63	23.14	2.62	23.98	2.63	23.31	2.62	25.24	2.61	32.41
		2.52	6.28	2.53	6.78	2.52	7.84	2.51	7.83
2.54	6.48	2.34	2.62					2.34	6.05
2.35	3.12	2.29	7.22	2.30	8.05	2.29	8.14	2.28	9.33
2.30	7.37	2.25	23.03	2.26	25.21	2.26	21.57	2.25	28.23
2.26	25.01	2.22	3.22	2.22	4.01				
2.22	3.23	2.14	7.22	2.15	8.26	2.15	8.14	2.14	10.01
2.15	2.64	2.06	5.76	2.06	6.14	2.06	8.14	2.05	10.16
2.11	7.48								
2.06	2.87	2.03	4.81	2.03	3.17	2.03	4.07	2.02	11.29
2.03	6.09	2.00	5.03	2.00	4.97	1.99	6.51	1.99	7.83
2.00	5.21	1.94	29.53	1.94	27.54	1.94	26.59	1.93	38.40
						1.91	4.13	1.91	4.14
1.95	29.61	1.88	13.45	1.89	12.71	1.89	13.70	1.88	18.67
1.88	5.07	1.86	5.34	1.87	5.51	1.86	6.10	1.86	8.50
1.86	5.34	1.83	33.24	1.84	29.87	1.83	32.56	1.83	45.03
1.84	32.72	1.80	17.27	1.80	16.73	1.80	13.83	1.80	20.48
1.80	17.41	1.77	12.56	1.77	12.07	1.77	11.53	1.77	15.81
1.77	12.56	1.75	13.29	1.75	13.13	1.75	11.39	1.72	16.18
1.75	12.91	1.71	14.87	1.72	16.95	1.72	16.14	1.71	21.46
1.72	14.98								

Listing of d-spacings vs intensities for the implants after heating to 900°C

1		2		3		4		5	
d	I	d	I	d	I	d	I	d	I
	-	4.39	16.39	4.39	13.62		-		-
4.05	10.67	4.07	23.18	4.05	22.81	4.07	9.94	4.09	17.25
3.88	10.37	3.89	17.33	3.88	5.18	3.88	10.36	3.89	14.36
3.49	6.02	3.49	11.49		-	3.50	6.17	3.51	7.41
3.43	36.84	3.43	58.03	3.43	45.78	3.43	37.48	3.43	70.65
	-	3.36	14.75	3.36	18.51		-		-
3.16	10.86	3.20	63.23	3.20	90.96	3.17	10.37	3.17	19.28
3.07	18.56	3.07	18.97	3.09	5.40	3.08	19.16	3.08	38.88
	-	3.00	22.25	3.01	29.62		-		-
	-	2.87	100	2.87	100		-		-
2.81	100	2.81	78.68	2.81	9.55	2.81	100	2.81	100
2.77	51.55	2.77	48.95		-	2.77	52.15	2.77	94.06
	-	2.76	34.89	2.75	41.33		-		-
2.73	66.47	2.72	62.53	2.72	21.48	2.72	61.98	2.72	97.73
2.63	24.69	2.64	14.51	2.67	16.51	2.65	5.86	2.63	46.21
	-	2.61	70.25	2.60	99.70	2.62	24.08		-
	-	2.54	16.39	2.55	22.07		-		-
2.51	6.71	2.51	17.56	2.51	20.88	2.52	6.91	2.52	12.80
	-	2.40	12.88	2.40	18.67		-		-
	-	2.37	11.24	2.37	12.74		-	2.34	6.40
2.29	7.71	2.29	9.36	2.29	3.92		-	2.29	13.66
2.26	25.58	2.25	31.38	2.25	22.22	2.23	7.01	2.26	52.92
2.22	33.58	2.19	16.39	2.19	25.11	2.19	23.03		-
2.14	7.11	2.15	14.75	2.16	19.85	2.16	3.14	2.15	15.61
2.09	2.96		-		-	2.09	7.64	2.11	4.91
2.06	5.72	2.06	43.90	2.07	16.00	2.05	3.87	2.06	10.53
2.03	2.95	2.02	14.05	2.02	28.00	2.01	5.65	2.02	15.84
1.99	5.03	1.99	11.71	2.00	12.59		-	1.99	9.36
1.94	29.23	1.93	32.08	1.93	10.29	1.95	5.44	1.94	58.78
1.89	13.63	1.88	23.63	1.89	27.11	1.91	29.63	1.89	27.11
1.86	5.53		-	1.88	25.03	1.87	12.56	1.87	11.47
1.83	29.63	1.83	25.76	1.83	3.92	1.83	30.47	1.84	61.67
1.80	27.06	1.80	18.73	1.81	10.81	1.79	15.70	1.80	35.91
1.77	11.95	1.77	17.09	1.77	17.25	1.77	11.94	1.78	28.49
1.75	13.33	1.75	13.11	1.74	7.92	1.74	12.46	1.75	27.16
1.72	12.34	1.72	34.89	1.72	41.70	1.72	14.24	1.72	27.71
	-	1.70	14.75	1.70	16.80		-		-

cont'd

6		7		8		9		10	
d	I	d	I	d	I	d	I	d	I
	-		-		-		-		-
4.09	6.36	4.05	9.10	4.07	13.90	4.09	10.41	4.05	9.38
3.88	6.96	3.88	9.50	3.88	12.38	3.88	9.93	3.88	9.10
	-	3.50	6.00	3.51	6.85	3.50	5.37	3.49	4.51
3.43	37.27	3.43	37.80	3.43	64.44	3.43	61.31	3.43	40.38
	-		-		-	3.34	4.48		-
3.17	10.68		-		-	3.20	13.86		-
3.07	15.45	3.15	11.80	3.17	18.92	3.17	17.10	3.15	10.76
	-	3.07	17.90	3.09	31.24	3.08	23.24	3.06	22.17
	-		-		-	2.99	4.69		-
2.80	100		-	2.89	3.49	2.87	20.68		-
	-	2.81	100	2.81	100	2.82	100	2.81	100
	-	2.77	53.10	2.77	78.10	2.79	80.76		-
2.72	49.09		-		-		-	2.76	62.07
2.64	21.74	2.71	63.50	2.72	82.86	2.72	72.97	2.73	78.71
	-		-	2.63	44.69	2.63	33.86		-
2.54	6.81	2.61	22.10		-	2.59	14.13	2.61	28.61
	-	2.52	6.50	2.53	10.48	2.53	8.89	2.51	7.36
	-		-		-	2.39	3.58	2.39	2.11
2.34	5.15		-	2.34	6.98	2.34	7.65	2.34	3.86
	-	2.29	6.90	2.30	11.43	2.30	9.86	2.29	7.82
2.26	18.56	2.26	22.00	2.26	39.74	2.26	29.10	2.25	30.26
	-	2.23	3.20	2.23	4.63	2.18	4.82		-
2.14	7.57	2.16	7.50	2.15	11.74	2.15	10.34	2.14	8.55
	-		-		-		-	2.10	2.20
2.06	7.58	2.06	6.00	2.06	10.79	2.06	10.89	2.06	6.99
2.03	9.09	2.04	2.50	2.02	14.85	2.02	18.41	2.03	12.69
2.00	6.81	2.00	5.10	2.00	8.38	2.00	8.76	2.00	5.70
1.94	23.40	1.94	27.50	1.94	50.35	1.94	35.31	1.94	34.96
1.89	14.31	1.89	19.00	1.89	24.69	1.89	20.69	1.89	16.74
	-	1.86	5.40	1.86	9.65	1.87	9.03	1.87	5.97
1.84	27.42	1.83	30.10	1.83	58.44	1.84	45.31	1.83	28.33
1.80	16.51	1.80	16.00	1.80	29.58	1.80	20.07	1.80	20.42
1.78	12.87	1.77	12.40	1.77	22.54	1.78	14.21	1.78	16.09
1.75	13.63	1.75	12.60	1.75	23.61	1.75	16.55	1.75	15.63
1.72	15.07	1.72	14.00	1.72	26.15	1.72	16.69	1.72	16.74

Listing of d-spacings vs intensities for the bones after heating to 650°C

1		2		3		4		5		6	
d	I	d	I	d	I	d	I	d	I	d	I
4.11	14.60	4.12	12.90	4.11	13.16	4.14	13.27	4.11	12.67	4.07	13.14
3.91	13.09	3.91	12.34	3.89	13.26	3.98	13.18	3.91	13.75	3.89	13.89
3.44	37.41	3.44	33.68	3.45	37.85	3.44	31.41	3.44	34.28	3.45	34.55
3.19	14.96	3.18	14.03	3.18	14.49	3.20	15.04	3.19	14.73	3.17	14.27
3.10	29.64	3.09	10.57	3.09	20.41	3.11	21.95	3.10	21.43	3.08	20.65
2.83	100	2.82	100	2.81	100	2.84	100	2.82	100	2.81	100
2.72	90.95	2.73	58.56	2.73	55.51	2.72	67.30	2.71	59.73	2.72	57.65
2.64	28.20	2.66	23.38	2.63	24.59	2.65	25.57	2.65	24.10	2.64	23.66
2.54	10.79	2.55	8.84	2.52	9.48	2.54	11.68	2.54	10.53	2.53	9.57
2.35	7.48	2.36	13.19	2.37	11.73	2.35	12.39	-		2.35	9.38
2.27	11.15	2.27	23.29	2.29	22.75	2.28	26.28	2.30	24.38	2.26	22.53
2.15	12.37	2.16	9.35	2.17	9.08	2.15	13.98	2.15	11.78	2.15	9.38
2.06	7.23	2.07	7.48	2.08	8.47	2.08	13.36	2.07	11.42	2.06	8.35
2.03	12.44	2.04	22.83	2.04	19.59	2.03	19.46	2.03	11.42	2.03	12.95
2.00	6.69	2.00	7.84	2.02	8.57	-		2.00	10.35	2.00	17.37
1.95	10.43	1.93	25.01	1.95	25.51	1.95	30.17	1.95	27.13	1.94	24.32
1.90	18.06										
1.88	9.92	1.88	15.88	1.89	15.71	1.90	19.47	1.90	17.32	1.89	15.58
1.85	36.73	1.84	27.16	1.85	29.08	1.85	31.68	1.84	28.57	1.84	26.48
1.81	27.91	1.80	17.73	1.80	18.36	1.81	23.00	1.81	10.08	1.80	18.78
1.78	30.80	1.77	15.40	1.78	15.82	1.79	20.00	1.79	17.41	1.78	16.15
1.76	18.71	1.76	14.00	1.76	14.79	1.76	17.69	1.76	15.17	1.76	14.27
1.72	15.82	1.71	14.00	1.72	15.30	1.73	16.81	1.72	14.28	1.72	13.99

Listing of d-spacings vs intensities for the bones after heating to 900°C

1		2		3		4		5		6	
d	I	d	I	d	I	d	I	d	I	d	I
4.09	15.51	4.11	15.41	4.09	13.72	4.12	12.81	4.09	16.41	4.11	13.59
3.89	13.04	3.91	14.44	3.91	13.64	3.94	11.87	3.91	15.28	3.89	11.81
-		3.53	10.22	3.53	9.73	3.54	11.33	3.53	10.58	3.51	8.15
3.45	37.02	3.45	49.48	3.44	45.49	3.45	30.63	3.44	41.66	3.44	37.22
3.19	14.47	3.19	15.92	3.19	15.52	3.20	17.58	3.19	15.02	3.18	12.35
3.09	31.10	3.09	32.22	3.10	28.78	3.11	28.51	3.09	30.39	3.09	28.87
2.81	100	2.82	100	2.83	100	2.83	100	2.83	100	2.82	100
2.77	63.89	2.79	77.03	2.79	73.80	2.80	59.37	2.79	72.92	2.76	64.52
2.71	86.74	2.73	81.85	2.73	90.58	2.73	83.59	2.72	93.45	2.73	91.75
2.63	28.91	2.64	36.22	2.64	34.51	2.64	30.86	2.64	33.19	2.64	29.11
2.59	7.05					2.61	15.63				
2.52	11.14	2.54	11.34	2.54	10.04	2.54	17.58	2.54	10.92	2.54	9.62
-		-		2.41	6.11	-		-		2.40	3.41
2.34	8.81	2.34	9.57	2.35	19.24	-		2.34	8.21	2.34	3.88
2.29	10.58	2.30	11.48	2.30	10.98	2.31	19.38	2.30	12.05	2.30	9.94
2.27	42.67	2.27	42.70	2.26	14.98	2.27	44.61	2.27	43.23	2.26	40.52
-		2.24	5.52	2.23	5.49	-		-		2.23	4.19
2.14	12.55	2.15	13.25	2.15	12.15	2.16	27.89	2.15	13.27	2.15	11.33
2.07	7.54	2.11	4.07	2.11	4.78	2.13	42.26	2.11	4.45	2.11	3.41
-		2.06	9.12	2.06	9.09	2.07	30.39	2.06	9.43	2.06	6.98
2.04	15.58	2.03	18.77	2.03	19.21	2.03	30.54	2.02	12.66	2.03	4.65
2.00	6.20	2.00	7.36	2.00	7.84	2.01	30.54	2.00	8.21	2.00	6.21
1.95	41.68	1.95	46.53	1.95	44.00	1.95	54.68	1.94	46.81	1.94	41.14
1.89	19.74	1.89	22.08	1.89	21.96	1.90	31.64	1.89	23.14	1.89	20.10
1.87	10.51	1.87	9.72	1.87	9.02	1.88	23.43	1.87	10.56	1.87	9.31
1.84	37.66	1.84	46.53	1.84	46.27	1.85	50.47	1.84	47.25	1.84	39.20
1.80	29.12	1.81	30.18	1.81	28.00	1.81	36.56	1.80	31.61	1.81	27.63
1.78	22.92	1.78	22.45	1.78	21.80	1.78	30.46	1.78	24.80	1.78	21.29
1.76	18.82	1.76	20.84	1.76	20.39	1.76	26.56	1.76	21.92	1.76	19.01
1.72	14.95	1.72	20.02	1.72	20.47	1.72	23.83	1.72	19.83	1.72	15.91